Electronic Thesis and Dissertation Repository

8-15-2014 12:00 AM

Studies of Anode Electrodes for the BioGenerator

Vahid Vajihinejad, *The University of Western Ontario*

Studies of Anode Electrodes for the BioGenerator

(Thesis format: Monograph)

by

Vahid <u>Vajihinejad</u>

Graduate Program in Chemical and Biochemical Engineering

A thesis submitted in partial fulfillment
of the requirements for the degree of
Master of Engineering Science

The School of Graduate and Postdoctoral Studies
The University of Western Ontario
London, Ontario, Canada

© Vahid Vajihinejad 2014

Abstract

The BioGenerator as a fundamentally new type of H_2-to-electricity conversion system offers a quite sustainable and cost effective solution to the challenges associated with the use of fuel cells in renewable power grids. The development of an anode electrode for the BioGenerator was subject of this work. The unique features of the BioGenerator require unique electrodes, and more specifically anode. The combination of biological cathodic liquid and the hydrogen gas fuel require specific hydrophobic/hydrophilic properties of the anode. Several different methods for anode formation were studied. The spreading technique was found to be most appropriate for the conditions in the BioGnerator. It was employed to fabricate three-layer hydrophobic PTFE-bound anode electrodes. The reproducibility, durability and performance stability of the mentioned electrodes were studied using i-V curves, ex-situ cyclic voltammetry, and through-plane gas permeability. In addition, the effect of hydrophobic polymer content (PTFE) in the backing substrates, including woven-fiber carbon cloth and nonwoven-fiber carbon papers, on the gas permeability, hydrophobicity, and long-term durability of anode electrodes was studied. Results showed that woven-fiber carbon cloth impregnated with 80-100 wt.% PTFE gives an enhanced durability towards flooding in the course of continuous operation at 100 mA cm^{-2}. Moreover, causes of failure in the performance of the anode electrodes were assessed and results showed that the mass transfer is the main source of limitation in the long-term operation.

Keywords

The BioGenerator, micro-porous layer (MPL), backing layer (BL), catalyst layer (CL), hydrophobicity, long-term durability, liquid flooding.

Co-Authorship Statement

Vahid Vajihinejad was the principal author. The supervisors Dr. Dimitre Karamanev and Dr. Shahram Karimi made revisions and recommendations. Based on some portions of results in this thesis, two papers are under preparation for submission to peer reviewed journals. The contribution of each author is given below

1- Effect of PTFE in Gas Diffusion Backing Layer of Hydrogen Oxidation Anode Electrode of a Microbial-based H_2/Fe^{3+} Redox Flow Fuel Cell

To be submitted to: *International Journal of Hydrogen Energy*

Authors: Vahid Vajihinejad, Paul Brouwers, Dimitre Karamanev, Shahram Karimi

Experimental work and data analysis were performed by Vahid Vajihinejad. Paul Brouwers contributed to the gas permeability analysis and fabrication of electrodes. Dimitre Karamanev and Shahram Karimi provided consultation regarding experimental work and data analysis. The manuscript was written and revised by Vahid Vajihinejad and reviewed by Dimitre Karamanev and Shahram Karimi.

2- Performance Stability Studies of Hydrogen Oxidation Anode Electrodes used in a Microbial-based H_2/Fe^{3+} Redox Flow Fuel Cell

To be submitted to: *The Canadian Journal of Chemical Engineering*

Authors: Vahid Vajihinejad, Ricardo Cuello, Dimitre Karamanev, Shahram Karimi

Experimental work and data analysis were performed by Vahid Vajihinejad. Ricardo Cuello contributed to SEM analysis and fabrication of CV cell. Dimitre Karamanev and Shahram Karimi provided consultation regarding experimental work and data analysis. The manuscript was written and revised by Vahid Vajihinejad and reviewed by Dimitre Karamanev and Shahram Karimi.

Acknowledgment

Table of Contents

List of Tables

List of Figures

xiii

Nomenclature

a_{H^+}	Activity of Proton (unitless)
a_{H_2}	Activity of Hydrogen (unitless)
a_{O_2}	Activity of Oxygen (unitless)
$a_{Fe^{3+}}$	Activity of Ferric Ion (unitless)
$a_{Fe^{2+}}$	Activity of Ferrous Ion (unitless)
$E_{r,cell}$	Reversible Cell Voltage (V)
ε_{th}	Thermodynamic Reversible Efficiency (unitless)
ε_{real}	Real Efficiency (unitless)
F	Farady's Constant (C mol^{-1})
i	Current Density (A cm^{-2})
i_0	Exchange Current Density (A cm^{-2})
i_L	Limiting Current Density (A cm^{-2})
V_{cell}	Cell Voltage (V)
R	Universal Gas Constant (J mol^{-1} K^{-1})

Abbreviations

BL	(Gas diffusion) Backing Layer
BOL	Beginning of Life (Operation)
BPL	Bipolar Plate
CL	Catalyst Layer
CV	Cyclic Voltammetry
ECSA	Electrochemical (Active) Surface Area
EOL	End of Life (Operation)
GDL	Gas Diffusion Layer
GDE	Gas Diffusion Electrode
MEA	Membrane Electrode Assembly
MIP	Mercury Intrusion Porosimetry
MPL	Micro-Porous Layer
PEMFC	Polymer Electrolyte (Proton-Exchange) Membrane Fuel Cell
PTFE	Polytetrafluoroethylene
SEM	Scanning Electron Microscopy
XPS	X-Ray Photoelectron Spectroscopy
XRD	X-Ray Diffraction

1 Introduction

1.1 Motivation

The Necessity of finding alternatives to fossil fuels is no longer a question in the 21st century because fossil fuels are not renewable, and they lead to major impacts on the environment. These reasons have created the rationale for developing alternative energy technologies (Glaser 1968). According to the US Department of Energy, over the last two decades, about 75% of human-caused emissions have come from the burning of fossil fuels (DOE, FOSSIL 2013).

In the last few years, there has been a considerable growth in the share of renewables in the generation of electricity, heat, and in fuel production. In respect to the generation of electricity, renewables fall into two major categories: hydropower and new renewables (Renewables 2013 Global Status Report, 2013). The share of renewable primary energy sources for global electricity generation at the end of 2012 accounted for 16.5% and 5.2% for hydropower and other renewables, respectively (Renewables 2013 Global Status Report 2013). Among the latter, one can mention alternatives such as wind and solar power, bio-power, geothermal power and ocean (wave) power (John and Weir 2006; Lindley 2010). In electricity generation on a global scale, wind and sun are the most important sources mainly due to their environmentally friendly nature and unlimited quantity. For example, in 2010, the power generated from wind turbines accounted for almost 70% of the worldwide electricity generation from non-hydro renewable sources of energy (Renewables 2011: Global Status Report 2011).

However, in order to take advantage of the unlimited potency of wind and sun for generating electricity, there is one big challenge. The intermittency of wind and solar power generation brings the viability of these natural resources into question (Lindley 2010). No intermittent power generation can be introduced to the electrical grid without smoothing. In other words, the output of such sources needs to be smoothed out by storing their excess energy in the form of intermediate energy. Recently, systems such as rechargeable and redox flow batteries, hydrogen storage, pumped hydro, compressed air storage, supercapacitors and flywheels have been proposed as energy storage systems for renewable-based power plants (Hadjipaschalis *et al*., 2009). Of these choices, the only well-established technology is pumped hydro, but

unfortunately, it has a big drawback- it is very limited by geographical location (Buenoa and Carta 2006). Among the existing energy storage methods, hydrogen is probably the best overall power storage medium. Electrolysis is a highly efficient and well-established technology for the conversion of surplus electricity to hydrogen (Figure 1-1). Compression or liquefaction is commonly used for the storage of the produced H_2 (Zhou 2005). However, the current bottleneck in hydrogen-based energy storage of renewable power is the conversion of the stored hydrogen back into electricity, since there is no well-developed H_2-to-electricity conversion technology.
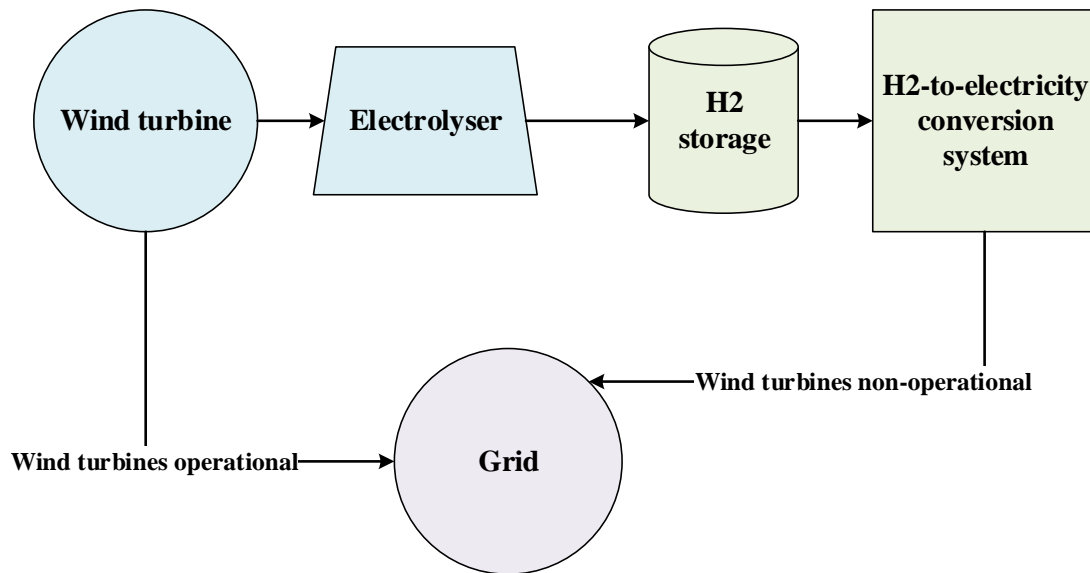
Figure 1-1 A schematic diagram of integrating renewable energies and electrical grids

Currently in wind and solar power plants, a balance between demand and supply is achieved by mixing hydrogen with natural gas and burning it in turbines as a NG-H_2 mixture (Lee and Gushee 2009). Major impacts of doing so are: 1- Cycling for baseload power plants will increase maintenance cost and decrease the plant life. 2- In some cases, cycling emits pollutants like SO_2 and NO_x more than conventional natural gas plants (Barnes & Levine, 2011) (Drouineau, Maïzi *et al.*, 2014).

When hydrogen is used as an intermediate fuel, fuel ce=lls are theoretically considered promising H_2-to-electricity conversion systems. However, the two significant challenges associated with these technologies are high cost and low durability (DOE, Technical Plan- Fuel Cells 2012). Due to sluggish kinetics of the oxygen reduction reaction (ORR), it is almost

practically impossible to run a PEM fuel cell with no nobel metal catalyst (Shao 2013). What is the solution?

The BioGenerator as the first biologically based H_2-to-electricity conversion technology, to be successfully demonstrated on a laboratory scale, is a promising alternative capable of generating power densities over 1800 W m^{-2} (Karamanev *et al.*, 2013 and this study). The BioGenerator is a microbial hydrogen redox flow fuel cell, in the cathode of which the oxygen reduction is replaced with the reduction of ferric ions which are continuously generated by respiration of special types of microorganisms (Hojjati *et al.*, 2013). Because of the bio-regeneration of the oxidant, there is no need to use any metal catalyst in the cathodic reaction. This capability of the BioGenerator will eliminate the cost issue as a significant barrier to the commercialization of H_2/O_2 fuel cells (Wang *et al.*, 2011). The BioGenerator has a unique configuration and is targeted to be employed in certain stationary applications for smoothing the output of wind and solar power plants. It looks like the BioGenerator is a good alternative to conventional fuel cells. It offers a quite sustainable and cost effective solution. However, one important step towards the commercialization of this technology is to demonstrate the durability of its performance. One of the main components of interest in improving the lifetime durability of the BioGenerator is improving durability of its anode electrode, where the hydrogen oxidation reaction takes place. Unfortunately, available gas diffusion electrodes are very limited, costly and designed for use in PEMFCs. Therefore, they do not properly respond to the requirements of the BioGenerator.

1.2 Objectives

On the basis of this introduction, the main objectives of the present work are:

1. To study and develop an anode electrode, based on an appropriate and reproducible method, to be used in the BioGenerator that meets the unique requirements of this system.
2. To study the effect of hydrophobicity of the gas diffusion layer of hydrogen oxidation anode electrodes and the subsequent performance stability of the BioGenerator.
3. To study the causes of failure in long-term operation of the anode electrode.

1.3   Thesis outline

Based on the objectives, this thesis is presented in the following chapters:

Chapter 1 is the introduction, discusses background of the work, and outlines the objectives of the present study.

Chapter 2 introduces the fundamentals of fuel cells, and further describes the BioGenerator by discussing its fundamentals, constitutive components, and involved reactions. Following that, solutions to manage mass transport within the gas diffusion electrodes are reviewed. At the end, methods for dealing with anode flooding are briefly assessed.

Chapter 3 describes the materials, methods of fabrication, different measurements and the set up used in the development and study of the anode electrodes.

Chapter 4 shows the results obtained in this study. It starts with selecting the appropriate gas diffusion medium by investigating the effect of hydrophobic content and gas permeability characteristics of the backing layer and the consequent performance in the BioGenerator system. In addition, it discusses the results obtained from the introduction of different amounts of PTFE in the catalyst layer of the anode electrode using the spreading technique. Moreover, it brings the results from the study of the long-term stability of the developed anode electrodes based on the spreading technique and compares them with the results obtained from the use of commercially available electrodes. Moreover, in this chapter, some modes of performance failure are discussed.

Chapter 5 summarizes the conclusions obtained in this study and by providing recommendations, directs the reader towards future research on the BioGenerator electrodes.

<div align="center">Chapter 2</div>

2 Background and Literature Review

2.1 What is a Fuel Cell?

A fuel cell is an electrochemical device that converts the chemical energy of a fuel directly into electricity. Fuels and oxidants- either in gas or in liquid form- are fed into two separate compartments. In one compartment, the oxidation reaction of the fuel takes place and electrons are released, while in the other the electrons are consumed in the reduction reaction of the oxidant. The former is called the anodic reaction, whereas the latter is referred to as the cathodic reaction (O'Hayre *et al.*, 2006). To better understand the working concept of a fuel cell, Figure 2-1 shows a conventional H_2/O_2 polymer electrolyte membrane fuel cell (PEMFC).
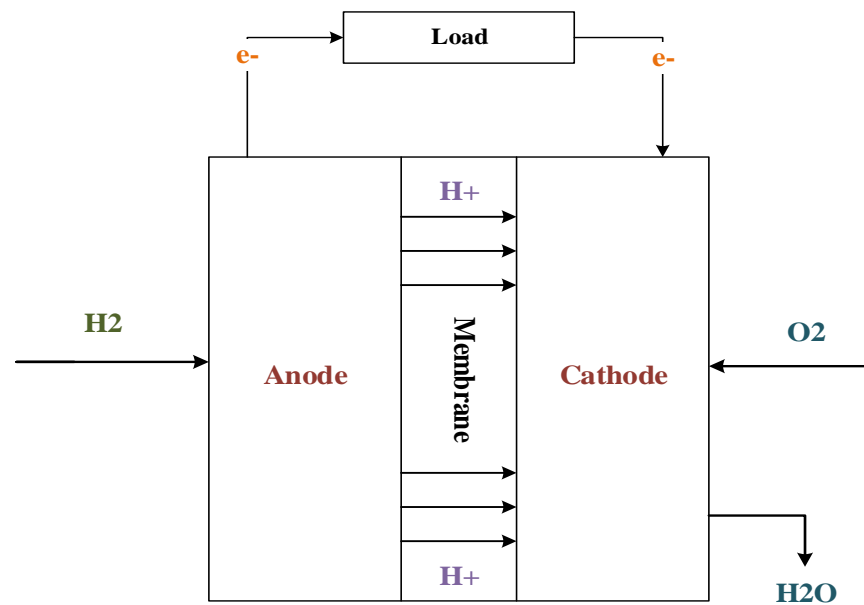
Figure 2-1 Scheme of a PEM fuel cell

In order for the electrical circuit to be charge-balanced and the overall reaction to be complete, the generated protons must migrate to the cathode side through a proton exchange membrane (PEM- a solid polymer electrolyte).

Anode: $\quad H_2 \xrightarrow{Pt} 2H^+ + 2e^-$ $\qquad$ (2-1)

Cathode: $\quad O_2 + 4H^+ + 4e^- \xrightarrow{Pt} 2H_2O$ $\qquad$ (2-2)

Overall: $2H_2 + O_2 \xrightarrow{Pt} 2H_2O$ (2-3)

Both reactions (2-1) and (2-2) require to be catalyzed by usually a precious metal such as platinum. This is especially true in the oxygen reduction reaction (2-2), whose rate is vitally dependent on an adequate catalyst. A practical operation voltage of a single H_2/O_2 fuel cell is 0.7 to 0.8 V and for obtaining larger values, more cells need to be connected in series, forming a fuel cell stack (Karimi 2011).

Fuel cells are mainly classified based on the electrolyte they use (Okada and Yokoyama 2001). Of the most popular fuel cells, there are six types as follows:

1-   Polymer Electrolyte Membrane (PEM) Fuel Cells

2-   Direct Methanol Fuel Cells (DMFCs)

3-   Alkaline Fuel Cells (AFCs)

4-   Phosphoric Acid Fuel Cells (PAFCs)

5-   Molten Carbonate Fuel Cells (MCFCs)

6-   Solid Oxide Fuel Cells (SOFCs)

Table 2-1 gives a brief description of some of these technologies.

Table 2-1 A quick overview on fuel cell technologies (EERE 2011)

Fuel Cell Type	Common Electrolyte	Temp.	Stack Size	Efficiency	Application	Advantages	Disadvantages
Polymer Electrolyte Membrane (PEM)	Perfluoro-Sulfonic acid	Typically 80°C	<1- 100kW	60% Transport 35% Stationary	. Backup power . Portable power . Transportation . Specialty vehicles . Distributed generation	. Solid electrolyte reduces corrosion & electrolyte management problems . Low temperature . Quick start-up	. Expensive catalyst . Sensitive to fuel impurities . Low temp waste heat

Alkaline (AFS)	Aqueous solution of KOH soaked in a matrix	90-100°C	10-100kW	60%	. Military . Space	. Cathode reaction faster in alkaline electrolyte, higher performance . Low cost components	. Sensitive to CO_2 in fuel and air . Electrolyte Management
Phosphoric Acid (PAFC)	Phosphoric acid soaked in a matrix	150-200°C	400kW 100kW Module	40%	. Distributed generation	. Higher temperature enables CHP . Increased tolerant to fuel impurities	. Pt catalyst . Long start-up time . Low current and power
Molten Carbonate (MCFC)	Solution of lithium, sodium, and/or potassium carbonates soaked in a matrix	600-700°C	300 kW-3 MW 300 kW module	45-50%	. Electric utility . Distributed generation	. High efficiency . Fuel flexibility . Can use a variety of catalyst . Suitable for CHP	. High temperature corrosion and breakdown of cell components . Long start-up time . Low power Density
Solid Oxide (SOFC)	Yttria stabilized zirconia	700-1000°C	1 kW–2 MW	60%	. Auxiliary power . Electric utility . Distributed generation	. High efficiency . Fuel Flexibility . Can use a variety of catalysts . Solid electrolyte Suitable for CHP & CHHP . Hybrid/GT cycle	. High temperature corrosion and breakdown of cell components . Long start-up time

2.2 Fuel Cells Thermodynamics

The overall reversible fuel cell voltage is sum of the anodic and the cathodic half-cell potentials. For example, in the case of a H_2/O_2 fuel cell, for

Anode:

$$H_2 \xrightarrow{Pt} 2H^+ + 2e^- \qquad E_{r,a} = E^0{}_a - \frac{RT}{2F}\ln\left(\frac{a_{H^+}{}^2}{a_{H_2}}\right); \; E^0{}_a = 0 \; (vs. SHE) \qquad (2\text{-}4)$$

Cathode:

$$O_2 + 4H^+ + 4e^- \xrightarrow{Pt} 2H_2O \quad E_{r,c} = E^0{}_c - \frac{RT}{4F}\ln\left(\frac{1}{a_{H^+}{}^4 \, a_{O_2}}\right); \; E^0{}_c = 1.23 \, V \; (vs. SHE) \qquad (2\text{-}5)$$

Overall:

$$2H_2 + O_2 \xrightarrow{Pt} 2H_2O \quad E_{r,cell} = E_{r,c} - E_{r,a} = E^0{}_{cell} - \frac{RT}{2F}\ln\left(\frac{1}{a_{H_2} \, a_{O_2}{}^{0.5}}\right); \; E^0{}_{cell} \; 1.23 \, V \; (vs. SHE)$$

$$(2\text{-}6)$$
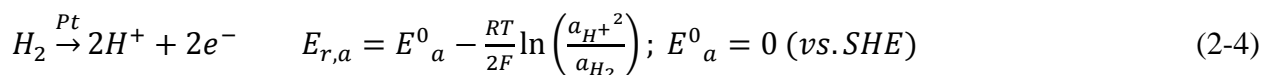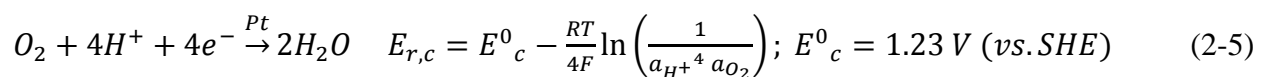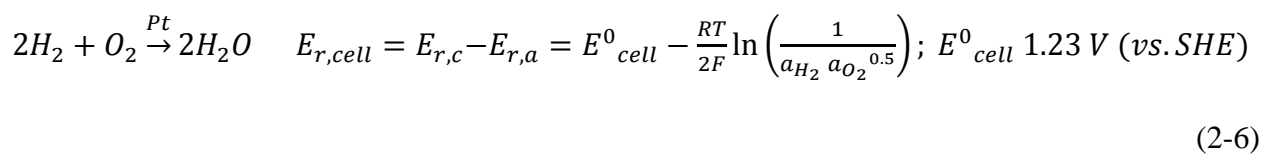
In reality, however, the fuel cell voltage is less than that of given by Equation 2-6. The fuel cell performance is associated with irreversible losses. These are activation, ohmic and mass transport losses.

2.2.1 Activation loss

Some portion of the voltage generated by any fuel cell is dedicated to drive the electrochemical reactions on the surface of the electrodes. It makes sense that activation losses are dominant in low current densities. The Tafel equation models the activation loss for an electrode as

$$\Delta V_{act} = a \ln \left(\frac{i}{i_0}\right) \tag{2-7}$$

, where i= current density (A cm^{-2}), i$_0$= exchange current density (A cm^{-2}), and a is a constant.

In thermodynamic equilibrium, the forward and reverse current densities are equal in a way that the net current density is zero. Therefore, one can say i$_{forward}$ = i$_{reverse}$= i$_{equilibrium}$. This very small dynamic equilibrium current density (i$_{equilibrium}$) is known as the exchange current density (i$_0$) (O'Hayre *et al*., 2006). Different reactions in the presence of different catalysts exhibit different exchange current densities. For example, at standard conditions, the exchange current density for the hydrogen oxidation reaction at the surface of Pt in an acidic environment is 10^{-3} A cm^{-2}, whereas for the oxygen reduction reaction this value is 10^{-9} A cm^{-2} (Vielstich *et al*., 2003).

2.2.2 Ohmic loss

In middle current densities, the dominate source of the loss is migration of ions and electrons within the membrane and through the external circuit, respectively. This causes a drop in voltage and this loss is estimated by Equation 2-8.

$$\Delta V_{ohmic} = iR_{ohmic} = i(R_{elec} + R_{ionic}) \tag{2-8}$$

2.2.3 Mass Transfer loss

At higher current density, the performance of a fuel cell is mainly limited by mass transport of reactants to the electrodes. Mass transfer limitation (fuel cell concentration loss) is given by Equation 2-9 (O'Hayre *et al*., 2006).

$$\Delta V_{conc} = c \ln \left(\frac{i_L}{i_L - i}\right) \tag{2-9}$$

, where c is a constant and i_L is known as the limiting current density of a fuel cell. The limiting current density is the full potential of a fuel cell in generating the highest possible current density. At this point, the dominant source of current limitation is feeding the active electrochemical sites with fuels. Consequently, this current is mostly limited to mass transfer of reactants within the fuel cell. The limiting current density is expressed as

$$i_L = nFD^{eff} \frac{C_R{}^0}{\delta} \tag{2-10}$$

, where n is the number of electrons generated or consumed by the reaction; F is the Faraday constant C mole^{-1}; D^{eff} is the effective reactant diffusivity within the catalyst layer m^2 s^{-1}; C$_R{}^0$ is the bulk (flow channels) reactant concentration mole L^{-1}; δ is the electrode (diffusion layer) thickness m.

Considering all the losses, one can model the net voltage generated by a fuel cell as:

$$V_{cell} \equiv E_{cell,r} - losses = E_{cell}^0 - \frac{RT}{2F} \ln \frac{1}{[H_2]^2[O_2]} - \Delta V_{act} - \Delta V_{ohmic} - \Delta V_{conc} \tag{2-11}$$

On this basis, current density- voltage (i-V) measurement is used to quantify the overall electrochemical performance of a fuel cell system. It represents the behavior of a fuel cell in a full range of current densities. An i-V curve consists of three regions that each represents the influences of special limitations on the system performance. Figure 2-2 shows a typical i-V curve that could be obtained from a fuel cell. As seen, there are three regions: activation loss, ohmic and mass transfer loss. Each of these regions represents the dominant source of overvoltage in the system working under specific range of current density.
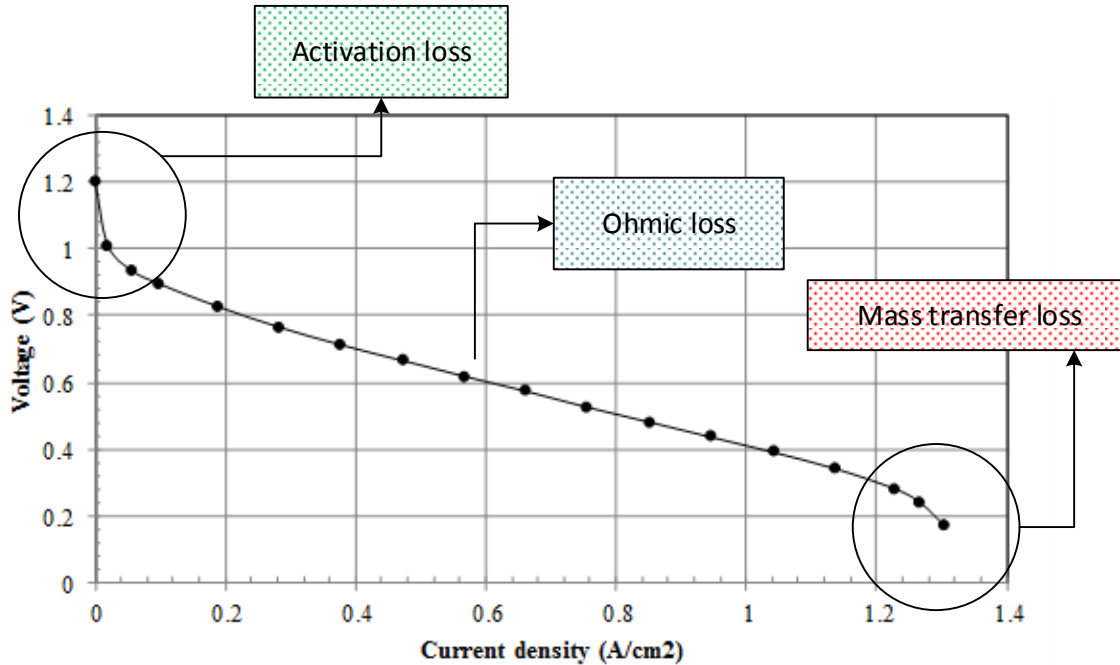
Figure 2-2 A typical i-V curve obtained in a fuel cell

2.2.4 Fuel Cell Efficiency

The efficiency of a fuel cell in reversible conditions is given as

$$\varepsilon_{th} = \frac{\Delta G}{\Delta H} \tag{2-12}$$

Equation 2-12 tells us that efficiency of a fuel cell, even under reversible conditions, does not reach 100% because usually $\Delta G < \Delta H$ ($\Delta G = \Delta H - T \Delta S$). This is known as the reversible loss and the efficiency of the Carnot cycle is a well-known example of that. Considering thermodynamic reversible effects, irreversible losses and losses in fuel supply, the fuel cell efficiency in practice is given as

$$\varepsilon_{real} = \left(\frac{\Delta G}{\Delta H}\right)\left(\frac{V_{cell}}{E_{cell,r}}\right)\left(\frac{i/nF}{v_{fuel}}\right); \ v_{fuel} = rate \ of \ fuel \ supply \ (mol/s) \tag{2-13}$$

Equation 2-13 shows that by increasing the V_{cell} (V_{real}), the fuel cell efficiency will also increase.

2.3   Fundamentals of the BioGenerator

2.3.1 Idea

The idea behind the invention of the BioGenerator was to eliminate the cost and sluggish kinetics associated with the oxygen reduction reaction in PEMFCs. In fact, the BioGenerator tries to use the capability of microorganisms in the sustainable regenerative production of oxidants for the reduction reaction in conventional fuel cells (Karamanev *et al.*, 2013). Therefore, it is considered the first biologically based technology for H_2-to-electricity conversion that is capable of being employed as part of the intermediate energy storage in renewables grid.

2.3.2 Structure and Reactions

Hydrogen is the preferable fuel for the anode of the BioGenerator. Through a catalytic oxidation reaction, hydrogen is electrochemically split into protons and electrons (Equation 2-14). We know that electricity is the flow of electrons. Therefore, on the other side of the electrical circuit, a reaction is needed to consume these generated electrons. Ferric ions (Fe^{3+}), the oxidants, are responsible for consuming these electrons in the BioGenerator and helping the anodic reaction produce more electrons so we can have more electricity. Simply on the surface of graphite felt, ferric ions accept electrons and are converted to ferrous ions (Fe^{2+}) (Equation 2-15). The formed ferrous ions flow to a bioreactor, where through a microbial reaction, are oxidized back into ferric ions, and in doing so, the bioregenerative cycle of the oxidant supply to the fuel cell is completed (Equation 2-16 and Figure 2-3).

$$H_{2\,(g)} \xrightarrow{Pt} 2H^+{}_{(aq)} + 2e^- \tag{2-14}$$

$$2Fe^{3+}{}_{(aq)} + 2e^- \rightarrow 2Fe^{2+}{}_{(aq)} \tag{2-15}$$

$$2Fe^{2+}{}_{(aq)} + 2H^+{}_{(aq)} + 1/2O_{2\,(g)} \xrightarrow{iron\ oxidizing\ bacteria} 2Fe^{3+}{}_{(aq)} + H_2O_{\,(l)} \tag{2-16}$$
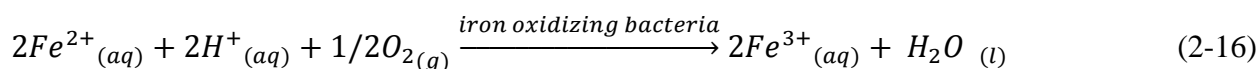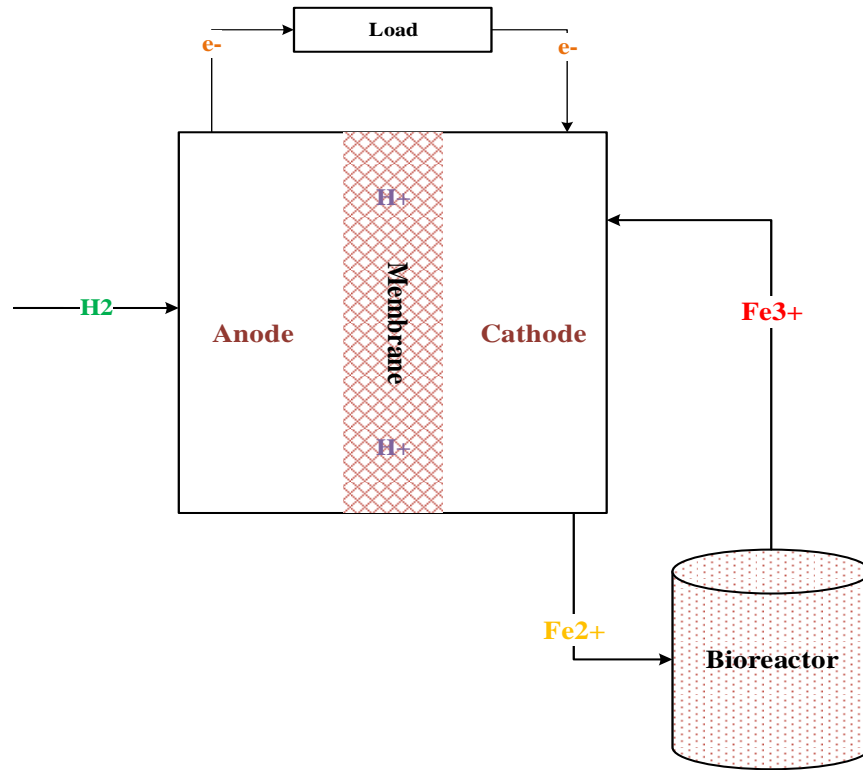
Figure 2-3 Scheme of the BioGenerator system

Based on the Nernst equation (Stock and Omra 1989), the reversible half-cell potentials and the total reversible voltage of the BioGenerator are given as (Hojjati *et al.*, 2013)

Anode: $\qquad E_{r,a} = E^0{}_a - \frac{RT}{2F}\ln\left(\frac{a_{H+}{}^2}{a_{H2}}\right)$ $\qquad\qquad\qquad\qquad\qquad\qquad\qquad$ (2-17)

Cathode: $\qquad E_{r,c} = E^0{}_c - \frac{RT}{2F}\ln(\frac{a_{Fe2+}{}^2}{a_{Fe3+}{}^2})$ $\qquad\qquad\qquad\qquad\qquad\qquad\qquad$ (2-18)

Overall: $\qquad E_{r,BioGen} = E_{r,c} - E_{r,a} = E_{r,BioGen}{}^0 - \frac{RT}{2F}\ln(\frac{a_{Fe2+}{}^2\, a_{H+}{}^2}{a_{Fe3+}{}^2\, a_{H2}})$ $\qquad\qquad\qquad$ (2-19)

2.3.3 Bipolar Plate (BPL)

In the BioGenerator, bipolar plates serve as dispensers for the reactant gas in the anode, and the liquid electrolyte in the cathode (Figure 2-4). They also separate mechanically the anode from the cathode. Here, the general features of bipolar plates will be discussed based on PEMFCs.

BPLs function as an electrical conductor, and help manage heat conduction and water convection within the fuel cell stack (Hermanna *et al*., 2003). They also provide structural support for the whole stack. In view of these functions, properties such as good electrical and thermal conductivity, corrosion resistivity and mechanical stability are among those that a bipolar plate must meet (de Waalb *et al*., 2003; Hermanna *et al*., 2003). Taking into account these factors, bipolar plate can be among the most critical component of a fuel cell stack. This is true to the extent that bipolar plates can account for about 40% of the cost and 80% of the total weight of a stack (Brady *et al*., 2004). In terms of conductivity, metallic materials such as gold, having an electrical conductivity of 45000×10^3 S/cm; Fe alloys, 5300×10^3 S/cm; Ti, 2400×10^3 S/cm with higher electrical conductivity as compared to materials like carbon-polymer composites, ~ 1 S/cm and graphite 10^3 S/cm, are prime choices (Steele and Heinzel 2001). In addition, since the graphite is normally porous, in order to prevent the crossover of reactants, a binder or resin is added to decrease its porosity (Steele and Heinzel 2001). Furthermore, plates are usually machined to make channels and these channels carry the reactant gases from the inlet all the way to the outlet of the plates (Cunningham *et al*., 2007). The configuration of channels such as depth and width as well as the flow field pattern have a large impact on how reactants are distributed across the electrodes, where they take place in the oxidation or the reduction reactions (Li and Sabir 2005). For example, in a patent, an increase of 50% in performance was obtained through optimizing only the flow field network and the reactant gases distribution fields (Watkins *et al*., 1992). Currently, different flow field designs are used in fuel cell research (Figure 2-5). The parallel and the serpentine, however, are the most widely-used designs. The former configuration is simple to make, has lower pressure drop between inlet and outlet, and more uniform distribution of reactant gases over the surface of the electrodes. However, one drawback of the parallel flow field is its higher susceptibility to be blocked by liquid water. However, due to the structure of the serpentine flow field, a higher gas flow rate can push the liquid water out of the channels more easily than in the case of parallel channels (Hongthong *et al*., 2007, Li and Sabir 2005).

All in all, bipolar plates are crucial for a fuel cell stack and extensive research is being undertaken to come up with a suitable design for flow channels as well as optimum chemical compositions that meet targeted durability, mechanical stability, electrical and thermal conductivity. For the BioGenerator, one of the challenges is the design of chemically durable

plates with flow fields for the cathode side, since there is highly corrosive liquid coming from the bioreactor, flowing in the cathode side bipolar plate channels.
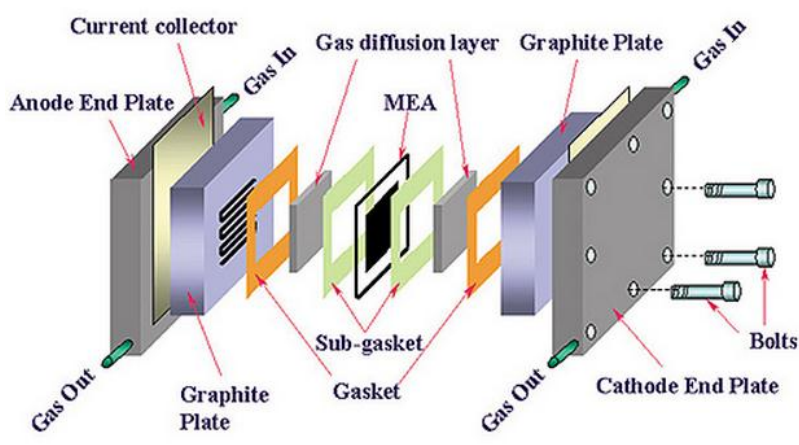
Figure 2-4 A complete scheme of a fuel cell system. Graphite plates refer to bipolar plates in this picture (Scientific Computing World 2003)
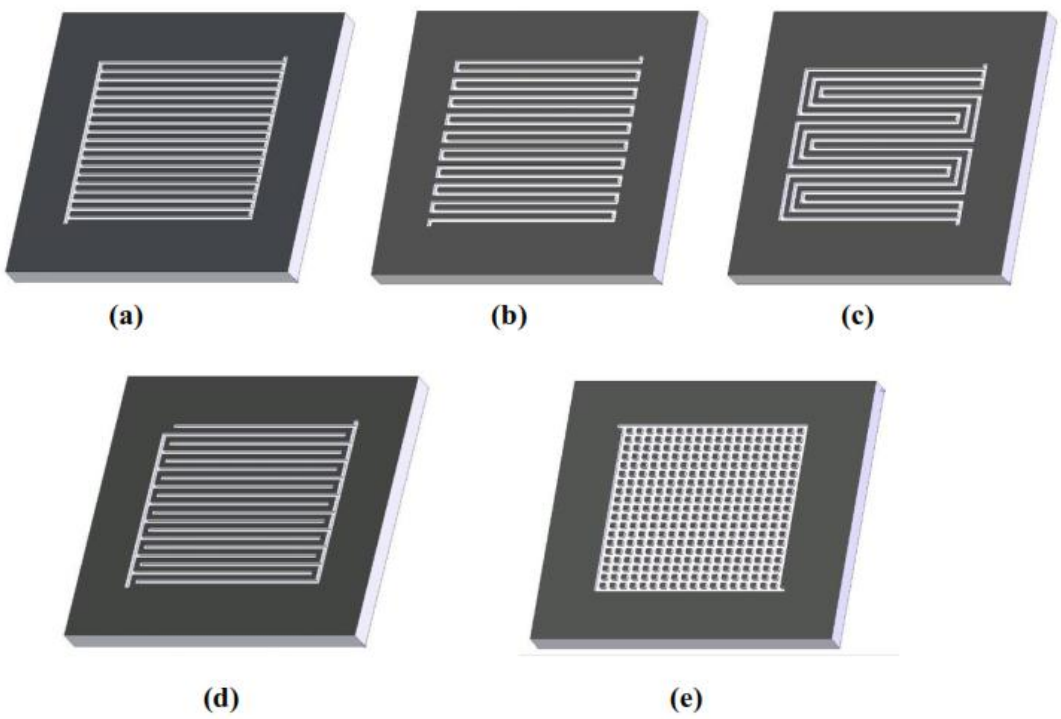
Figure 2-5 Different flow field configurations: a) parallel, b) serpentine, c) parallel-serpentine, d) interdigitated, e) pine or grid type (Karimi 2011)

2.3.4 Gas Diffusion Layer (GDL)

The GDL in the BioGenerator is used at the hydrogen anode electrode. Here, as a baseline, discussions begin with the role of GDLs in conventional PEM fuel cells. The anode and cathode conventionally consist of two layers. The first faces the bipolar plates and is called the Gas Diffusion Layer (GDL) and the second faces the membrane and is known as the Catalyst Layer (CL). A GDL is a carbon-filled porous media composed of two sub-layers. A macro-porous substrate (the backing layer) is the first sub-layer that serves as a mechanical support as well as a conductor for electrons flowing between the catalyst layers and bipolar plates. The backing Layer (BL) also facilitates gas and liquid mass transport within the GDL (Figure 2-6). Often to enhance mass transfer and to provide better electrical contact between the BL and the CL, a very thin sub-layer known as the Micro-Porous Layer (MPL) is formed on the top of the BL and usually contains carbon particles mixed with binders such as Polytetrafluoroethylene (PTFE) or/and a sulfonated tetrafluoroethylene-based-fluoropolymer ionomers such as Nafion. When flooding is an issue, carbon particles are impregnated with PTFE and if the GDL suffers from drying, Nafion usually is the option. Sometimes to obtain higher porosity, a pore-forming agent such as Li_2CO_3 or ammonium carbonate is added to the MPL.

1 Anode backing layer

2 Anode micro-porous layer

3 Anode catalyst layer

4 Nafion membrane

5 Cathode catalyst layer

6 Cathode micro-porous layer

7 Cathode backing layer
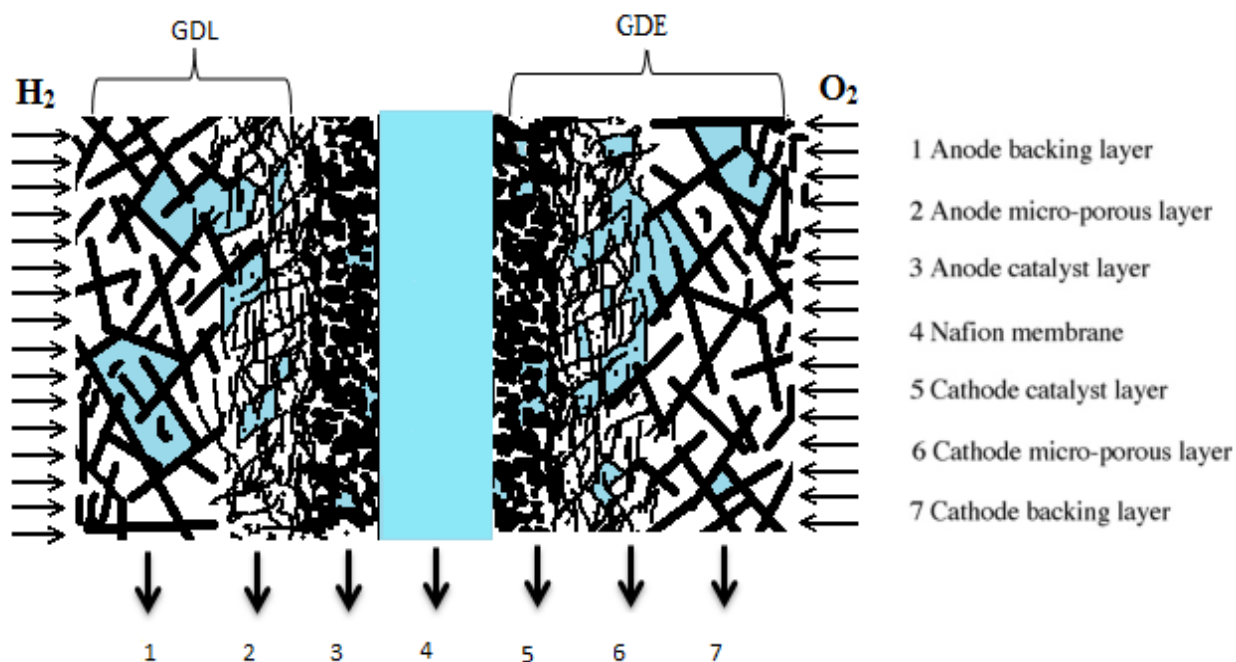
Figure 2-6 A schematic picture of a seven layer Membrane Electrode Assembly (MEA)

2.3.4.1   Backing Layer (BL) and Mass Transport

As already mentioned, the GDL is often constructed of two sub-layers; the BL and the MPL. The BL is usually made of carbon cloth or paper. Carbon paper structure is very random (non-woven), while cloth consists of an orderly network of fibers (woven). Figure 2-7 shows microscopic images of these materials.
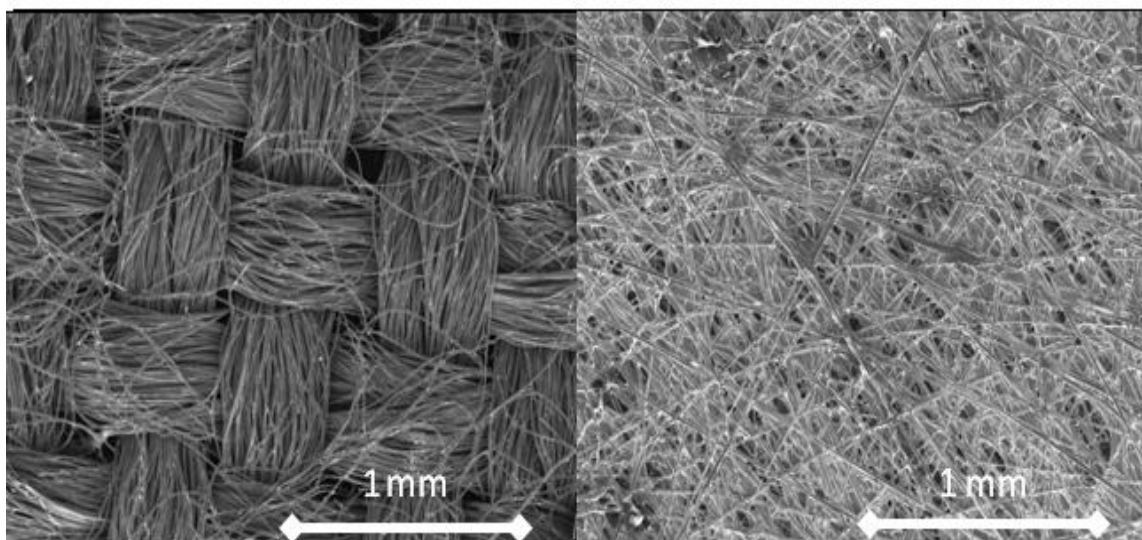
Figure 2-7 Microscopic pictures of left) carbon cloth and right) carbon paper (FuelCellEtc 2013)

The thickness of the BL is an important parameter. A thinner BL has lower electrical resistance plus the gaseous reactants can move easily, but it is not preferable since having smaller pore volume can cause water flooding. For example, the optimal thickness for a carbon paper is between 275- 370 µm. The backing layer is usually treated with a hydrophobic polymer such as PTFE or FEP to enhance liquid water transport. The same trend is valid for PTFE. Too low of a PTFE will cause liquid flooding while too high of a PTFE content will increase the electrical resistivity as well as decrease the gas permeability due to decreasing pore volume. In one study, different GDLs impregnated with 10 to 40 wt.% PTFE were prepared, where 10% gave the best performance for PEMFCs (Lim and Wang 2004). It is generally agreed that higher pore volume will enhance mass transfer. In addition to the total porosity, pore size distribution is a crucial element that plays an important role in controlling mass transfer properties within the GDL.

Kong *et al* (2002) defined the distribution of pores in their GDLs (treated carbon cloths) based on pore diameter in three zones: micro-pores (0.03- 0.06 µm), meso-pores (0.06- 5.0 µm), and macro-pores (5.0- 20 µm). Their experiments with different levels of humidity showed that the distribution of pore size is a more crucial morphological factor in controlling mass transport than total porosity. They concluded that macro-pores in the BL could prevent flooding better and lead to a higher performance in PEMFCs (Kong *et al*., 2002).

2.3.4.2   MPL and Mass Transport

In addition to the BL, the MPL plays a dominant role in the performance of a fuel cell. The MPL is a micro-porous layer consisting of carbon particles and a hydrophobic binder such as PTFE. The role of the MPL is to 1- provide micro-size paths of pores (between 0.01–0.05 μm in diameter) resulting in better mass transfer 2- provide better mechanical compaction and electrical contact between the BL and the catalyst layer. Like the BL, in the MPL also, the amount of PTFE can influence the performance. Park *et al* (2008) investigated the amount of PTFE in the MPL on the performance of PEMFCs, where it was altered from 10 wt.% to 40 wt.%, and the best performance was obtained when the PTFE content occupied only 20 wt.% of the MPL loading. Increasing PTFE, especially in high current densities, decreases the chance of blocking pores by water droplets, enhancing liquid mass transport, which can result in better cell performance.

The carbon loading can influence the performance of the MPL as well. A low carbon loading is not desirable because it can cause flooding in the MPL, whereas too much carbon will increase the diffusion resistance of the gaseous reactant within the GDL. Usually a loading of 1.5- 2.0 mg cm^{-2} is selected for the MPL of PEMFCs. Park *et al* (2006) changed the carbon loading in their MPL from 0.2 to 2.0 mg cm^{-2} and observed that the best performance (air as the oxidant) was obtained with the micro-porous layer loaded with 0.5 mg cm^{-2} (Park *et al*., 2006).

Recently, there has been growing interest towards controlling the properties of the MPL such as porosity, electrical conductivity, and hydrophobicity, by selecting different carbon materials. Passalacqua *et al* (2001) studied various kinds of carbon in the MPL and their results showed that Acetylene Black (ASB) could exhibit the best performance in a PEM fuel cell as compared to others. They state that it was due to the highest pore volume and lowest average pore diameter

of ASB (Passalacqua Squadrito *et al*., 2001). In another study conducted by Priyanka *et al* (2008), the influence of pore size distribution of different carbon papers prepared by various laminates on performance of a PEM fuel cell was examined. Results show a better performance was achieved when pore size distribution mostly fell in the range of 30- 50 μm (Priyanka *et al*., 2008). For example, Black Pearls 2000 has larger pore volume (2.67 cm^3 g^{-1}) than Acetylene Black (0.23 cm^3 g^{-1}). Wanga et al (2006) proposed a high efficiency MPL of composite carbon black consisting of 20 wt.% Black Pearls 2000 (Cabot Corp, Boston, Mass.) and 80 wt.% Acetylene Black. That team rationalized that presence of a large number of hydrophobic meso-pores (0.05– 7.0 μm) is essential for ensuring a reliable liquid mass transport (Wang *et al*., 2006).

2.3.4.3   GDL and Electrical Conductivity

The electrical conductivity of a GDL is usually measured in two directions: through (cross-) plane and in plane. Since PTFE is a non-conductive polymer, the conductivity of the GDL drops by adding PTFE. Ismail *et al* (2010) investigated the effect of the PTFE-treatment of different backing layers and MPLs on the electrical conductivity of the GDL. They concluded that through-plane conductivity decreased as PTFE content increased in both the backing layer and the MPL. However, the conductivity of the BL for in-plane directions remained almost constant, and the reason for this was that the structure of carbon fibers is fixed and does not change with change in PTFE. The in-plane conductivity of the MPL, on the other hand, decreased as PTFE content increased (Ismail *et al*., 2010). In Xua *et al* (2007) experiments, PTFE loading in the cathode GDL of a direct methanol fuel cell was the subject of a study and it was found that 40% PTFE is optimal (Xua *et al*., 2007).

2.3.4.4   GDL- Summary

Overall, the GDL serves some very important roles including mechanical support for the catalyst layer, electrical conductor for electrons reaching or leaving the catalyst layer, and enhancement of gas and liquid transport. The fulfillment of each of these functions requires special modifications and often improving one will cause a decline in the others. Therefore, whenever each function needs to be improved, the impact of any changes must be checked with the functionality of the others. In the systems suffering from flooding, the treatment of the backing

layer to an extent that does not affect the electrical conductivity, the fuel permeability, and also the lamination of a micro-porous layer on that backing layer are often the options chosen. Adding a hydrophobic polymer like PTFE to both the BL and the MPL is a crucial step. However, the thickness of the backing substrate, type of the carbon materials, their loading, and the content of PTFE all have to be also considered thoughtfully.

2.4   A Brief Assessment of Flooding Management in Similar Hydrogen-Based Systems

2.4.1 Alkaline Fuel Cells

The anode and the cathode fuels in AFCs are usually the same as those in PEMFCs. However, the difference is in the electrolyte. The electrolyte in AFCs is an aqueous alkaline solution such as 30% KOH. The anodic and the cathodic reactions are (O'Hayre *et al*., 2006):

Anode: $2H_2 + 4OH^- \rightarrow 4H_2O + 4e^-$ (2-20)

Cathode: $O_2 + 2H_2O + 4e^- \rightarrow 4OH^-$ (2-21)

Overall: $2H_2 + O_2 \rightarrow 2H_2O$ (2-22)

AFCs operate at temperatures around 90- 100 ℃. Water is the byproduct of the anodic reaction and removed by evaporation through recirculating of the electrolyte (De Geeter *et al.*, 1992). The AFCs initially used in space applications (the Apollo project) were operating at 80- 149 ℃ and pressures between 29 psig to 299 psig, while in the atmospheric applications, they operate at 1.0- 3.0 psig and 40- 75 ℃ (McLean *et al.*, 2002). The electrodes are usually fabricated by coating a hydrophobic catalyzed layer onto a surface of a GDL and then these two layers are laminated onto the surface of a porous metallic baking layer to form a three-layer electrode. The catalysts used for the anode electrode are Pt or Pd (0.12- 0.5 mg cm^{-2}), Ni and Ag. Although using Ni and Ag as the catalyst reduces the manufacturing cost, it will make the electrode degradation faster because the electrolyte is highly corrosive (Gülzow 1996).

2.4.2 Phosphoric Acid Fuel Cells

The reactions in phosphoric acid fuel cells (PAFCs) are the same as those in PEMFCs. However, the difference is that the electrolyte in PAFCs is composed of phosphoric acid (H_3PO_4). The operating temperature is 150- 200 ℃. The phosphoric acid electrolyte is maintained in between a

0.1- 0.2 mm silicon carbide (SiC) matrix (Larminie and Dicks 2003). PAFC electrodes are usually made of a hydrophobic binder such as PTFE and Pt/C as the catalyst. PTFE content in the catalyst layer is varied between 20- 40 wt.%.

2.4.3 Immersed-Tank Electrowinning

Electrowinning or electroextraction is referred to the process of extracting metals from their ores via metal electrodeposition (Free, *et al.* 2012). In a patent (Allen *et al.* 1994), hydrogen anodes immersed in a tank containing zinc sulfate ($ZnSO_4$) were used as the electron generator in a zinc electrowinning system.

Cathode: $Zn^{2+}_{(aq)} + 2e^- \rightarrow Zn_{(s)}$ (2-23)

Anode: $H_{2(g)} \rightarrow 2H^+_{(aq)} + 2e^-$ (2-24)

A three-layer hydrogen anode electrode was made as shown in Figure 2-8.
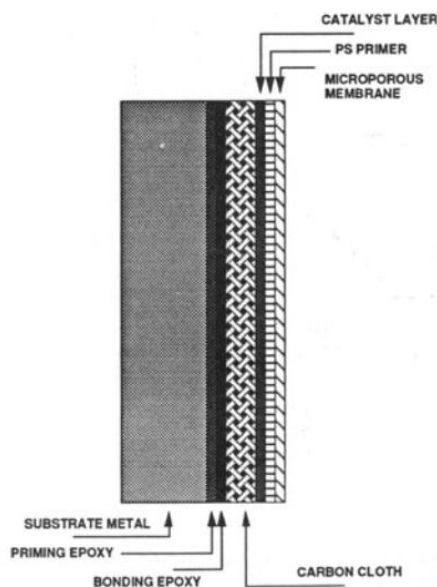
Figure 2-8 Scheme of an immersed hydrogen electrode used in zinc electrowinning (Allen *et al.*, 1993)

A catalyst layer composed of platinum and PTFE as the binder was coated onto the surface of a thick (1.6 mm) tightly woven graphite-fiber cloth. Furthermore, a polysulfone adhesive layer was placed in between a porous membrane (Celgard®) and the electrode, in order to bind the catalyst layer and the membrane better together. The electrolyte penetrated to the catalyst layer through the membrane but did not flood the catalyst layer.

2.5 Summary

By looking into the fuel cell systems that employ liquid electrolytes, one can conclude that the effort has been to prevent the flooding of the gas-fed electrodes by making them hydrophobic, employing multilayer gas diffusion electrodes to enhance mass transfer, and/or making some configurations to prevent penetration of the electrolyte into the electrodes. The idea of making GDLs hydrophobic is to hinder water immovability in pores structure and is usually achieved by impregnation of the backing layer by PTFE and/or adding PTFE to the MPL ink. In addition, porosity can be controlled by altering hydrophobicity content, carbon material, curing temperature, and compression of the GDL and so on. For better mass transport in the GDL, the effort should be in providing an ideal path structure for gas to flow evenly through the GDL and liquid to move easily within the GDL. The fundamentals of two-phase transport in the gas diffusion electrode is the same, either for liquid electrolyte fuel cells or polymer electrolyte fuel cells. Therefore, PEMFCs, as the most developed and well-studies types of fuel cell are good baselines to begin with in order to understand water management in the BioGenerator system. From the perspective of patterning the electrode fabrication, in the first observation, the problem of flooding in some of the liquid electrolyte fuel cells such as PAFCs or AFCs looks very similar to the BioGenerator. However, one should take it to account that the operating conditions and configurations and the electrolyte nature of those fuel cells are quite different from the BioGenerator's. As such, PAFCs operate at relatively high temperatures (150- 200 ºC) and this factor, to a notable level, helps evaporation of liquid penetrated into the gas diffusion electrodes. For example, Hydrogen-based electrowinning employs a very thick GDL that in the case of the BioGenerator could decrease the performance due to high electrical resistivity. Therefore, because of the unique configuration and operating conditions of the BioGenerator, based on the information from other types of fuel cells, research conducted to develop electrodes that could meet the performance requirements of the BioGenerator.

3 Materials and Methods

3.1 Anode Electrodes

3.1.1 Preparation of the Backing Layer (BL)

As mentioned earlier, anode electrodes were composed of three layers; the backing layer (BL), the micro-porous layer (MPL), and the catalyst layer (CL). Untreated carbon cloths and papers were hydrophobized by impregnation in 30 wt.% PTFE dispersion (DuPont Teflon®). In order to vaporize the remaining emulsifiers, the treated materials were heated in oven for 10 minutes at 270 ºC. Toray T-120 and CC4 Plain (Fuel Cell Earth LLC) were used as carbon papers and cloths, respectively.

3.1.2 Preparation of the Micro-porous Layer (MPL)

To enhance mass transfer, mechanical adhesion, and electrical contact between the BL and CL, a thin layer composed of carbon and PTFE was laminated on top of the BL. A dense ink of carbon powders (Vulcan XC72) and PTFE with isopropyl alcohol as the solvent was mixed ultrasonically for five minutes and then laminated onto the surface of BLs using a height-adjustable blade-contained apparatus (spreading technique). To obtain better compaction, prior to the baking, the prepared GDLs were hot pressed at 80 ºC under 100-psi pressure for 15 seconds The prepared gas diffusion layers (GDLs) were cured in oven for 2 hours at 345 ºC. Total loading of MPLs were 1.5 ± 0.17 mg cm^{-2} with 30 wt.% content for PTFE.

3.1.3 Preparation of the Catalyst Layer (CL)

There are four conventional widely used ways plus three comparatively new methods mostly employed on lab scale, each of which has relative advantages and disadvantages in terms of practice and fundamentals. The four are brushing, spreading, spraying, and screen printing while the three are electrodeposition, catalyst powder deposition, and sputtering.

In conventional methods, catalyst ink is directly applied onto the surface of the GDL. Catalyst ink is referred to a mixture of Pt/C particles and a binder (often PTFE or/and Nafion) that is uniformly mixed with the help of a solvent. Depending on the required degree of viscosity, different solvents such as glycerol, isopropanol, or normal-butyl acetate might be employed.

3.1.3.1   Brushing

In brushing (painting) method, a wet mixture of catalyst and binder is directly applied onto the surface of the GDL with a paintbrush (Figure 3-1). For better paintability, a higher viscous solvent like glycerol is usually used. Painting (brushing) seems to be easy and low cost, but the problem associated with this method is its non-uniformity that will result in lack of reproducibility and uniformity. In addition, it will require art and can be very time consuming for large-scale production of electrodes. When PTFE is the binder, often for achieving three-phase contact in the electrode, a thin layer of Nafion solution will be brushed onto the surface of the GDE. The catalyst layer together with the GDL makes the gas diffusion electrode (GDE). The former is named ionomer impregnation or Nafion post-coating. The Nafion post-coting was not used in this study because the lowest possible degree of hydrophilicity was desired.

Pt/C+PTFE+ Solvent
(Catalyst Ink)
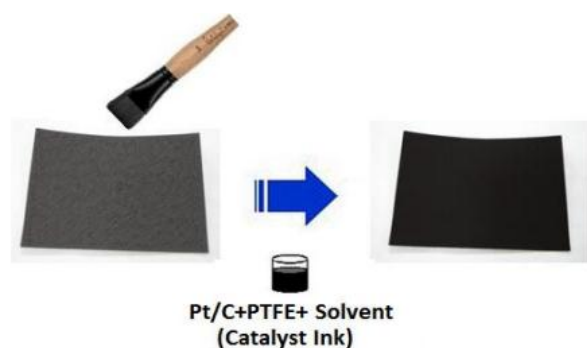
Figure 3-1 Scheme of brushing method

3.1.3.2   Spraying

In the case of spraying, a mixture of Pt/C and ionomer is sprayed (usually using an airbrush apparatus) onto the surface of the GDL (Figure 3-1). It is obvious that less viscous mixture is required for spraying. The benefit of this method is its ease of use, being fast and eventually you could fabricate a very thin and uniform layer of catalyst. However, one drawback of spraying is that due to its watery (thin) structure, the ink, to some extent, will penetrate into the GDL and decrease the catalyst utilization. Furthermore, this may possibly cause flooding in the GDL if the ink is hydrophilic.

Figure 3-2 Badger Airbrush Co 150-5-PK Professional used to apply the catalyst layer onto the surface of the GDL

3.1.3.3 Spreading

Spreading, on the other hand, is a widely used method for the CL lamination, in which with help of an adjustable blade-contained apparatus or a heavy stainless steel cylinder, a paste of catalyst mixture is applied onto the surface of the GDL. One drawback of this technique is that most probably a thin solution cannot be used because it has to be in paste form. However, it has two advantages to other methods: it can give a uniform and reproducible catalyst layer and a good control over the thickness of the CL. Beside all; it is a suitable option for large scale of electrode production.

Figure 3-3 Knife spreader (Mitutoyo, TQC Co.) used in this study to laminate MPLs and CLs. Height of the knife is adjustable to obtain different uniform thicknesses

3.1.3.4 Catalyst Coating

In all the mentioned methods, catalyst layers loaded with 40 wt.% PTFE and 0.5± 0.08 mg Pt cm^{-2} (Platinum, nominally 40% on carbon black; Alfa Aesar Company) were laminated on MPLs using painting, spraying, or spreading techniques. The catalyst ink was a hydrophobic composition of Pt/C particles and PTFE powder. First, the catalyst powder was soaked with a

few drops of distilled water, then isopropyl alcohol was added, and the entire solution was mechanically mixed for 30 minutes. After that, the PTFE powder was added to the mixture and followed by mixing for at least 30 minutes until a viscous ink formed. To obtain better compaction, prior to the baking, the prepared GDLs were hot pressed at 80 ºC under 100-psi pressure for 15 seconds. The prepared catalyst layers (CLs) were cured for 2 hours at 345 ºC to ensure all the PTFEs were melted within the structure of the CL and bound the carbon particles together. The ink for spreading and painting comprised a dense mixture, while for spraying a diluted ink was prepared.

3.1.3.5   Electrodeposition

Electrodeposition is a technique performed under either DC or pulse current. The advantage over pulse-electrodeposition is that it will allow us to control the growth of metal ion clusters that will enable us to produce very small catalyst particles and a high surface area. In addition, due to the presence of the ionomer (e.g. Nafion) on the surface of the GDL, metal ions will sit on places where ionomer is present, and it can ensure a good number of catalyst particles deposited near regions both ionic and electronic pathways are present (Kim and Popov 2004; Kim *et al.,* 2004; Summer *et al.*, 1998 Rao and Trivedi 2005). In addition to electrodeposition, sputtering method is capable of fabricating very thin layer of catalyst layer (~10 nm) and loading as low as 0.04 mg cm^{-2} as compared to the state-of-art methods with loading in neighborhood of 0.4 mg cm^{-2} (O'Hayre *et al.*, 2002).

For the fabrication of the BioGenerator anode electrode, platinum electrodeposition was tested to coat a layer of catalyst particles onto the surface of a hydrophobic GDL. 0.1 M Pt $(NH_3)_4Cl_2$ was used as the electrolyte solution containing platinum ions. Different constant and pulse current densities ranging from 20 mA cm^{-2} to 400 mA cm^{-2} were employed using different duty cycles. (karimi and Foulkes 2012). However, no platinum deposition was obtained and the reason might be the absence of the ionomer on the surface of the MPL to help exchange platinum ions on the surface of the MPL. Figure 3-3 illustrates the working configuration of the electrodeposition method used in this study.
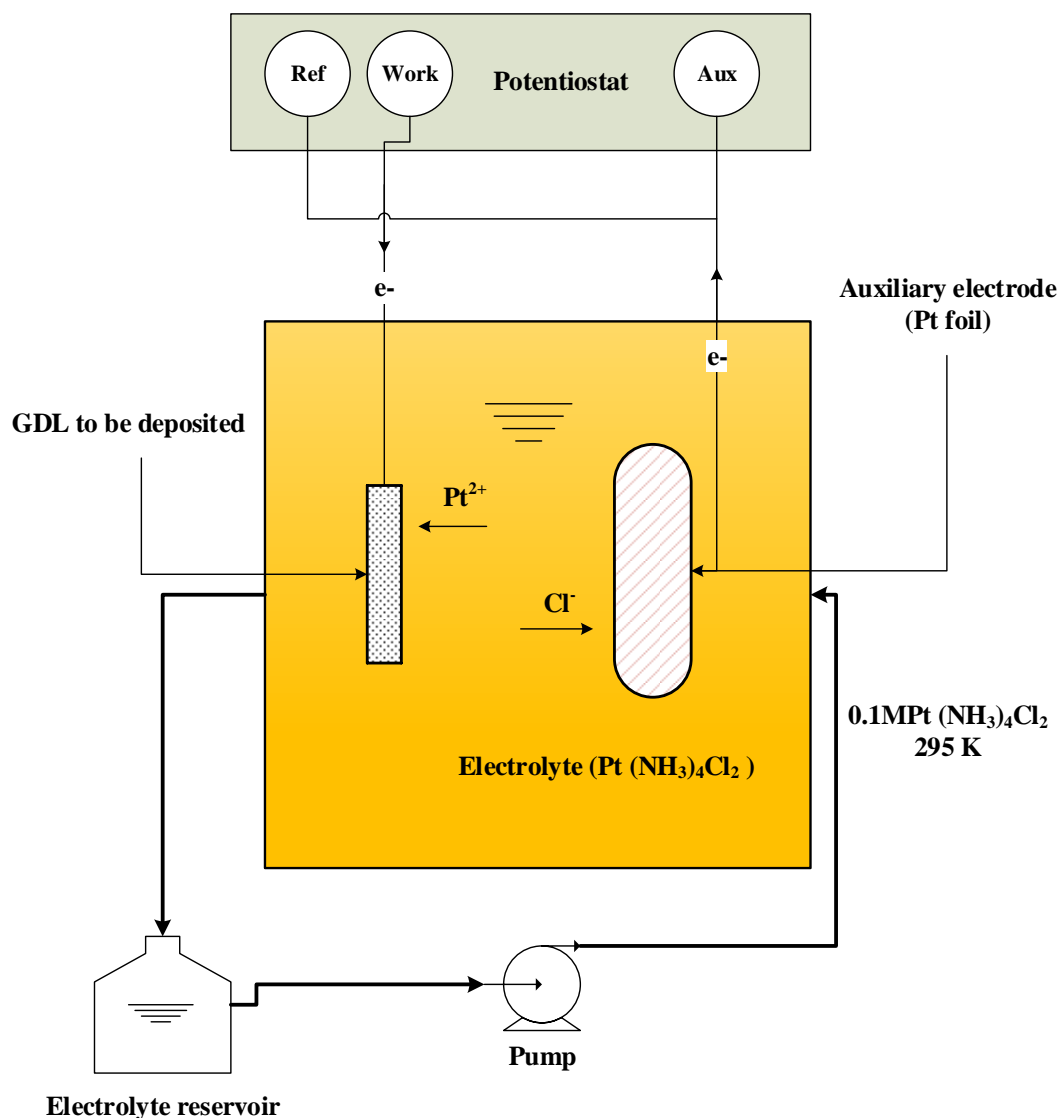
Figure 3-4 Illustration of the continuous flow Pt- electrodeposition system. 0.1 M Pt (NH$_3$)$_4$Cl$_2$ was used as the electrolyte, and the electrodeposition bath volume was 15 mL.

3.2 Flow Fields, Cathode and Membrane

As a fuel cell, the BioGenerator uses a fuel and an oxidant. The anode fuel is hydrogen gas and the cathodic oxidant is the solution of ferric ions coming from the bioreactor. Graphite plates were machined using CNC (Computer Numerical Control) milling machine. For smaller cells (5 cm^2), a serpentine structure (Figure 2-5-b) was chosen for both the gas and the liquid side. However, for larger area (400 cm^2), to help the back-diffused water exit the anode channels more easily, a parallel serpentine flow field with narrow channels was proposed (Figure 2-5-c) for the gas side. On the other hand, parallel flow fields (Figure 2-5-b) with wider channels were

proposed for the liquid side. The reason of using parallel flow field in the liquid (cathodic) side was to avoid pressure drop and more uniform distribution of the oxidant concentration in the cathode. The depth and width of channels for the gas side were 2 mm and 1.5 mm, while the depth and width of channels for the liquid side were 2.5 mm and 3 mm, respectively.

Figure 3-4 shows picture of bipolar plates fabricated for 10 kW BioGenerator fuel cells having active area of about 20cm by 20cm.
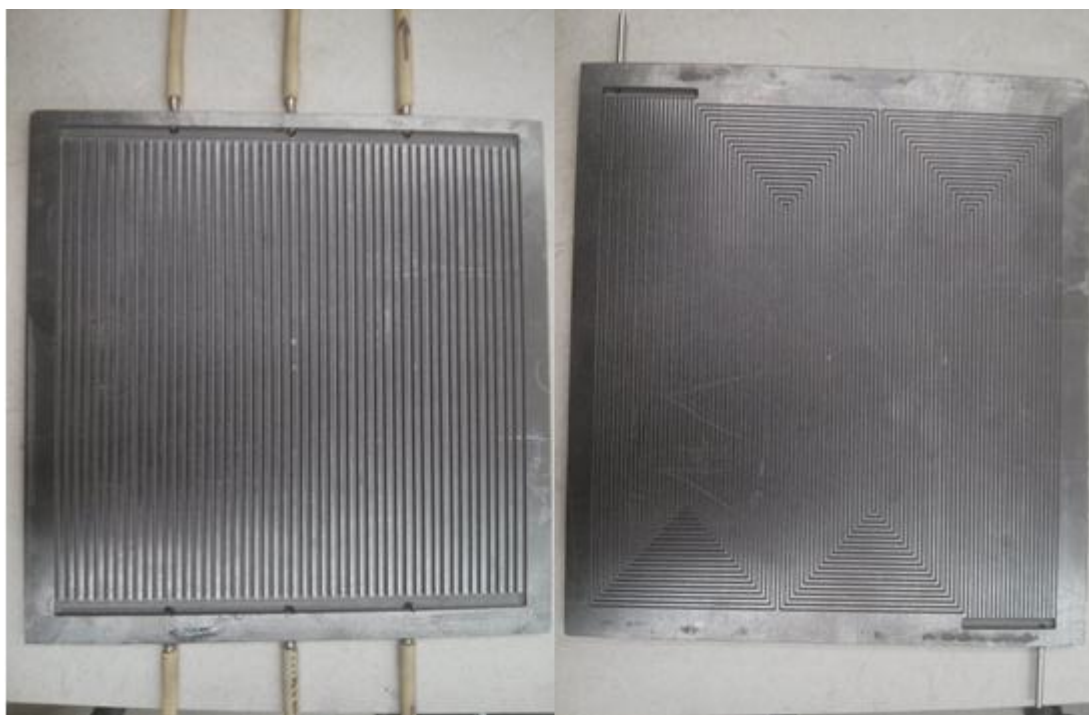
Figure 3-5 Left hand side is picture of the bipolar plate used for the liquid side. Wider parallel channels help avoid pressure drop and decrease the chance of blocking channels with particulates found in liquid flow. The picture at the right shows parallel-serpentine flow fields for the gas side.

A cation exchange HSF Selemion membrane (Pupkevich *et al*., 2013) was used as the membrane. For conditioning, membranes were placed in distilled water for 24 hours prior being used in the fuel cell. Graphite felt (SIGRATHERM KFA-5, SGL, Wiesbaden, Germany) was used as the cathode electrode. Activation of the graphite felts was performed as described in Pupkevich *et al*., 2007.

3.3   Laboratory Set-up of Fuel Cells for the BioGenerator

Figure 3-5 shows the continuous flow test station used in this work.

Figure 3-6 BioGenerator fuel cells laboratory set-up

The BioGenerator fuel cell test station consisted of membrane electrode current collectors assembly, pumps for the supply of the cathodic electrolyte and a Chroma 6312 electronic load for maintaining a constant current within the fuel cells. The same cathodic electrolyte was run through series of fuel cells electrically connected together. A 600 L airlift bioreactor (Karamanev *et al.*, 2013) was used for continuous supply of the electrolyte to the fuel cells cathode compartment. The iron oxidizing bacteria were a mixed culture dominated by *L. ferriphilum*. *L. ferriphilum* is an autotrophic microorganism that uses CO_2 as the only carbon source. The pH in the bioreactor was between 0.7- 0.9 (2- 3% H_2SO_4). The temperature in the bioreactor was 20ºC. For the experiments in this study, electrolyte flow rate was 33 ml min^{-1}, and the total concentration of iron ions was 40 g L^{-1}. Deionized water was added periodically to compensate for the evaporation of water in the bioreactor. In addition, H_2 pressure and flow rate were kept at 3 ± 0.5 psig and 200 ml min^{-1}, respectively.

3.4 Ex-situ Characterization Techniques

3.4.1 Through-Plane Gas Permeability

Through-plane gas permeability of the prepared backing layers was measured with air using an in-house fabricated apparatus (Figure 3-6) since using hydrogen as the experimental gas was not safe. However, it is a valid assumption that hydrogen permeability will follow the same trend

observed in the case of air (Phillips et al., 2012; Gostick et al., 2006). Darcy's law proposes the following equation for measurement of gas permeability:

$$K = \mu \, \nu \, \frac{\Delta X}{\Delta P} \tag{3-1}$$

, where ν is superficial fluid flow velocity through the medium m s^{-1}; K is permeability of the medium m^2; ΔP is the applied pressure difference Pa; μ is the fluid viscosity (Pa s); and Δx is the thickness of the medium m.
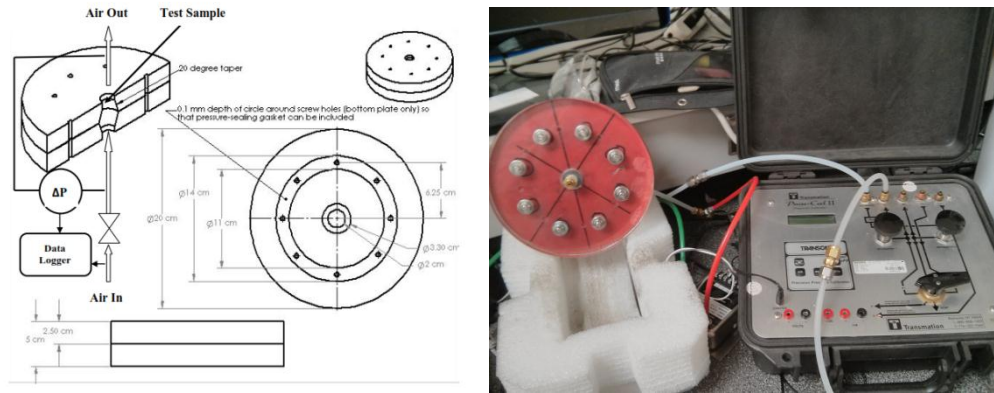
Figure 3-7 Scheme of the apparatus used for permeability measurements of the BLs (Karimi 2011)

However, Equation 3-1 is given for calculating the permeability of incompressible fluids, constant properties, laminar flows under steady state conditions. Equation 3-2 represents the solution of Darcy's law for compressible fluids for one-dimentional flow (Geertsma 1974; Gostick *et al.,* 2006):

$$\frac{P_{in}^2 - P_{out}^2}{\frac{2LRT}{MW}_f} = \frac{\mu}{K} m' \tag{3-2}$$

, where P_{in} is the inlet pressure; P_{out} is the outlet pressure; L is the length of sample; T is the temperature; R is the universal gas constant; MW_f is the molecular weight of fluid; μ is the viscosity of fluid; K is permeability of the medium m^2; and m$^{'}$ is the fluid mass flux through the sample kg s^{-1}m^{-2}.

Samples were placed into the experimental apparatus (Figure 3-6) and checked to ensure no air leakage. Compressed air was passed through the system at different pressures from 0.0 to 30.0

inches of water. The pressure difference between the inlet and outlet of the sample was converted in mV using an electronic apparatus and the volumetric flow rate was measured at the end of the system. The K value was then calculated using equation 3-2. Samples with large error in their K values were checked under a microscope for possible clogged of the fibers. Any clogged samples were removed from the set of samples. Procedures were repeated for each sample at least three times in different apparatus to ensure accuracy of analysis.

3.4.2 Contact Angle

Contact angle measurement is a technique, which quantifies the wettability of a solid surface with a liquid phase. In the wettability of a surface, some important parameters are involved. One can mention roughness of the surface, surface coating, and surface energy between the materials are among influencing parameters in determining contact angle of a surface. We do not have a specific number that determines the border between hydrophobicity and hydrophilicity. However, 90^0 is widely used as the transition angle from hydrophobicity to hydrophilicity.

A straightforward technique for measuring contact angle is sessile drop method, where a drop of liquid is placed on the surface of the material of interest and the angle between the liquid and surface gives the contact angle (Figure 3-7). In the case of fuel cell electrodes and GDLs, especially cloth-based, it is difficult to measure the actual value of the contact angle because the surface is so rough and porous that the droplet contacts only fractions of the solid surface (J. Gostick *et al*., 2012). However, this method is still quite useful in observing the hydrophobicity changes caused by surface aging due to fuel cell performance.
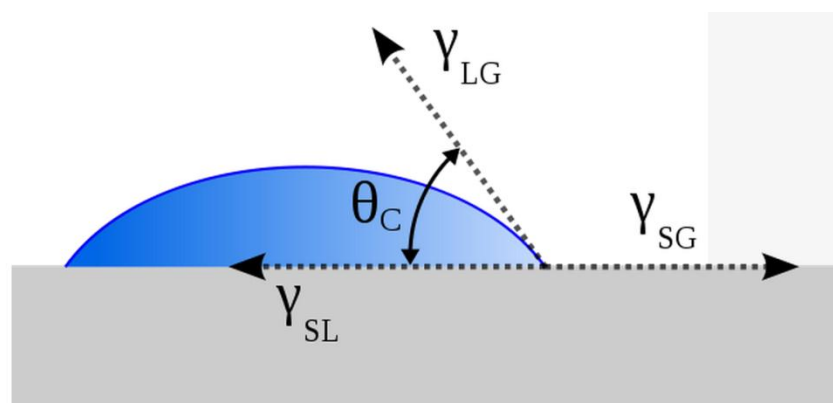
Figure 3-8 Scheme of the sessile drop technique. Θ_c is the contact angle (Sessile drop technique 2014).

3.4.3 Mercury Intrusion Porosimetry (MIP)

The mercury intrusion porosimetry (MIP) is an analysis used to gain information on material porous nature features like pore diameter, total pore volume and pore size distribution. MIP involves intrusion of mercury into the material at different pressures via porosimeter. In MIP technique, different pressures of mercury are applied and pore diameters are evaluated from the Equation 3-3 known as Wash-burn equation (Giesche 2006).

$$\Delta P = \frac{2\gamma cos\theta}{r_{pore}} \tag{3-3}$$

, where γ is the surface tension of mercury; θ is the contact angle between the material surface and the mercury; ΔP is the applied pressure difference; r_{pore} is the material pore diameter. By applying pressures up to 60,000 psi, mercury intrusion porosimetry is capable of measuring pores as small as 3.5 nm (Webb 1993). A Micromeritics AutoPore IV Mecrcury Porosimeter was used in this study.

3.4.4 Scanning Electron Microscopy (SEM)

In fuel cell research, Scanning Electron Microscopy (SEM) is a technique used to obtained detailed information on microstructure, surface morphology, as well as chemical compositions of the materials and fuel cell components. In SEM technique, a beam of high-energy electrons is focused towards a sample to generate different signals at the surface. These signals are generated as a result of sample-electrons interactions and contain useful information about the surface structure of the sample. This information includes surface morphology, chemical composition, orientation of constitutive materials and chemical compositions (Egerton 2005). Figure 3-8 shows a scheme that how a scanning electron microscope works.
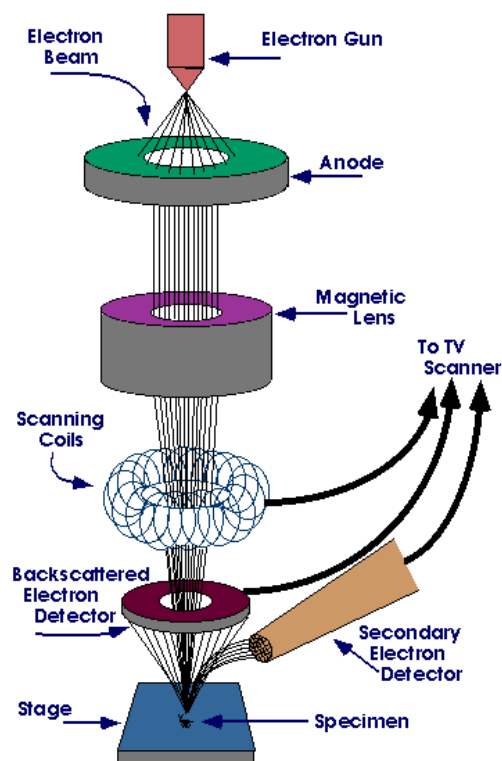
Figure 3-9 Scheme of an electron scanning microscope (SEM) (Schweitzer n.d.)

In the electrode fabrication for fuel cells, SEM can be used to obtain information about the surface morphology of electrodes and help observe morphological changes of the catalyst layer when studying lifetime durability of fuel cell components (Figure 3-9). In this study, samples were cut in small (1 cm^2) pieces, and after being coated by osmium, were analyzed using a LEO Zeiss1540XB FIB/SEM equipment.
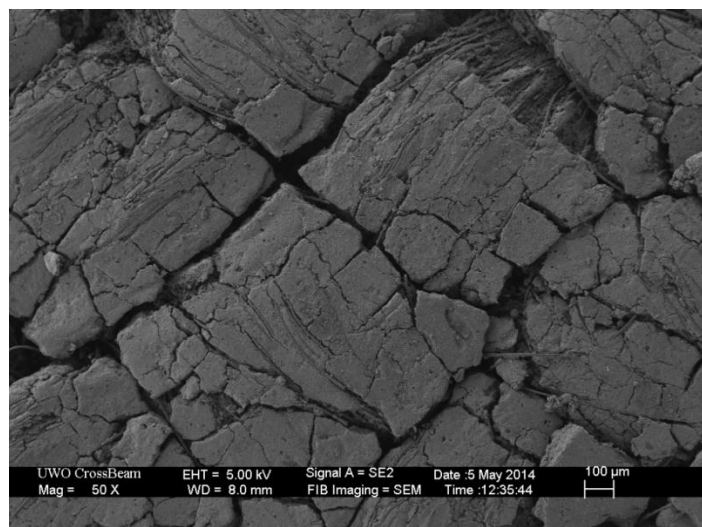
Figure 3-10 SEM image of a fuel cell catalyst layer fabricated by PTFE-bound spreading technique

3.4.5 X-Ray Diffraction (XRD)

XRD is a characterization technique used in obtaining information on chemical composition and crystallographic structure of materials. One of the advantages of XRD is that it is not a destructive test. It is well agreed that activity of a catalyst layer is a strong function of its particles size, orientation, shape, and distribution. In fuel cell research, activity of the catalyst layer is dependent on the size of catalyst particles, and whether they are present near the three-phase zone or not. This definitely guarantees the activity of a catalyst layer. XRD is a powerful technique to help obtain size of catalyst particles and their crystals structure (Shijun *et al*., 2008).

Beams of x-rays are directed to the surface of the catalyst layer (Figure 3-10). Each crystalline component reflects the incidence beam in its own unique way. Therefore, each element will give its on angle of reflection. William Lawrence Bragg and his father, Sir William Henry Bragg, got the Nobel Prize in physics in 1915 for their work in determining crystal structures. They proposed Equation 3-3 that became the basis of XRD (Sadoway 2010).

$$n\lambda = 2d_L \, sin\theta \tag{3-3}$$

, where n is the reflection order; λ is the wavelength of incident wave; θ is the angle between the incident ray and the scattering planes; d_L is the spacing between the planes in the atomic lattice.
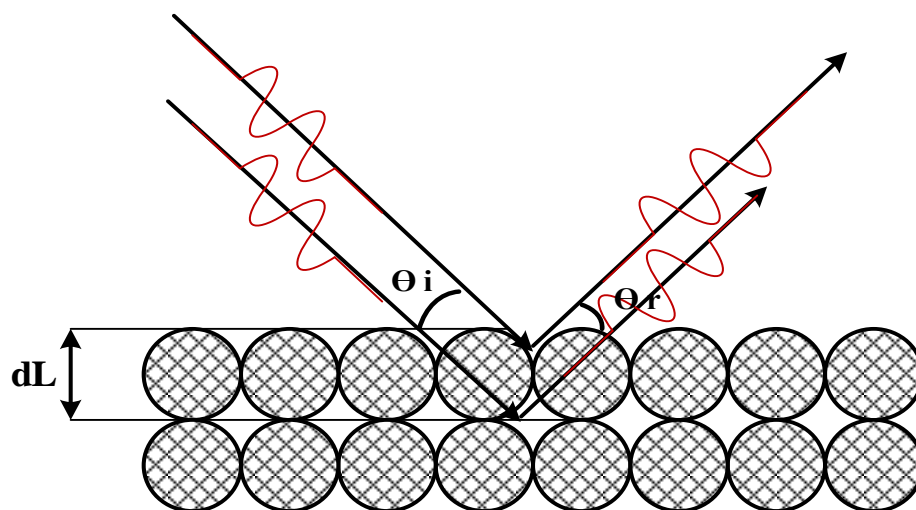
Figure 3-11 An illustration of XRD technique. Θ_i is the incidence angle (waves are going into the crystal structure); Θ_r is the reflection angle (waves are leaving the crystal structure); dL is the spacing between the planes in the atomic lattice.

3.4.6 XPS (X-Ray Photoelectron Spectroscopy)

XPS is a technique that uses X-ray beams to generate a pattern consisting elements in the surface of a material existing up to about 10 nm in depth. X-ray excites electrons in the outer layer of elements on the surface of material and some of the electrons are separated from the surface and will emit as a photoelectron. Therefore, this is a surface sensitive technique. XPS provides information about chemical state of an element, electron state, and empirical formula (Engelhard n.d.). In fuel cell research, XPS is a good technique to provide us with any source of trace element on the surface of the catalyst that interferes with the activity of the catalyst. It also shows the chemical state of the catalyst when exposed to dissolution, support corrosion and other sources of deactivation (Borup *et al*., 2007).

3.5 Electrochemical Analysis

3.5.1 i-V Measurements

Based on the concepts discussed in section 2-2, current density- voltage (i-V) measurement was used to quantify the overall electrochemical performance of the BioGenerator. At first, the fuel cell was put on a small current density for some time to become conditioned and reach the steady state. The time can vary depending on the dynamics of the system. For the BioGenrator fuel cell, 20-30 minutes was sufficient. Then, the current was swapped from zero to the maximum

possible (short circuit condition). Sufficient time must be given to each point to reach steady state. In this study, i-V curves were obtained using a Chroma 6312 Electronic Load.

3.5.2 Cyclic Voltammetry

Cyclic voltammetry (CV) is an electrochemical technique that enables us to analyze the activity of fuel cell catalysts in more details. In fuel cell research, cyclic voltammetry can be performed in-situ or ex-situ. Figure 3-11 shows a typical three-electrode electrochemical cell configuration used to perform an ex-situ cyclic voltammetry.
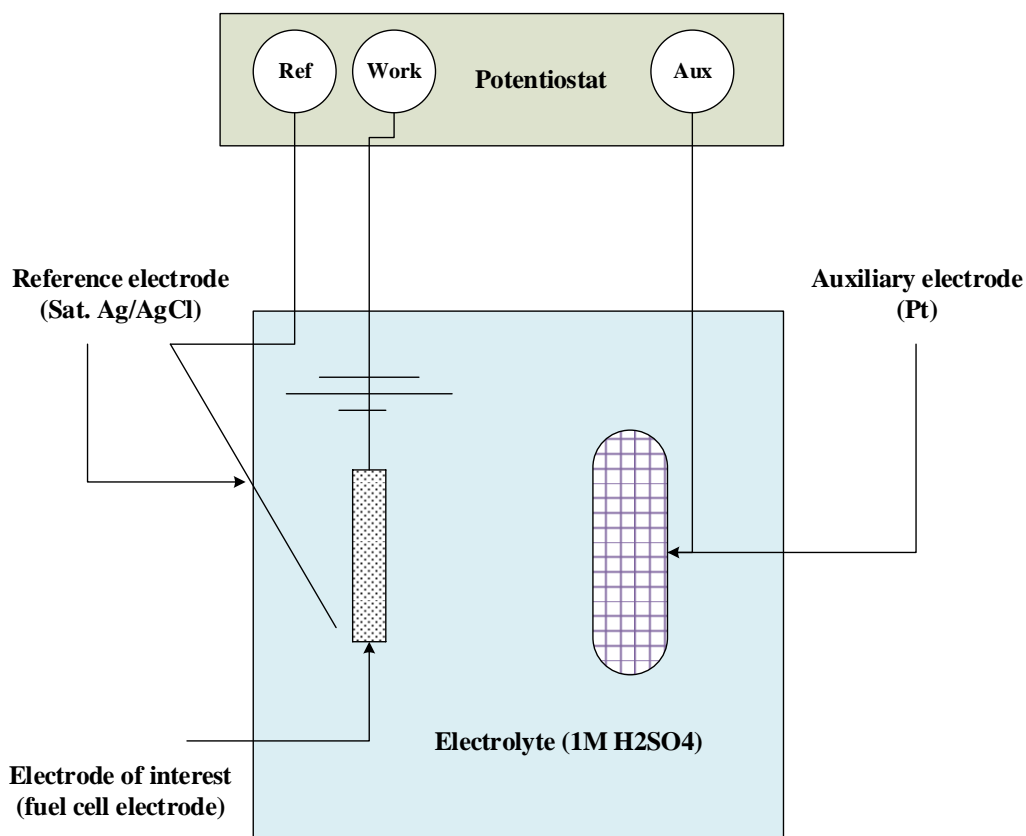
Figure 3-12 A scheme of the electrochemical cell used for ex-situ cyclic voltammetry measurement of the fuel cell electrodes in this work.
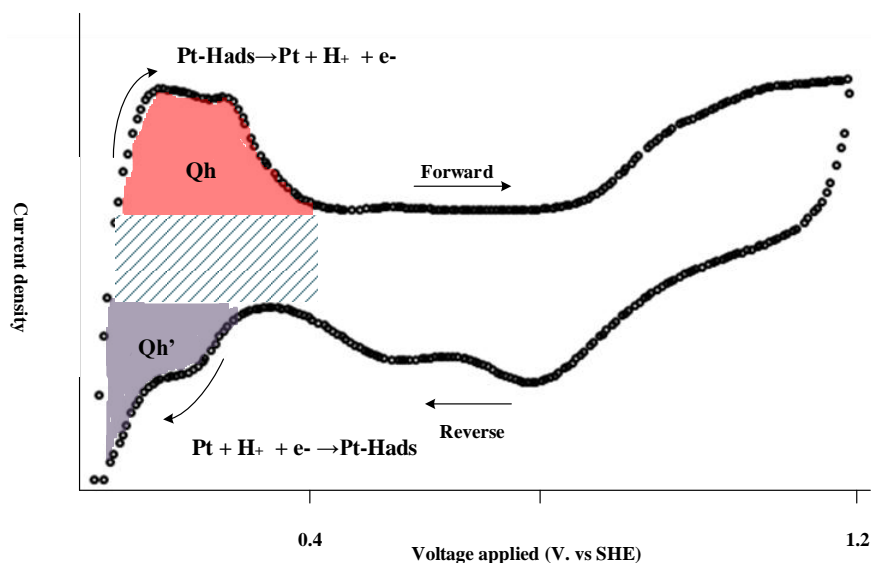
Figure 3-13 A typical fuel cell electrode CV curve. Q_h and $Q_{h'}$ represent charges associated with hydrogen adsorption and desorption on platinum.

A CV curve (Figure 3-12) can be used to calculate the electrochemically active catalyst surface area in the following manner (Cooper 2009):

$$ECSA = \frac{Q_{pt}}{Q_m L}$$
(3-8)

, where ECSA is the electrochemical catalyst surface area ($cm^2_{Pt}\ g_{Pt}^{-1}$); Q_{pt} is the charge density calculated from the area under the curve when plotting current density versus time (C $cm^{-2}_{electrode}$); Q_m is the charge required to reduce a monolayer of protons on the surface of platinum (210 µC/ cm^2_{Pt}); L is the loading of platinum in the electrode ($g_{pt}\ cm^{-2}_{electrode}$). In this work, CV tests were performed ex-situ in 1.0 M H_2SO_4 with scan rate of 50 mV s^{-1}. For obtaining steady state results, electrodes were conditioned for 15 minutes under a constant voltage followed by 10-15 cycles for the peaks to appear and the surface of catalyst layer to become conditioned.

Chapter 4

4 Results and Discussions

4.1 Outlook

The long-term stability of fuel cells is highly dependent on the structure of the fuel cell, the nature of the anode, cathode, and the membrane and on the nature of the electrolyte. In the case of a typical anodic process, the hydrogen oxidation is represented as

$$H_2(gas) \xrightarrow{Pt} 2H^+(electrolyte) + 2e^-(solid) \tag{4-1}$$

This typical three-phase reaction (4-1) guarantees the electrochemical hydrogen oxidation reaction to take place. Considering this, the presence of hydrophobic voids for the gas phase, an ionic conductive media for the electrolyte phase and a conductive solid phase for the transport of electrons is essential.
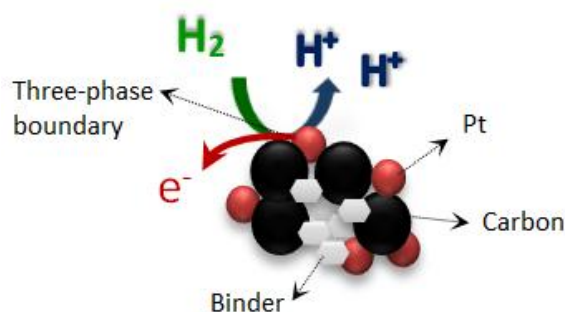
Figure 4-1 Scheme of the three-phase hydrogen oxidation reaction on a typical H$_2$-based fuel cell

In PEMFCs, both the fuel (H$_2$) and the oxidant (O$_2$) are gases under standard conditions. The product of the electrochemical reaction is water, which is produced as a result of the oxygen reduction reaction on the cathode (4-2) (Sridhar *et al*., 2001).

$$2H^+{}_{(aq)} + 1/2O_{2\,(g)} + 2e^- \xrightarrow{Pt} H_2O_{\,(l)} \tag{4-2}$$

The fluid structure in the BioGenerator, however, is quite different compared to PEMFCs. In the cathode, the gas phase containing oxygen is replaced with a liquid phase containing oxidants. The oxidant in the cathode reaction is ferric ions (Fe^{3+}). Ferric ions accept the electrons generated in the anode reaction as follows:

$$2Fe^{3+}{}_{(aq)} + 2e^- \rightarrow 2Fe^{2+}{}_{(aq)} \qquad (4\text{-}3)$$

The formed ferrous ions (Fe^{2+}) flow to the bioreactor, where they are consumed in the respiration reaction of the microorganisms:

$$2Fe^{2+}{}_{(aq)} + 2H^+{}_{(aq)} + 1/2O_{2(g)} \xrightarrow{microorganisms} 2Fe^{3+}{}_{(aq)} + H_2O_{(l)} \qquad (4\text{-}4)$$
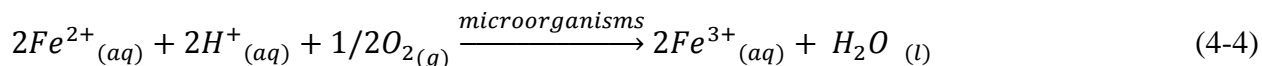
Reactions 4-3 and 4-4 represent the bio-regenerative cycle for continues supply of the oxidant to the fuel cell. One can combine 4-3 and 4-4 and the result will be:

$$2H^+{}_{(aq)} + 1/2O_{2(g)} + 2e^- \xrightarrow{microorganisms} H_2O_{(l)} \qquad (4\text{-}5)$$
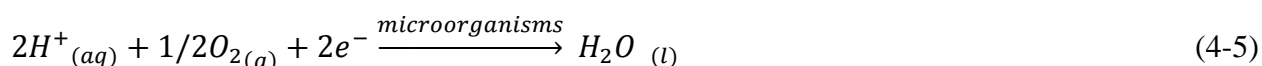
Reaction 4-5 is the same reaction happening in a PEM fuel cell (4-2). However, there is one big difference. The PEMFC cathode reaction will not proceed without the presence of a precious metal catalyst such as platinum, while microorganisms indirectly catalyze the cathodic reaction in the BioGenerator.
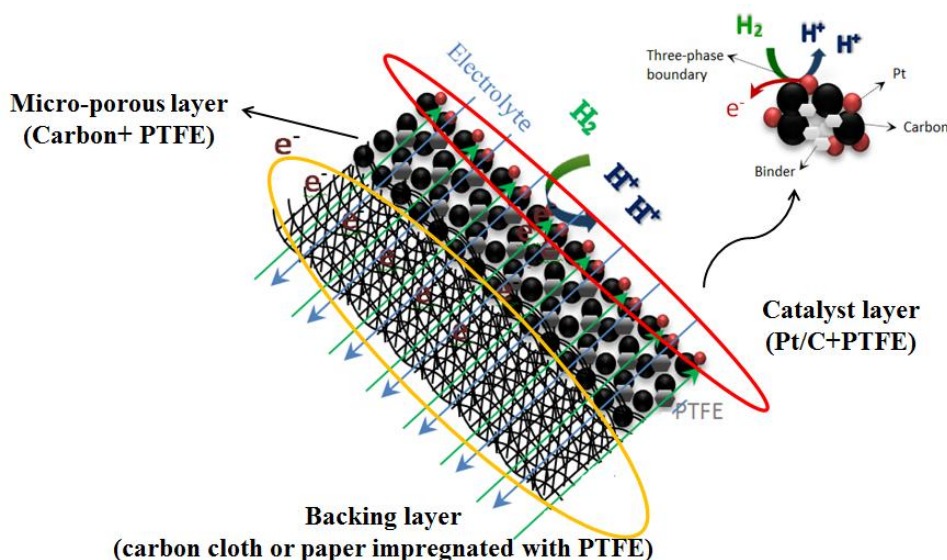
Figure 4-2 A schematic diagram of the two-phase transport within the anode electrode of the BioGenerator

The gas diffusion electrode (GDE) comprising the backing layer (BL), the micro-porous layer (MPL), and the catalyst layer (CL) plays the most important role in the performance and long-term durability of the BioGenerator (Figure 4-2). There is a tradeoff between the short-term performance and long-term durability of the GDE. In other words, not all the changes targeted to

increase the short-term performance can enhance the long-term durability. A well-understood example is the amount of hydrophobicity in the structure of the GDE. PTFE is a non-conductive polymer often used to make electrodes hydrophobic and can decrease the performance of the system due to decreasing the electrical conductivity. The catalyst layer is agreed to be the most crucial layer governing the performance of the fuel cell electrodes. The BioGenerator anode electrode is hosting considerable amount of liquid that comes from the cathode side by passing through the membrane. Depending on what membrane is used, the flux of liquid varies. For example, the water flux from the cation exchange Selemion HSF membrane is 0.0352 ml. cm^{-1}. hr^{-1}, while this value for Phosphorylated polyvinyl alcohol (p-PVA) membranes is approximated to be 0.0608 ml. cm^{-1}. hr^{-1} (Pupkevich *et al*., 2013). Presence of the three-phase boundary near catalyst particles is essential. The gaseous reactants flow through the GDL and will reach the sites in the CL to take part in the reaction (gas phase), an electrolyte is needed to carry protons (electrolyte phase), and finally carbon particle surface will help electrons to flow (solid phase) (Figure 4-1). In the fabrication of the catalyst layer, all effort is to provide these three zones near the catalyst sites. To ensure there is enough adhesion between particles and space for gas to diffuse and react, a hydrophobic binder such as PTFE is usually applied. With the invention of Nafion and polymer exchange membranes, PTFE, as a binder, gave its place to Nafion. Nafion is a sulfonated tetrafluoroethylene based fluoropolymer-copolymer introduced in the late 1960s by Walther Grot of DuPont (Church 2006) and show great advantages over PTFE: 1- By looking at the structure of Nafion, simultaneous presence of hydrophobic ($-CF_2-CF_2-$) and hydrophilic ($-SO_3H$) heads can ensure ionic conductivity and gas diffusivity of catalyst sites, besides, it works as a reliable binder for particles. 2- Because of strong ionic conductivity of Nafion, the catalyst utilizations will increase noticeably. In the case of PTFE-bound catalyst layers, platinum utilization in the cathode reaction remains in the order of 20% (Murphy *et al*., 1994; Cheng *et al.*, 1999). Nafion can be brushed on the surface of PTFE-bound catalyst layer and/or impregnated within the catalyst particles. Basically, in PEM fuel cells, the CL can be applied either on the surface of GDL or membrane. The former is referred to as PTFE-bond catalyst layer and the latter known as thin-film method (Litster and McLean 2004). Type and the chemical stability of catalyst, support of the catalyst, level of hydrophobicity (hydrophilicity), porosity, thickness of the CL, deposition of catalyst on support, and lamination method of the catalyst layer are all among those key features that must be adjusted considering the demand of

the system and existing conditions. For example, for PEMFCs, Song et al (2004) proposed 0.8 mg cm^{-2} as the optimal content of ionomer (Nafion) when the Pt loading was 0.4 mg cm^{-2} (Song 2001).

The BioGenerator, in particular, suffers from flooding of the GDE. Due to the presence of an acidic electrolyte, proton conduction within the surface of the CL can be obtained easily. Therefore, as a binder, Nafion as a relatively hydrophilic polymer was replaced with PTFE to ensure desired level of hydrophobicity within the structure of the CL could be obtained.

As mentioned earlier, a GDE consists of three layers (CL, MPL, and BL). The BL together with the MPL form the gas diffusion layer (GDL). Based on what mentioned above, in this chapter, the main goal was to enhance longevity of the anode electrode in the conditions of the BioGenerator. The following steps and experiments were done and comprise the content of this chapter:

- PTFE-bound catalyst layers were fabricated with different techniques and the performance of anode electrodes made using these catalyst layers laminated on commercially available GDLs was studied.

- Application of the catalyst layer using pulse-electrodeposition was performed.

- The effect of PTFE in the gas diffusion backing layer (BL) on the gas permeability, surface hydrophobicity, and on the performance of the BioGenerator anode electrodes made out of different amounts of PTFE were investigated.

- Using the results from the above experiments, a PTFE-bound hydrophobic three-layer anode electrode was developed and its performance in the conditions of the BioGenerator was studied and compared with the commercially available electrodes.

- As an important baseline for the future research, some preliminary experiments and characterizations were conducted to help better understand the causes of failure in the anode electrode.

4.2 Lamination of PTFE-Bound Catalyst Layers on Commercially Available Gas Diffusion Layers

Hydrophobic commercially available gas diffusion layers (GDL-CT) designed to avoid flooding in fuel cells were purchased from FuelCell Etc (College Station, TX) and hydrophobic catalyst layers were laminated on top of them using spraying and brushing techniques. Figure 4-3 shows the long-term durability results obtained by using the mentioned electrodes in the BioGenerator fuel cell.
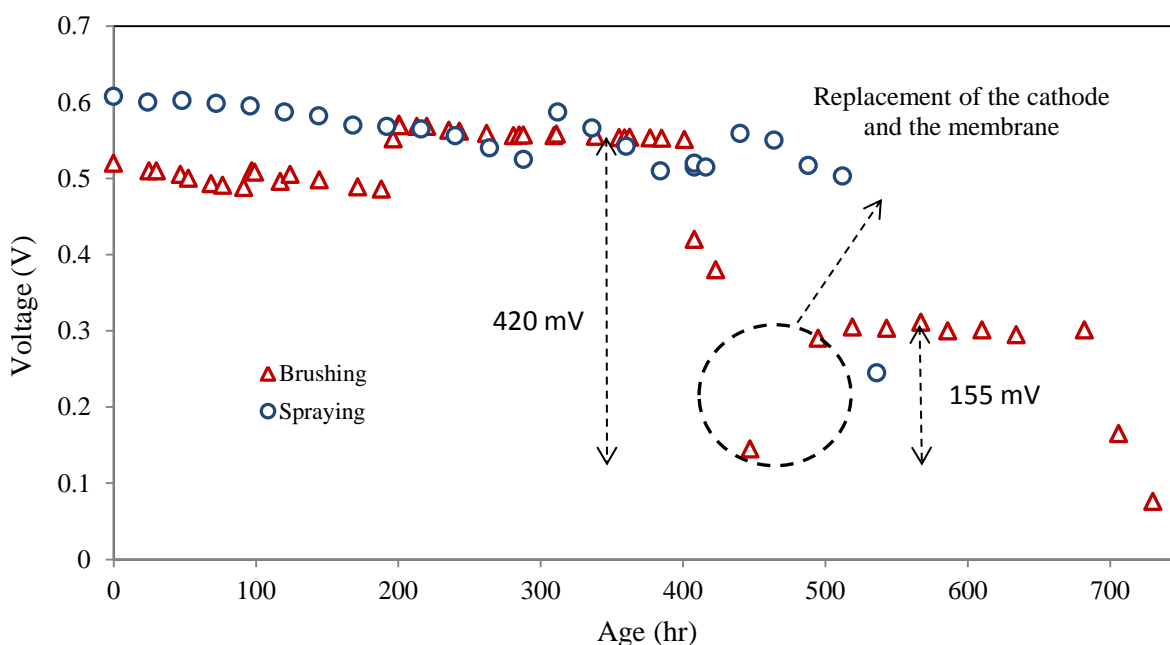
Figure 4-3 Continuous operation at 100 mA cm^{-2} for developed electrodes made by spraying and brushing the catalyst layer (0.5 mg cm^{-2}, 40 wt.% PTFE) onto the surface of commercially available GDLs (GDL-CT).

As Figure 4-3 shows, anode electrodes based on commercially available GDLs did not provide the desired long-term durability neither in the case of employing brush-made catalyst layers nor in the case of spray-made catalyst layers. To ensure that the main part causing the voltage loss was the anode electrode, one of the cells was opened and the used cathode and the membrane were replaced and put back into operation with the same anode. However, as it is clear, only about 35% of the voltage was recovered. We believe the reason was absence of sophisticated gas diffusion layer that led to flooding in the anode electrode. As it is evident, the durability of both types of the anode (spray and brush made) is almost the same and one should search the main

cause of failure in the gas diffusion layer. In addition to the need to re-construct and modify the gas diffusion layer, we needed to choose a method of electrode fabrication that would enable us for making larger area electrodes for 10 kW application of the BioGenerator in the future. The brushing technique is associated with a considerable chance of human error and non-uniformity of the physical properties. On the other hand, spraying technique seemed to generate more uniform layers of catalyst. However, spraying still suffers from lack of reproducibility and due to the low viscosity nature of its ink; the chances are that catalyst layer penetrates to the MPL. This would definitely result in decreasing the electrochemical active area. Figure 4-4 shows SEM images obtained from the surface of catalyst layers made by brushing and spraying technique.
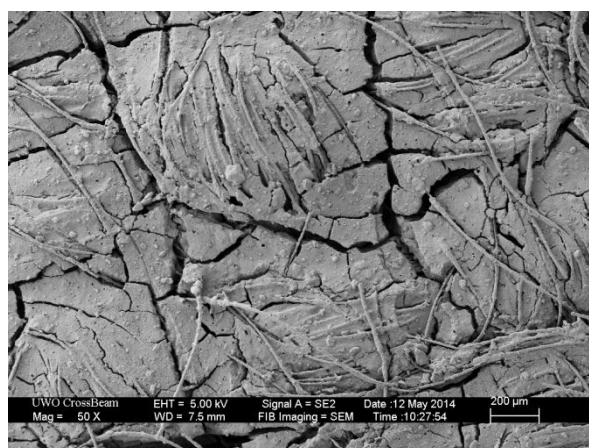
(a)
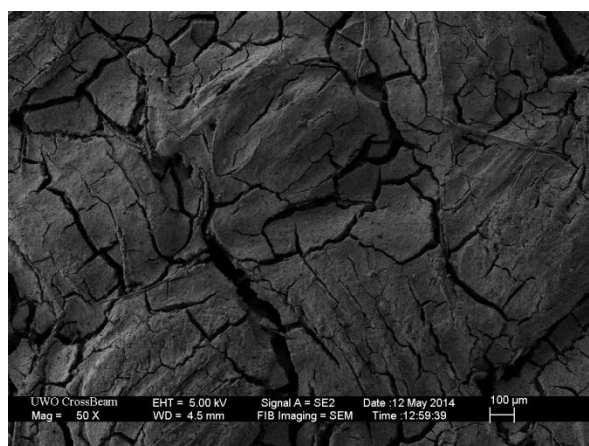
(b)

Figure 4-4 Top view SEM of catalyst layers. a) spray-made catalyst layers; b) brush-made catalyst layers

As the SEM pictures suggest, there is penetration of the catalyst layer into the middle layer (MPL). One can see that in the case of spray-made catalyst layers, fibers are clear while this is not the case for brush-made catalyst layers.

4.2.1 Application of Catalyst Layer using Pulse-Electrodeposition on Hydrophobic Gas Diffusion Layer

Electrodeposition of platinum particles directly onto the surface of gas diffusion layer is believed to give higher and more utilized electrochemical area. As described in 3-1-3-5, a continuous flow electrodeposition bath was constructed and Pt $(NH_3)_4Cl_2$ was used as the platinum salt. Our experiments showed that electrodeposition using Pt $(NH_3)_4Cl_2$ was not successful and no platinum was deposited on the surface of the gas diffusion electrode mainly because of absence of an ion-exchange agent. When Pt $(NH_3)_4Cl_2$ dissolves in water, it forms $(Pt (NH_3)_4)^{2+}$ complex. In the electrodeposition bath, the formed platinum complex is dragged to the cathode, while the Cl^- ions migrate to the anode side where they release electrons and form chlorine gas. An ionic force was needed to exchange Pt^{2+} cations and deposit them onto the surface of carbon. However, since there were no ionomer such as Nafion presented onto the surface of the carbon, no platinum deposition occurred.

On the basis of the above results, another technique, which would be capable of producing relatively uniform, reproducible, and controllable catalyst layers, was also used. A height-controllable-knife- based spreader (Figure 3-2), capable of fabricating small (1 cm by 1 cm) up to larger (20 cm by 20 cm) anode electrodes was used to form the MPL and the catalyst layer. From this perspective, research was directed towards making anti-flooding and high gas permeable electrodes based on modifications of gas diffusion backing layer.

4.3 Effect of PTFE Content in the Gas Diffusion Backing Layer on the BioGenerator Fuel Cell Performance

Now that the importance of transport phenomena in the GDL in controlling the longevity of the anode electrode became clear, the question was what material as the anode backing layer and what amount of PTFE as the hydrophobicity were desirable in the GDL. On this basis, a series of carbon cloth and paper samples were hydrophobized in a range from 0 to 200 wt.% PTFE (mass ratio of PTFE to the untreated material) and prepared for the gas permeability measurement (3-4-

1). Toray T-120 and CC4 Plain (Fuel Cell Earth LLC) were used as the materials of carbon papers and cloths, respectively. Figures 4-5-a, and 4-5-b show the results obtained from the gas permeability measurments of PTFE-treated carbon papers and cloths, respectively.
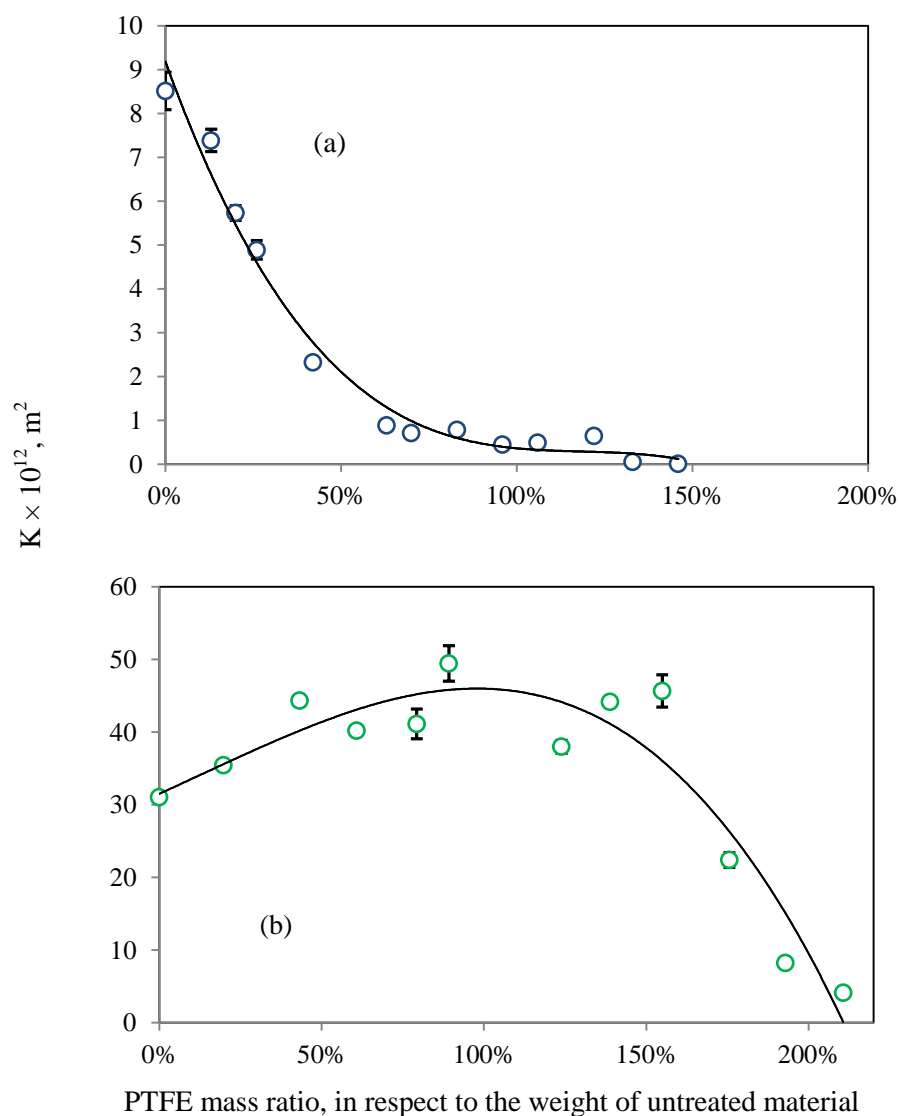
Figure 4-5 K permeability values of PTFE-impregnated a) carbon paper (Toray T-120); b) carbon cloth (CC4P- Fuelcell Earth).

As seen in Figure 4-5-a, by increasing the amount of PTFE in paper, the permeability decreases. This is in good agreement with the understanding of the texture of carbon paper (Figure 2-7). Figures 4-6-a and b are microscopic images obtained from carbon paper before and after the impregnation with PTFE. As observed, fibers in the paper are mechanically fixed in place, and

have a random structure. Therefore, when PTFE was added to them, it occupied the space between the fibers and reduced the available space for the gas to flow.

(a)

(b)

(c)

(d)
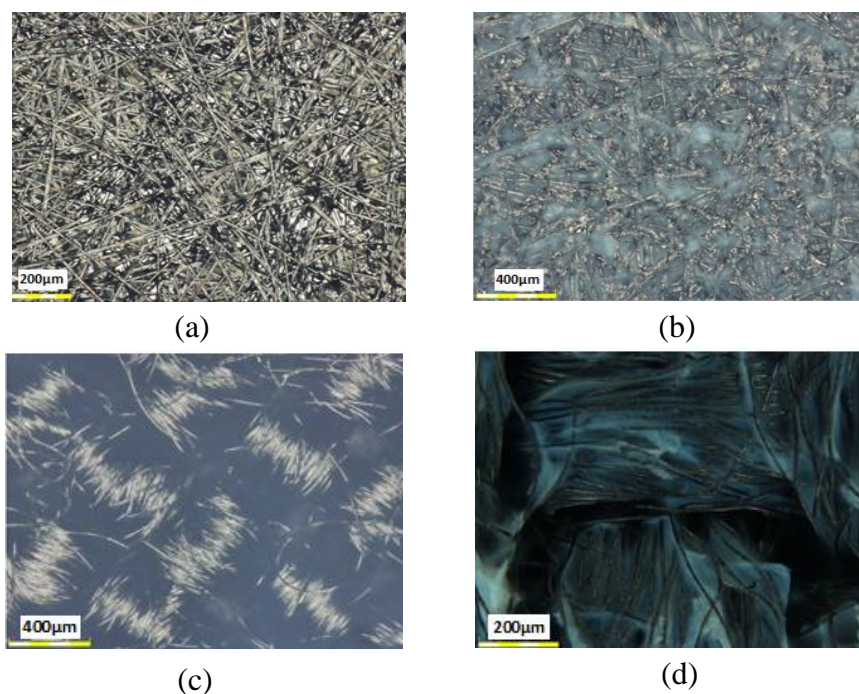
Figure 4-6 Microscopic images of carbon papers and cloths before and after impregnation with PTFE. (a) untreated paper; (b) impregnated paper; (c) untreated cloth; (d) impregnated cloth.

However, an interesting trend was observed in respect to changes in the gas permeability of the PTFE-impregnated wowen carbon cloths. As Figure 4-5-b shows, by increasing the amount of PTFE, in contrast with the paper, gas permeability initially increases gradually, but, at some point, by further increasing the PTFE, the gas permeability starts decreasing. Microscopic images of carbon cloths before and after the impregnation were obtained to help better understand the effect of PTFE on the cloth permeability. As it is clear from Figures 4-6-c and d, PTFE first occupies spaces between fibers and pushes them away, and by further increasing the amount of PTFE, it occupies more space between the fibers network. This observation might explain the trend observed in Figure 4-5-b, where first by increasing the amount of PTFE, the gas permeability increses until it reaches the maximum possible space in between the texture of fibers, and at this point, the space between the fibers becomes saturated and by further increasing the amount of PTFE, PTFE occupies the voids in the texture of cloth. As a result, the gas

permeability starts decreasing. The black spots in Figure 4-6-d are the voids between the wowen texture of cloth.

Based on the results obtained from the gas permeability analysis, anode electrodes were constructed based on carbon cloths with different amounts of PTFE in their backing layers. Cloth impregnated with 50, 85, 130 wt.% PTFE were selected and stability of anode electrodes employing these gas diffuion backing layers in the real application of the BioGenerator was evaluated. The electrochemical cells were run at 100 mA cm^{-2} and periodically current-voltage (i-V) measurements consisting of evaluation of the cells' performance at a full range of current densities were carried out to better understand the behaviour of the studied electrode with time. Figure 4-7 illustrates the current - voltage (i-V) measurements of these fuel cells during 250 hours of contineous operation.
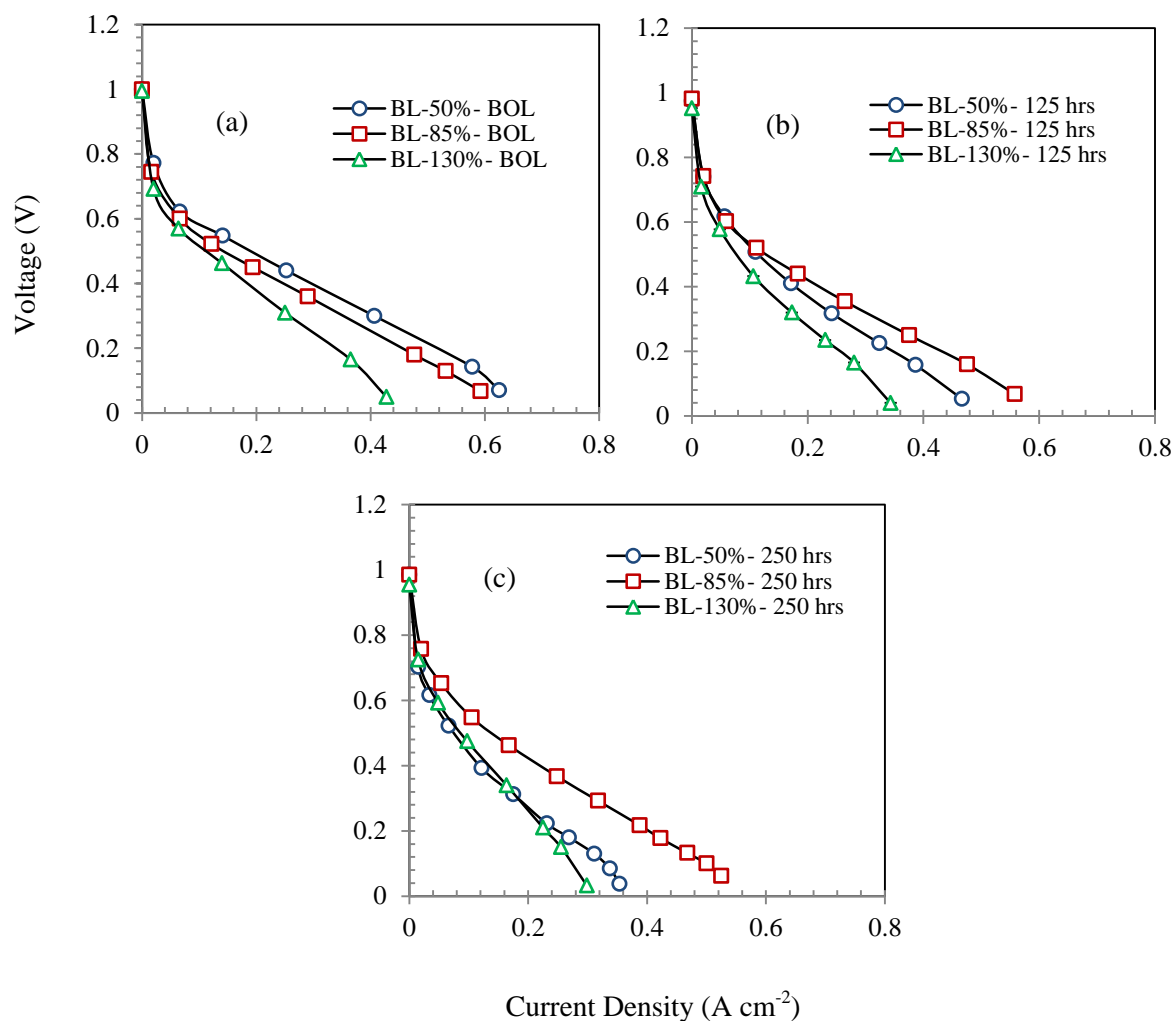
Figure 4-7 i-V curves obtained for anode electrodes with different amounts of PTFE in their gas diffusion backing layers (e.g.BL-50%= backing layer impregnated with 50 wt.% PTFE) a) beginning of operation (BOL); b) after 125 hours of continuous operation at 100 mA cm^{-2}; c) after 250 hours of operation at 100 mA cm^{-2} .

At the beginning of the operation, as expected (Figure 4-7-a), BL-50% exhibited a higher voltage at all the given current densities and the lowest performance was registered by BL-130%. Due to the non-conductive nature of PTFE, electrical resistivity increased upon adding more PTFE to the backing layer and, as a result, the cells' performance (voltage) decreased. However, after 125 hours of operation (Figure 4-7-b), when electrodes became almost conditioned, a considerable drop in performance was observed for BL-50% and BL-130% as opposed to BL-85%. As evident, the difference between the maximum current density that system could deliver was quite different from cell to cell at different periods of time. In addition, since the only diffrentiating parameter in these anode electrodes was hydrophobicity of their GDLs, then any difference in

the limiting current density should be attributed mostly to the state of two-phase transport within the anodic gas diffuion electrode.

To better explain the observations and conclud about the effect of PTFE in the GDL on the BioGenerator fuel cell performnce, we can say that PTFE increases the hydrophobicity. This is desirable for the conditions of the BiGenerator but at the same time it increses the electrical resistivity, and the electrical resistivity decreases the fuel cell voltage. This effect is clear where 130% PTFE exhibited lower voltage from the beginning of the operation in all the given current densities. Therefore, contact angle measuemment was conducted on a series of cloth impregnated with PTFE to observe the effect of PTFE on the hydrophobicity of backing layers. Figure 4-8 shows the results obtained from the contact angle measurement. As seen, the change in surface hydrophobicity in respect to the change in the PTFE added into the cloth follows almost a smooth logarithmic trend. The contact angle increses by increasing the PTFE from 0 to almost 50 wt.% while, it does not significantly change by further increasing the PTFE up to higher values like 160 wt.%. What this trend tells us is that higher the PTFE does not always mean higher the hydrophobicity. In other words, considering both the effect of PTFE on the hydrophobicity and on the electrical resistivity, one can claim that PTFE has a optimumn range. This is also in good agreement with the results from gas permability analysis.
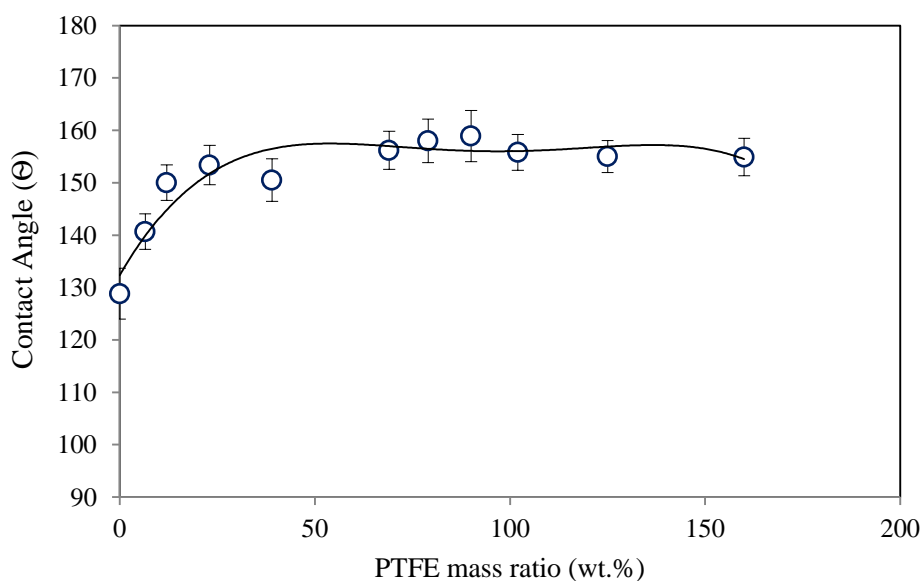
Figure 4-8 Surface contact angle of cloth-based gas diffusion backing layers impregnated with different amounts of PTFE

However, it is important to realize that Figure 4-8 shows the surface contact angle and it is a good assumption that the total volume of the cloth follows the same trend, as well. The other important point to mention is that hydrophobicity in the conditions of the Biogenerator is subject to change (discussed in Section 4-8) and for choosing the right amount of PTFE, one should also take into account losses of hydrophobicity during the course of operation.

So far, we realized that PTFE exhibits an optimum range in respect to its effect on gas permeability, contact angle and fuel cell voltage all together. As mentioned earlier, it is the state of two phase transport in the conditions of the BioGenerator that controlls the performace and logevity of the anode elcetrode. The reason why GDL backing layers impregnated with PTFE between 80-100 wt.% perform better for the conditions of the BioGenerator is to be realized through the analysis of pore structure and pore-size distributions of the GDL. In this respect, mercury intruion porosimetry (MIP) was performed on cloth-based gas diffuion backing layers impregnated with different amounts of PTFE. Figure 4-9 shows the results obtained from porosity analysis of these BLs. As seen, as more PTFE was added, the pore diameter decreased.
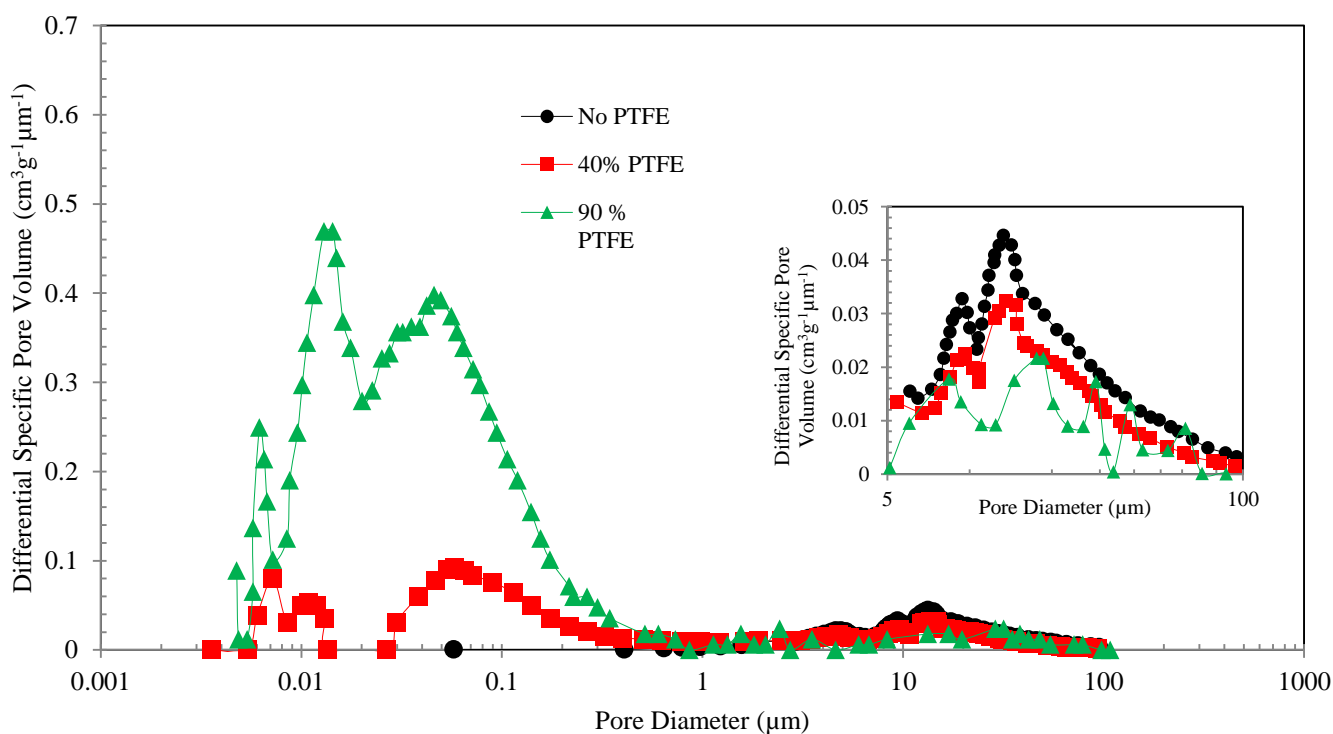
Figure 4-9 Pore size distribution curves as a function of PTFE loading in the gas diffuion backing layer

By looking into the literature on PEMFCs gas diffuion layers, depending on the system condition, the targeted performance, the range of pore diameter that is suitable for enhancing mass transfer is different. Fore instance, Kong *et al* (2002) show that larger number of macro-pores (5- 20 µm) can better enhance water managemnet in PEMFCS, while Wang et al (2006) show that presence of a large number of hydrophobic meso-pores (0.05– 7.0 µm) is essential for ensuring a reliable liquid mass transport. Considering the results obtained from Figure 4-7 and the results of porosity analysis (Figure 4-9), we can say that 80-100 wt.% PTFE showed an enhance mass transfer because they had larger number of hydrophobic meso-pores (0.08- 6 µm).

4.4   Catalyst Layers Bound with Different Amounts of PTFE

PTFE was used as the binder of Pt/C particles in the catalyst layer. Since the anode electrode suffered from flooding, higher amounts of PTFE were desirable. While, the higher PTFE migh help prevent flooding in the catalyst layer, at the same time it would decrease the catalyst utilization due to covering catalyst particles. Different amounts of PTFE, 15%; 30%, 40%, 60%, were studied and anode electrodes were made using the spreading technique. Figure 4-10 shows i-V curves obtained from the BioGenrator employing these electrodes. As observed, CL 15% exhibited a better performance in terms of a full range of current densities. However, our interest was in low current densities (100 mA cm^{-2}) and as the i-V curves suggest, there is not a significant diffrence in the perormance at low current densities. In early development of catalyst layer for PEMFCs, usually when PTFE was used as a binder, 30% was the optimum value to chose (S Litster *et al*., 2004). It is believed that BioGenerator requires higher contents of PTFE and since there was not a considarable diffrence in performance between 30% and 40%, 40% was chosen as the amount of PTFE in the catalyst layer. The obtained i-V curves also show that the performance noticeably decreased when PTFE occupied 60% of the catalyst layer. The curvature at high current densies proves that 60 wt.% PTFE not only did not enhance mass transfer, but hampered the gas diffuion through the catalyst layer.
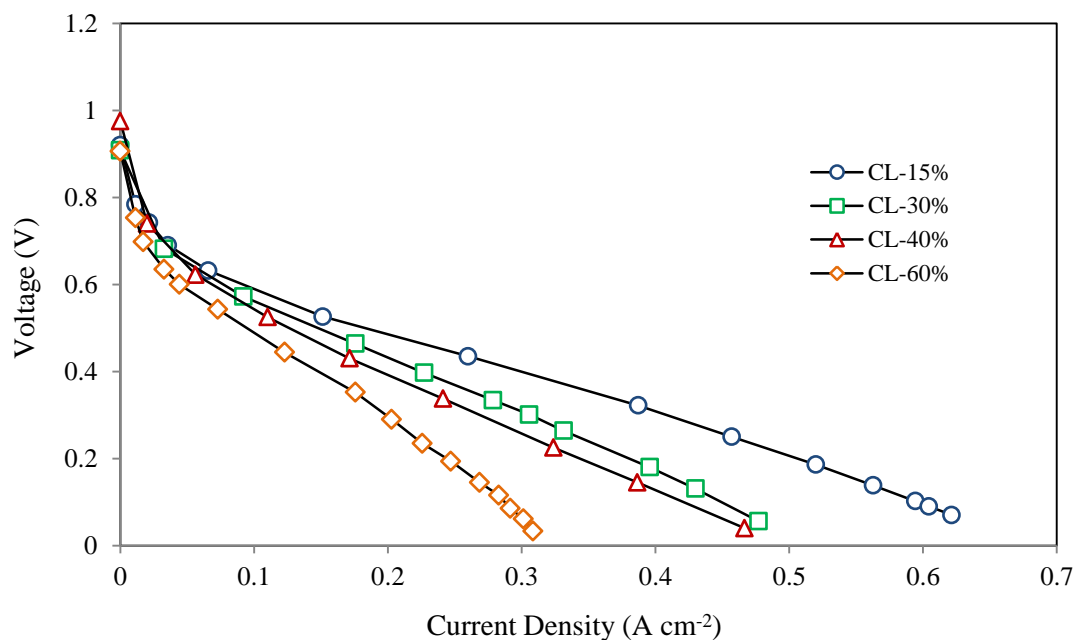
Figure 4-10 i-V curves obtained for fuel cells running with different contents of PTFE in their catalyst layers.

It was needed to prevent diffusion of aqueous cathodic electrolyte through the membrane to the anodic catalyst layer as much as possible. We expected to achieve hydrophobic catalyst layer by adding PTFE to its ink. The idea was that a hydrophobic surface would prevent the permeation of liquid to its pores. However, we needed to know whether by increasing the amount of PTFE, the surface hydrophobicity would change. To understand the impact of PTFE content on surface wettability of catalyst layers, contact angle measurements were performed on these surfaces. As shown in Figure 4-11, the changes in surface contact angle were not significant in respect to changes in the content of PTFE.
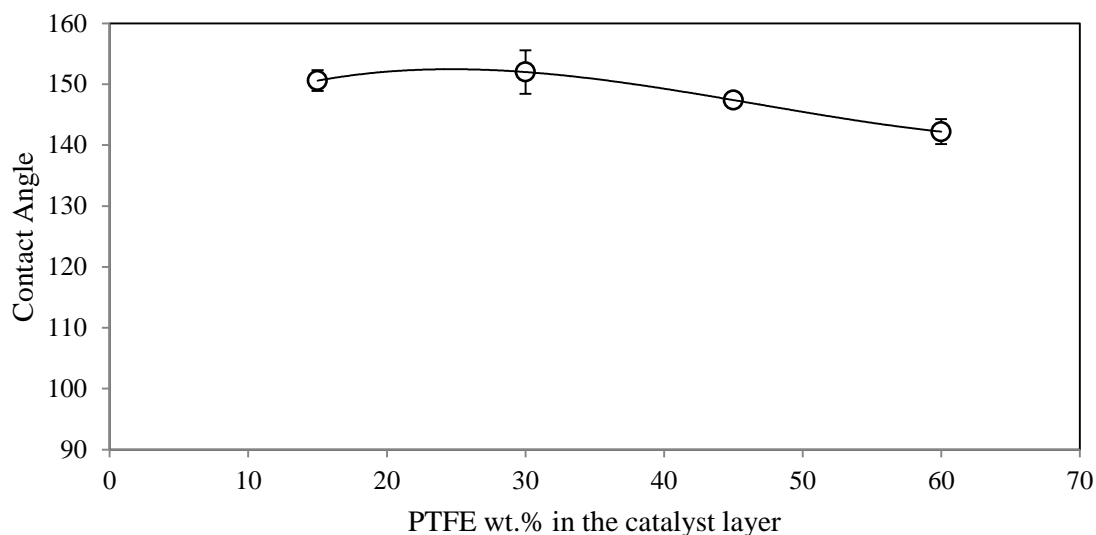
Figure 4-11 Surface contact angle of catalyst layers impregnated with different amounts of PTFE

Analyzing the performance of catalyst layers loaded with different amounts of PTFE was performed to estimate the range in which PTFE integration into the catalyst layer would work better. Figure 4-12 shows some schematic pictures that explain the role of hydrophobicity in the catalyst layer. As shown, a too low amount of PTFE would cause flooding by lettering liquid cover the surface of catalyst particles. In addition to that, a too low amount of PTFE does not provide a reliable binding between Pt/C particles that would results in detachment of the catalyst layer (Figure 4-12-a). On the other hand, a too high amount of PTFE might hamper diffusion of gas within the catalyst layer as well as to increase the electrical resistivity of the catalyst layer, which both can lead to decreasing the performance of the fuel cell (4-12-b). The former, as evident in Figure 4-10-CL 60%, can cause mass transfer loss. Therefore, an optimum amount of PTFE is needed in the catalyst layer to bind particles together, enhance mass transfer, and does not introduce large electrical resistance to the catalyst layer (4-12-c). This type of trend observed here has been observed in research conducted on PEM fuel cell cells where they were more interested in using Nafion as a binder. For instance, Passalacqua and co-workers (2001) tested different amount of Nafion (14- 66 wt.%) and found that 33 wt.% gave a better performance (Passalacqua, Lufrano *et al*., 2001). It is worth noting that this range of optimum value for PTFE in the catalyst layer is going to be different from system to system. It depends on the reacting

gas, the amount of liquid flux passing through the membrane, the targeted performance that system demand and so on.
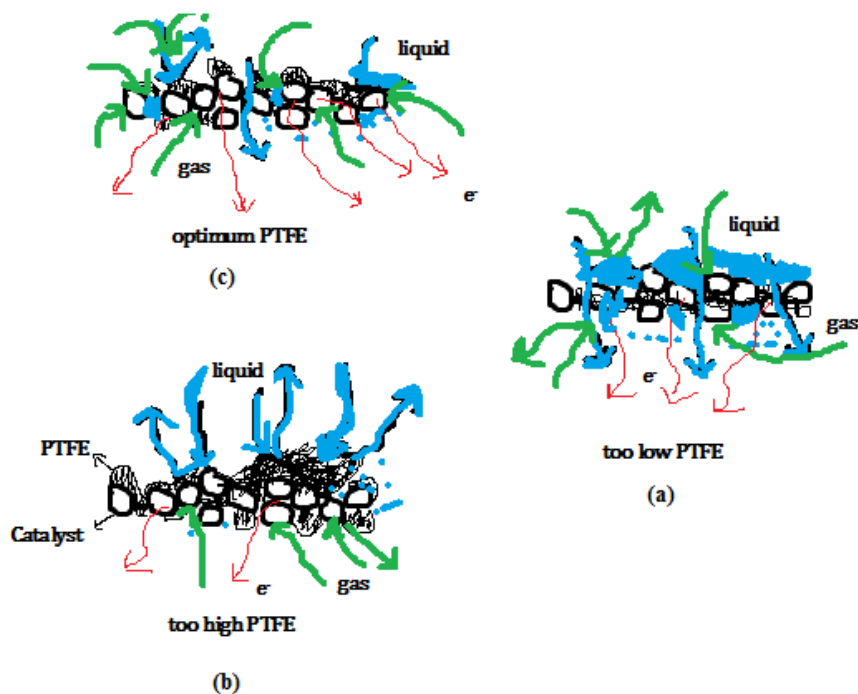
Figure 4-12 Scheme of impact of PTFE in mass transport within the catalyst layer

4.5 Comparing the Performance and Long-term Durability of Developed Electrodes Fabricated by the Spreading Technique with Commercially Available PEMFCs Electrodes

Based on the results from the previous section, anode electrodes were fabricated using a knife spreader described in 3-1-3-3. The anode backing layer was cloth impregnated with 85% PTFE. The MPL loading was 1.5 mg cm^{-2} and 30 wt.% PTFE. The catalyst loading was 0.5 mg Pt cm^{-2} bounded with carbon particles and 40 wt.% PTFE. Table 4-1 compares the specifics of the developed and commercially available electrodes.

Table 4-1 Physical characterizations of developed and commercially available electrodes

Electrode type	Thickness (mm)	Porosity			Contact angle (Θ)		Air permeability K (m²)
		Total pore area (m²/g)	Total pore volume (mL/g)	Average pore diameter (μm)	BL	CL	
This work	0.727 ± 0.007	2.7	0.59	0.85	151.3 ± 4.7	152.1 ± 3.6	1.66×10^{-11} ± 4%
SLGDE	0.420 ± 0.006	15.2	1.12	0.29	139.2 ± 2.3	102.2 ±4.3	2.62×10^{-13} ± 2%

Figure 4-13 shows the performance of different fuel cells employing commercial and the developed anode electrodes as a function of time when operating continuously at current density of 100 mA cm^{-2}. Evidently, the developed electrode comprising a hydrophobic backing layer impregnated with 85 wt.% PTFE and a PTFE-bound catalyst layer and a hydrophobic micro-porous in between, exhibited more stable and durable performance as opposed to SLGDE. As seen, after about 500 hours of operation, the commercial electrode (SLGDE) started to show instability and deterioration in the performance and after about 1800 hours of operation, it almost reached its end of life. On the other hand, the developed electrode exhibited that it was more durable in the continuous operation up to about 2500 hours. At some point in the operation, due to some issues in the bioreactor, the system was shut down and the hydrogen pressure was absent in the electrode. After the system went back on the normal operation, however, it is obvious that we had so many fluctuations in the performance.
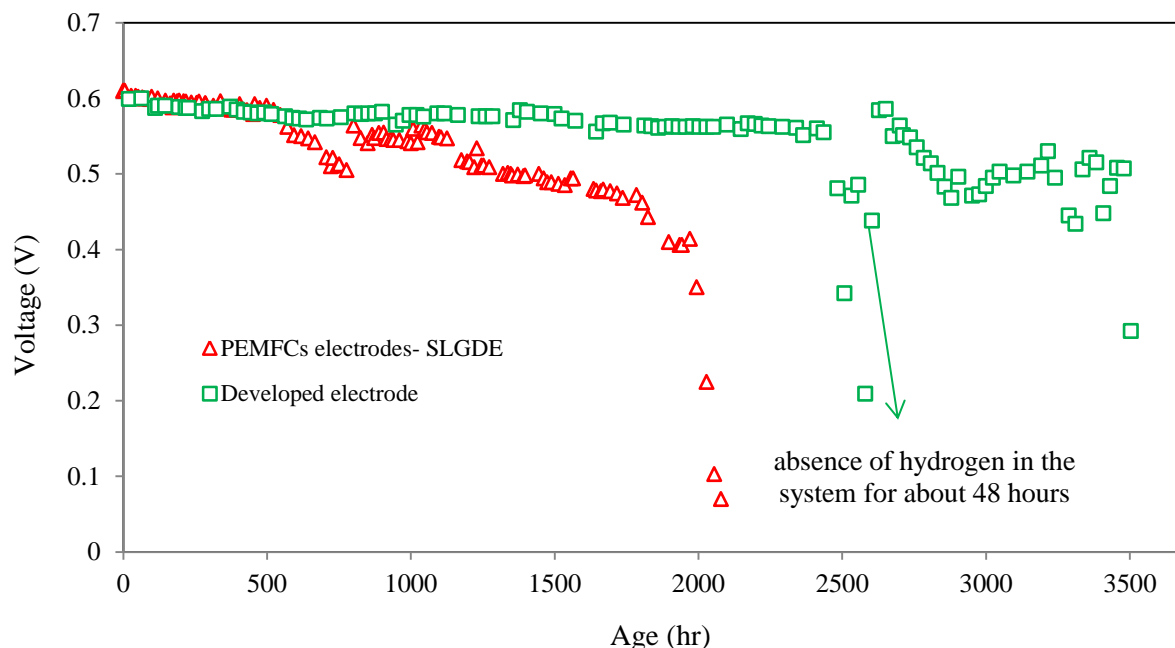
Figure 4-13 durability in performance for developed electrodes (PTFE: 85% in BL- 30% in MPL- 40% in CL- 5 cm^2 cell) and commercially available electrodes (SLGDE) running at constant current density of 100 mA cm^{-2}.

This instability in performance is due to flooding of the anode electrode due to creating negative pressure in the anode channels that resulted in a lot of back penetration of the electrolyte into the pores of the anode electrode. At this point, the cells were opened, the cathode and the membrane were changed and the anode electrode was dried and then cells were reassembled and system was put back on operation.

Because the system was operating at relatively low current density, it was hard to judge the ultimate stability of the cells towards flooding and other causes of the performance degradation. Therefore, in order to obtain more detailed information on differences in the stability of the electrodes, i-V measurements were periodically performed during the course of operation and Figure 4-14 shows these results. As observed, the cells using developed electrodes exhibit, in overall, more stable performance as compared to SLGDE.
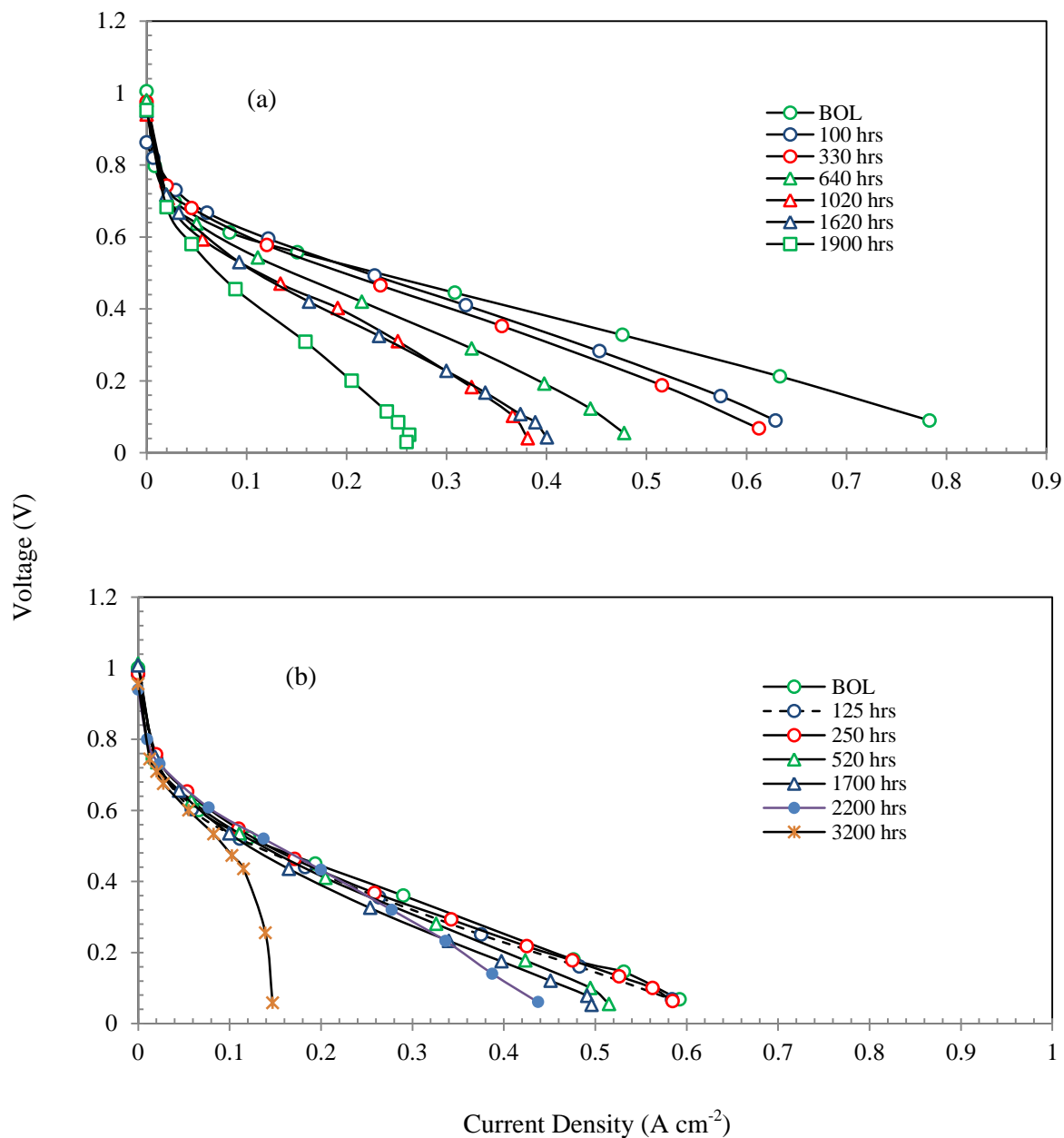
Figure 4-14 i-V curves obtained for fuel cells running with a) commercial PEMFCs anode electrode (SLGE); b) the developed electrode.

According to i-V curves, at the beginning, SLGDE exhibited better performance compared to that of the developed electrode. However, during the course of operation, a notable decline was observed in the performance of SLGDE. The developed electrode exhibited a higher degree of stability mainly because of an enhanced mass transport within its three layers. As evident, the developed electrode performed more stable in all the ranges of current densities as opposed to

SLGDE. To explain this, one should consider the hydrophobic structure of layers of the anode electrode as tunnels that gas and liquid from two opposite sides can pass through. During the course of operation, there is back diffusion of the cathodic electrolyte to the anode electrode and it penetrates all the way through the catalyst layer, MPL, and BL to finally exit from the gas channels. Liquid can occupy pores in all three of the layers with its movement and if pores are not hydrophobic enough to reject the liquid droplet out of their space and if enough paths are not availble for hydrogen gas to diffuse from channels to the catalyst sites, we will have a blockage of pores by liquid or what is referred to as flooding. In this basis, meso-pores of the GDL is more preferable to control the flooding. In other words, by proposing this three-layer hydrophobic structure for the anode, we tried to prevent penetration of the cathode electrolyte to the gas diffusion electrode. It is true that after some time, the driving force caused by back diffusion will suppress the repulsive forces formed by the hydrophobic surface of the catalyst layer and at this point, the anode electrode is susceptible to flood. However, hydrophobic structure of the catalyst layer and the gas diffusion layer provide hydrophobic paths to accommodate the penetrated liquid to pass through the gas diffusion layer and easily exit from the anode structure. Therefore, we have provided spaces for hydrogen gas to reach the catalyst layer. As SEM images (Figure 4-15) suggest, relatively larger number of meso-pores and macro-pores in the structure of the developed electrodes are evident for better mass transport within the catalyst layer. In addition to the size of the pores, hydrophobic structure of the developed electrodes make transport of liquid and gas through the catalyst layer easier. In other words, hydrophobic pores do not let liquid droplet stay in the pores and block the transport of gas but help them more easily rejected from the porous structure.

SEM images (Figure 4-15) that captured the top view of catalyst layers show the structural differences between commercially available electrodes and the developed electrodes in different magnifications.

(a)

(b)

(c)

(d)
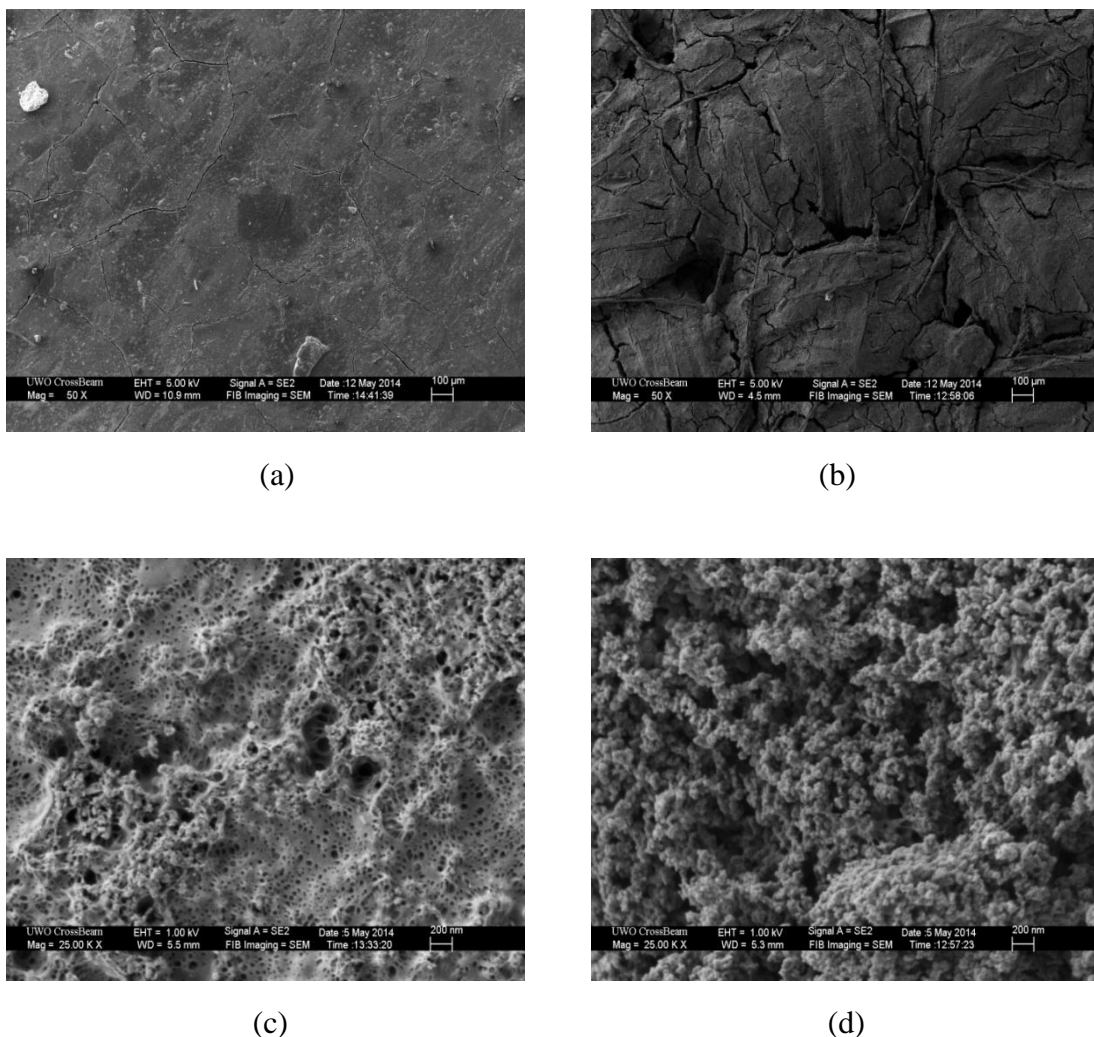
Figure 4-15 Top view SEM of catalyst layers. a) SLGDE-50 times magnification; b) the developed anode-50 times magnification; c) SLGDE-25000 times magnification; d) the developed anode-25000 times magnification

4.6 Failure Modes of Anode Electrodes

4.7 Electrochemical Degradation

Our results showed that electrochemical degradation of the catalyst layer and hydrogen mass transfer limitations due to flooding of the anode electrode were two sources of long-term performance failure. Cyclic voltammetry of fresh and deteriorated anode electrodes suggested that we had a considerable loss in electrochemical surface area. Figure 4-16 shows cyclic voltammetry results obtained from fresh PEMFC and the developed electrodes. As expected, hydrogen adsorption-desorption peaks appeared smaller for the developed electrode than that of Nafion-post coated SLGDE electrode. This lower exhibition of electrochemical surface area was

the consequence of impregnation of high content of PTFE (40 wt.%) which resulted in lower levels of electrochemical activity towards the hydrogen oxidation reaction. Based on calculations (Cooper 2009), electrochemical active area of the catalyst layer decreased to less than 40% of its initial value- from 32 m^2 Pt g^{-1} Pt to 11.5 m^2 Pt g^{-1} Pt. Ex-situ cyclic voltammetry ensures that we are only dealing with electrochemical activity of electrodes not mass transfer or ionic resistance. On the other hand, the developed electrode exhibits lower performance than even degraded SLGDE electrodes which proves the main limitation towards performance deterioration in this configuration was anode flooding. However, it is difficult to judge which layer (BL, MPL, or CL) had the most contribution to the mass transfer limitations.
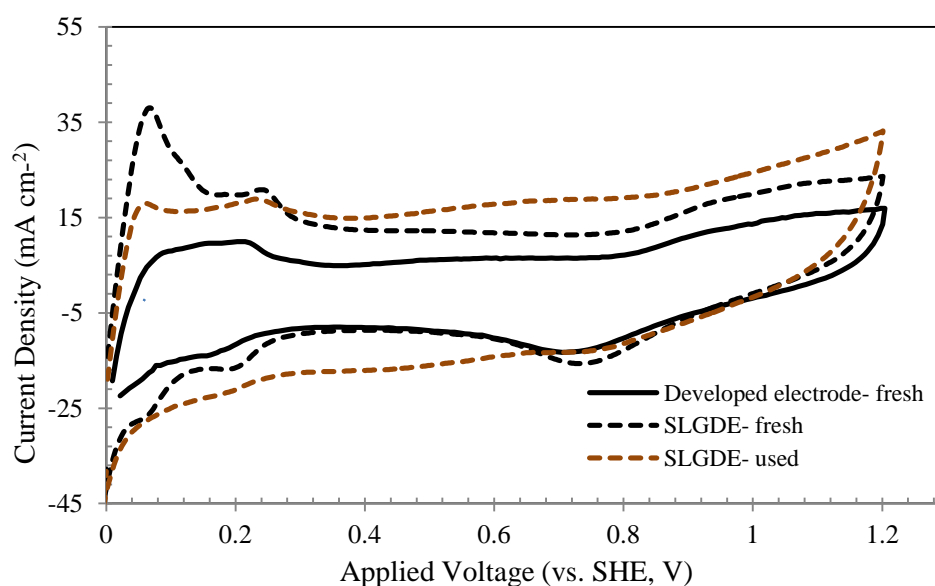
Figure 4-16 Ex-situ CV voltammograms obtained for fresh anode electrodes and after 2000 hours of continues operation at 100 mA cm^{-2} in the fuel cell.

One of the concerns in respect to the degradation of the catalyst layer in the BioGenerator was contamination of the catalyst layer by iron sulfate solution existing in the cathodic electrolyte (the ferric iron permeability is approximated to be 3.5×10^{-5} cm^2 min^{-1} (Pupkevich *et al.*, 2013)). XPS analysis was performed on both Nafion post coated commercial and the developed electrodes and it did not detect presence of iron element in the surface of the catalyst layer (Figure 4-17). The effect of iron poisoning is coverage of active sites of the catalyst layer by iron elements that could result in deterioration in the electrochemical active area of the anode electrode and the consequent performance.
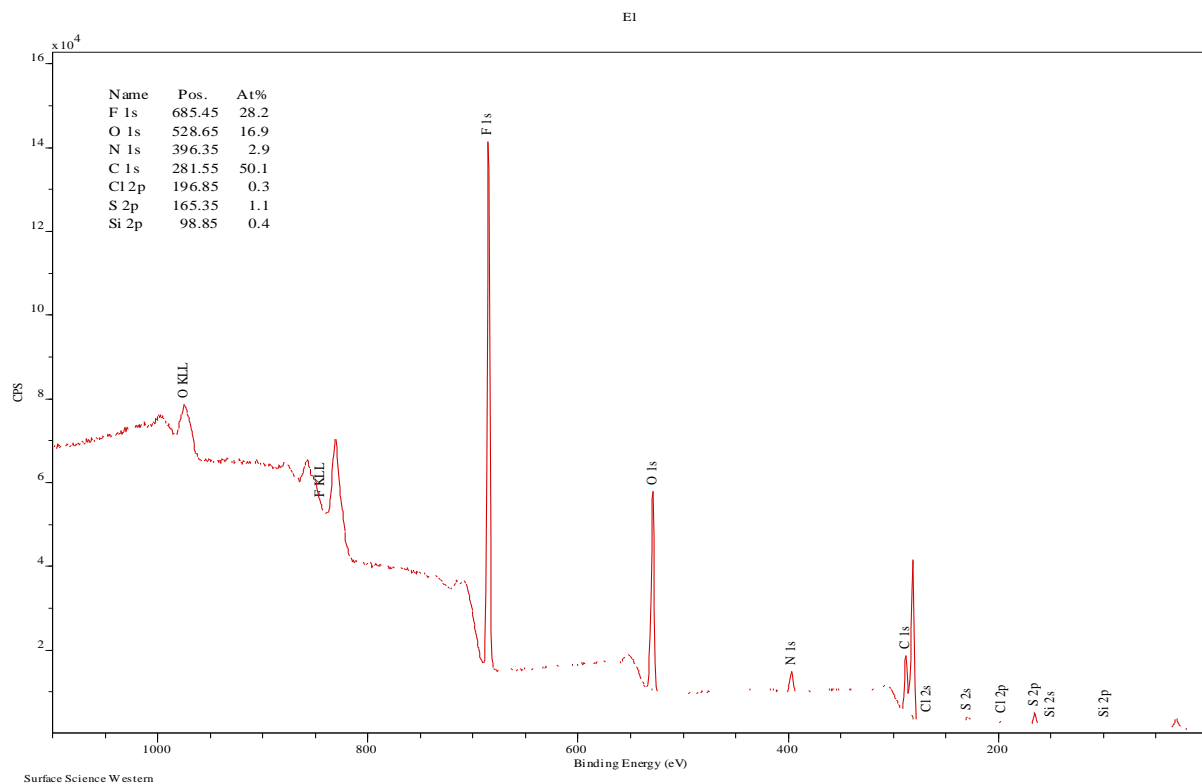
Figure 4-17 XPS analysis obtained from the surface of the catalyst layer of Nafion-post coated electrodes. As seen, there is no peak detecting presence of Fe element.

Figures 4-18 and 4-19 show SEM pictures obtained from surface of the catalyst layer before and after the operation in the system. It is evident that size of particles has grown and particle growth was one of the causes of decline in the activity of the catalyst layer.

Platinum agglomeration is known to happen as a result of two main processes. One of them is Ostwald ripening process. A well-understood example of Ostwald ripening process is Pt dissolution and redeposition (Borup *et al*., 2007). This specifically happens in high voltages. The second possible cause would be Coalescence.
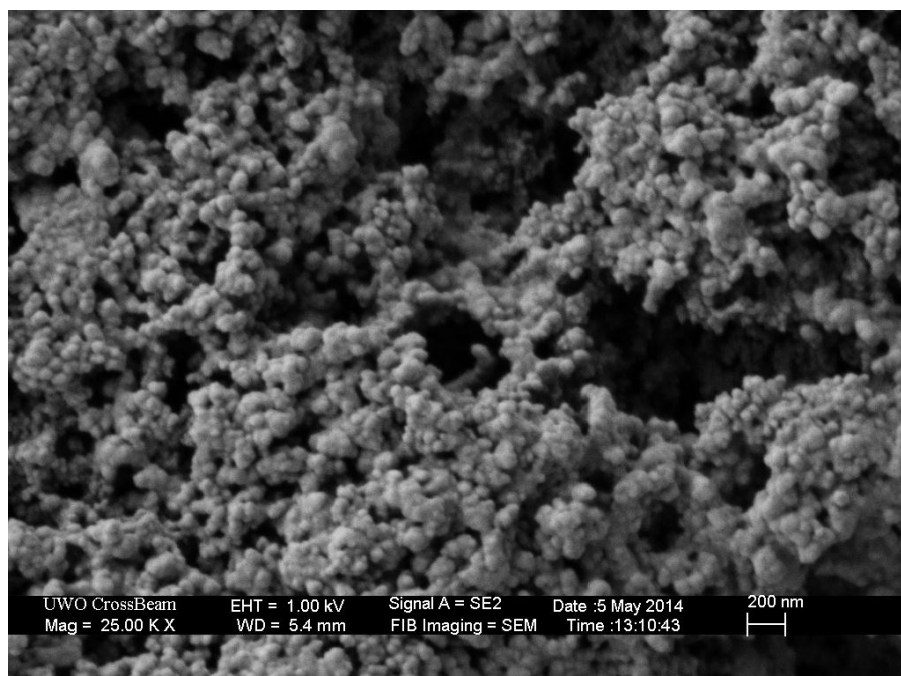
Figure 4-18 Top view SEM of the catalyst layer of used anode electrodes (after about 2500 hours of operation).
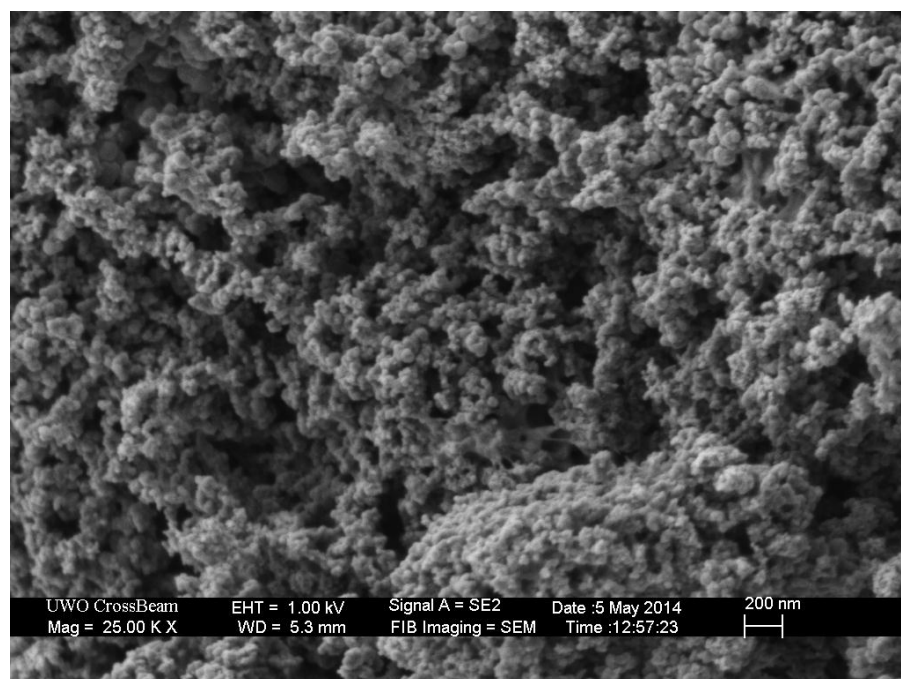
Figure 4-19 Top view SEM of the catalyst layer of fresh anode electrodes.

Coalescence mechanism is referred to as growth of catalyst particles. It can be due to growth of Pt nanoparticles through Pt nano-crystalline mitigation on the carbon support. The other

possibility would be Pt particles agglomeration caused by corrosion of the carbon support (X. Cheng *et al*., 1999; Ferreira *et al*., 2005; Yasuda *et al*., 2006).

4.8   Loss of Hydrophobicity

During the course of operation, a considerable loss was observed in the hydrophobicity of the surface of the anode electrode in both the CL and BL. Contact angle measurements of fresh and used electrodes suggest that hydrophobicity of the CL and the BL changed to some significant extent (Figure 4-20). This loss in hydrophobicity might be due to the degradation of PTFE particles or that PTFE content was washed away.
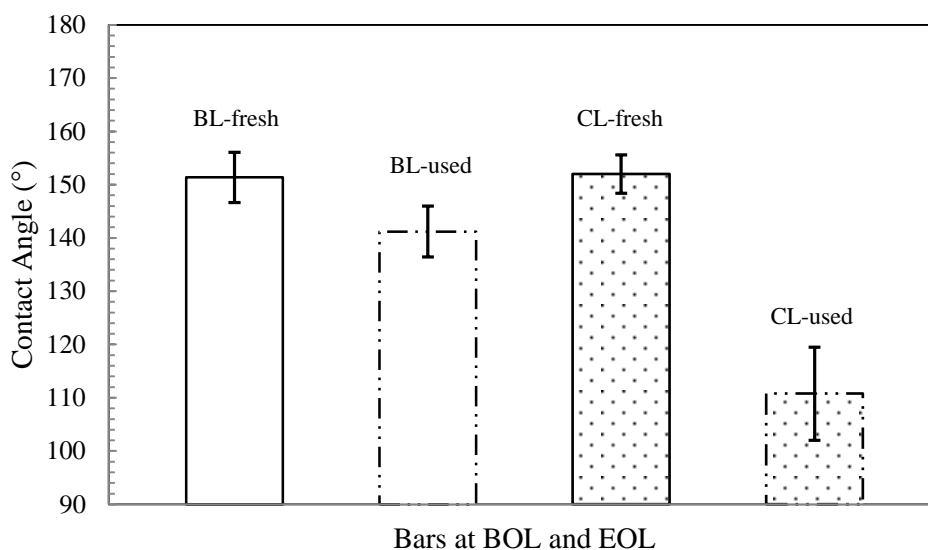
Figure 4-20 Contact angle values obtained for the developed electrodes at BOL (fresh) and EOL (used- after 2900 hrs of continuous operation at 100 mA cm^{-2}) for the backing layer and the catalyst layer sides.

4.9   Delamination

In some cases, that hot pressing was not used in the fabrication process, we had delamination of the catalyst layer from the MPL (Figure 4-21). In addition, for some electrodes, we had a sudden drop in voltage during the operation and when SEM was done on the used sample, detachment of the catalyst layer was evident (Figure 4-22). Hot pressing is a critical process. Its absence can result in delamination of the layers, while it can cause penetration of the layers to each other, which is undesirable. The pressure, temperature, and the time of press are factors that are

important in hot pressing. In this study, hot press was performed for 15 seconds at 100 psi, 80°C on both the MPL and the CL.
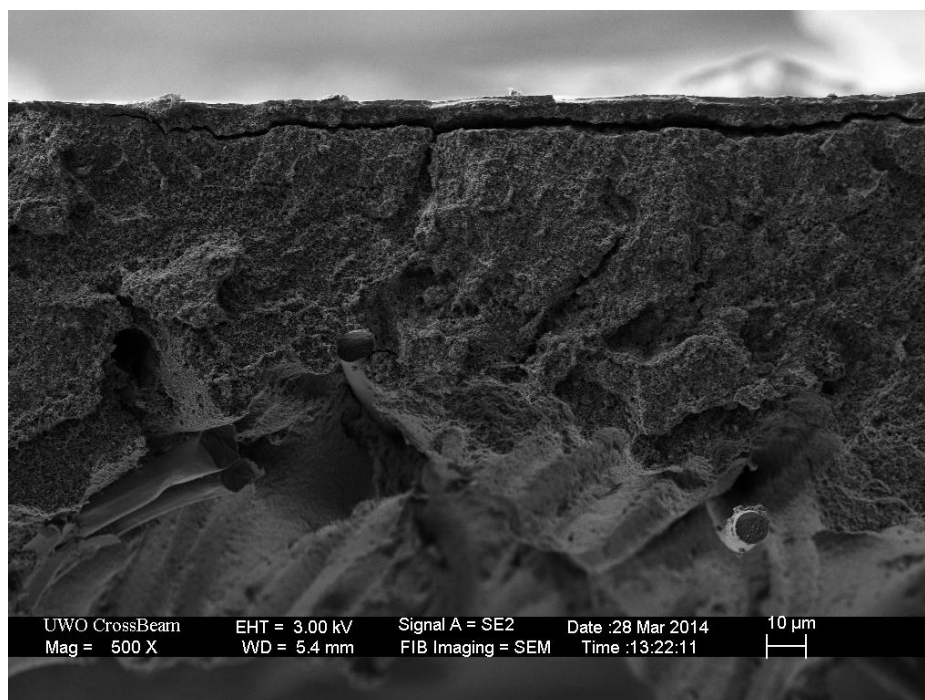
Figure 4-21 Cross-section image of the anode electrode. Delamination of the catalyst layer in a used anode electrode is shown in the SEM image
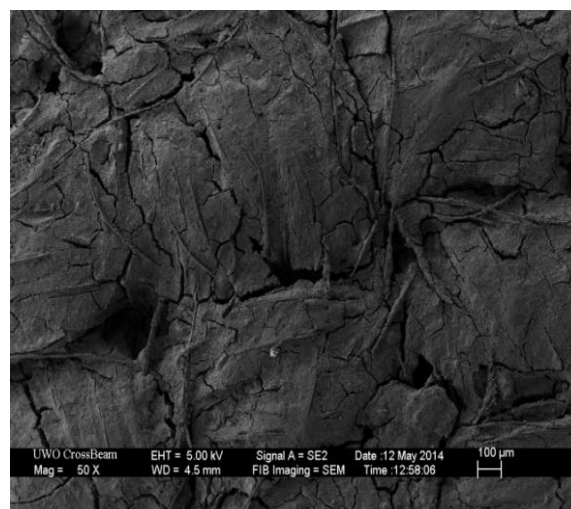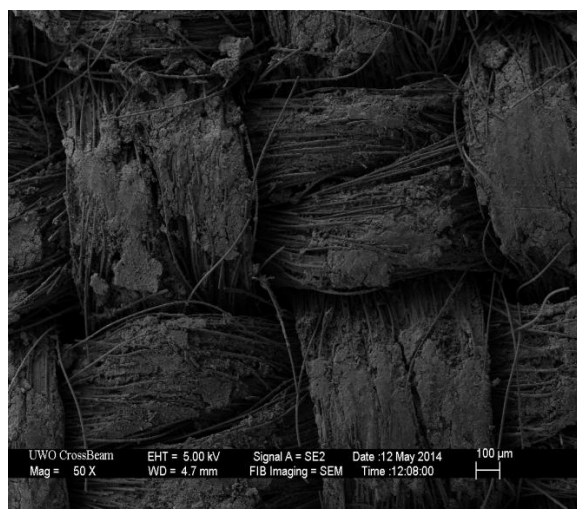
Figure 4-22 Top view SEM image of the catalyst layer of left) used electrode after 600 hours of operation and right) fresh electrode. The detachment of the catalyst layer is obvious.

5   Conclusions and Recommendations

5.1   Conclusions

In this work, three-layer-based hydrophobic anode electrodes for the application of the BioGenerator were proposed. Experiments showed that available commercial fuel cell electrodes are not suitable options for use in the BioGenerator. Although they give higher short-term performance, they do not exhibit a durable performance for long-term operations. The effect of hydrophobic polymer content in the backing layer was studied through both ex-situ experiments and in-situ performance analysis in the real BioGenerator. It was concluded that carbon cloths are preferable base-materials for the anode electrodes because they are mechanically flexible and our experiments showed they have a good capacity in accepting PTFE in their pore network to become very hydrophobic without hampering the gas permeability. In addition, results of the present work showed that gas permeability and contact angle of PTFE-treated backing layers represent an optimum range in the neighborhood of 80- 100 wt.% (in respect to the weight of untreated cloth) and presence of hydrophobic meso-pores in the GDL was essential to enhance mass transfer and prevent liquid flooding in the anode electrode. Another important result obtained from this work was that the dominant source of limitation in the performance of anode electrodes was mass transfer of hydrogen gas through the GDE or more correctly flooding of pore network by back diffusion of cathodic electrolyte through the membrane to the anode electrode. Additionally, some preliminary experiments were performed in order to understand other causes of failure in the BioGenerator anode electrodes. Our results showed that agglomeration of particles in the catalyst layer was evident after about 2500 hrs of continuous operation at 100 mA cm^{-2}. Moreover, activity of the catalyst layer could decrease to about 40-50% of its initial value; however, that was not the dominant source of deterioration. Hydrophobicity of the catalyst layer had a considerable reduction, while the backing layer hydrophobicity was not subject to as much reduction. This might direct our mind to think of carbon corrosion as one of the sources of the catalyst layer deterioration. Furthermore, an important hypothesis in respect to contamination of the catalyst layer surface by iron ions (present in the cathodic electrolyte) was investigated. XPS results did not detect elements of iron on the surface of the catalyst layer neither in the case of Nafion-post coated electrodes nor in the case of PTFE-bound electrodes. This might direct our future research towards employing to

some extend Nafion to the mixture of the PTFE-bound catalyst layer or alternatively as a thin layer coated onto the surface of the hydrophobic catalyst layer to enhance proton conduction within the catalyst layer-membrane interface. Followings briefly list the conclusions obtained from this work:

- Experiments showed that carbon cloth was the material of choice for the anode gas diffusion backing layer and could accommodate high contents of PTFE without hampering the gas permeability.

- 80-100 wt.% PTFE (in respect to the weight of untreated cloth) gave the highest through- plane gas permeability to the backing layers and provide larger number of hydrophobic meso-pores which could control the flooding more efficiently.

- The developed electrodes (proposed in this work) exhibited more stable performance within a full range of current density as compared to commercially available electrodes. In addition, they exhibited an enhanced longevity (at 100 mA cm^{-2} current demand) as compared to commercially available electrodes.

- Agglomeration and the consequent particles growth were evident in the catalyst layer as a result of long-term operations.

- Through long-term operations, contamination of the catalyst layer by iron element was not observed.

- A spreading technique was developed for the fabrication of the MPL and the CL suitable for large-scale production of the BioGenerator anode electrodes and gave relatively more reproducible results as compared to brushing and spraying.

- Although catalyst layer activity reduction was evident, limitations caused by gas mass transfer (liquid flooding within the pores) seemed to be the dominate source of the anode performance deterioration.

5.2 Recommendations

The BioGenerator fuel cell is a new system and has a unique structure. Therefore, other researchers can think of followings as proposals to continue the current work or study new elements and approaches in obtaining high performance and durable anode electrodes for the application of the BioGenerator

- The MPL loading, the amount of hydrophobicity and the type of carbon material are three parameters that can affect the performance of the MPL in the BioGenrator. Research might be conducted in determining the effects of these parameters in long-term operations of the BioGenerator. Carbon loading influences water management and electrical resistivity of the MPL. In addition, PTFE affects pore volume and the pore size distribution in the MPL as well as hydrophobicity. Moreover, carbon type can control the pore-volume and pore size distribution in the MPL.

- Catalyst loading, support material, the amount of hydrophobicity and use of an ionomer as a binder are among the parameters that can influence the performance of the BioGenerator for both short-term and long-term operations. Other than controlling the mass transport, the CL plays more important role that is driving the hydrogen oxidation reaction. Not all the parameters that help control the liquid flooding can have a positive effect on the electrochemical characteristics of the catalyst layer. As observed in this work, making the CL hydrophobic could help prevent flooding but had a negative effect on the electrochemical performance of the hydrogen oxidation reaction. Therefore, based on the demand, one should consider both sides. Since Nafion is highly proton conductive, and no iron contamination was detected on the Nafion post-coated catalyst layer, it would be useful to examine the influence of the Nafion in the catalyst layer on the long-term stability of the anode electrodes. Moreover, pulse electrodeposition could be a powerful technique in fabricating catalyst layer anode electrodes for the BioGenerator because we can have a good control over catalyst particle size and utilization of the catalyst particles. In this work, a continuous bath electrodeposition cell was proposed (Figure 3-3). Electrodeposition on hydrophobic GDLs was not successful mainly because the surface

of the GDL did not have any Nafion to exchange the Pt^{2+} ions. However, for the future research, one may try other salts such as $H_2PtCl_6.6H_2O$ that generate $PtCl_6^{2-}$ ions.

- One of the challenges in studying the long-term durability of the BioGenerator is that it is targeted to work at low current densities, and in this case, the effects of any deterioration will show up after relatively long periods of time (1700- 2500 hrs). That can become very time consuming. Therefore, an accelerated test protocol is needed for further research.

- One interesting research could be observing the influence of scale-up over long-term durability of the anode electrodes in the BioGenerator. There are at least two factors that play roles in mass transport management. One is pressure drop (liquid pressure distribution) in the cathode channels that influences the distribution of electrolyte back diffusion to the anode electrode plus the performance of the cathodic reaction. The other factor is influence of scale up on surface morphology of the anode layers.

- One can think of replacing the current structure of the BioGenerator fuel cell with series but separated tubular electrodes submerged in the bioreactor. It might bring us at least three advantages. One is eliminating the effect of liquid pressure distribution in the cathode side on the anode electrode and on the efficiency of the cathodic reaction. Second is avoiding clogging of cathode inlet and outlet due to growing microorganisms on the surface of the cathode electrode. Moreover, it will enable us to replace more easily the deteriorated or flooded electrodes with fresh ones.

6 References

Allen, Robert J, Peter C Foller, Ravindra J Vora, R Todd Bombard , and Michael DeMarinis . "Full-Scale Hydrogen Anodes for Immersed-Tank Electrowinning." *JOM* 45 (1993): 49-53.

Allen, Robert J, Ravindra J Vora, and Michael De Marinis. Antipercolation Gas-Diffusion Electrode and Method of Making Same. USA Patent US5300206 A. 04 05, 1994.

Antolini E. "Formation of Carbon-Supported PtM Alloys for Low Temperature Fuel Cells: a Review." *Mater Chem Phys* 78 (2003): 563–73.

Barnes, F, and J Levine . *Large Energy Storage Systems* . CRC, 2011.

Borup , R, J Meyers , B Pivovar B, YS Kim, and R Mukundan . "Scientific Aspects of Polymer Electrolyte Fuel Cell Durability and Degradation." *Chemical Reviews*, 2007: 3904–51.

Bouwman P, Teliska ME, and Lyons K. "Increased Poisoning Tolerance of Pt-FePO Oxygen Reduction Catalysts in: Proton Conducting Membrane Fuel Cells IV. Van Zee et al., editors." *Electrochemical Society Proceedings*, 2004.

Brady, M P, et al. "Cost-Effective Surface Modification for Metallic Bipolar Plates." DOE FY Progress Report, 2004.

Buenoa, C, and J.A. Carta. "Wind Powered Pumped Hydro Storage Systems, a Means of Increasing the Penetration of Renewable Energy in the Canary Islands." *Renewable and Sustainable Energy Reviews* 10, no. 4 (2006): 312-340.

Cheng , X, B Yi , M Han , J Zhang , Y Qiao , and J Yu . "Investigation of Platinum Utilization and Morphology in Catalyst Layer of Polymer Electrolyte Fuel Cells." *Power Sources* 79 (1999): 75–81.

Cheng, X, C Yi, Y Zhang, and J Yu Qiao. "Investigation of Platinum Utilization and Morphology in Catalyst Layer of Polymer Electrolyte Fuel Cells." *Power Sources* 79 (1999): 75–81.

Church, Steven. "Del. Firm Installs Fuel Cell." *The News* , 2006.

Cooper, Kevin R. "In-situ PEM Fuel Cell Electrochemical Surface Area and Catalyst Utilization Measurement." *Fuel Cell Magazine*, Jan/Feb 2009.

Cunningham, B D, J Huang, and D G Baird. " Development of Bipolar Plates for Fuel Cells from Graphite Filled Wet-Lay Material and a Thermoplastic Laminate Skin Layer." *Power Sources* 165 (2007): 764–773.

De Geeter, Eddy, Michael Mangan, Staf Spaepen, William Stinissen, and Georges Vennekens. "Alkaline Fuel Cells for Road Traction." *Power Sources* 80 (1992): 207–212.

de Waalb, E, E Middelmana, E Kouta, and B Vogelaarb. "Bipolar Plates for PEM Fuel Cells." *Power Sources* 118 (2003): 44-46.

DOE. *FOSSIL.* November 15, 2013. http://energy.gov/science-innovation/energy-sources/fossil (accessed May 04, 2014).

DOE. *Technical Plan- Fuel Cells.* Multiyear Research Plan, Washington, DC: DOE, 2012.

Drouineau, M, N Maïzi, and Mazauric Mazauric. "Impacts of Intermittent Sources on the Quality of Power Supply: The Key Role of Reliability Indicators." *Applied Energy* 116 (2014): 333–343.

EERE, DOE-. *Comparison of Fuel Cell Technologies.* EERE Information Center, 2011.

Egerton, R F. *Physical Principles of Electron Microscopy : An Introduction to TEM, SEM, and AEM.* Springer, 2005.

Engelhard, Mark . *X-Ray Photoelectron Spectroscopy XPS.* Prod. EMSL. n.d.

Ferreira, PJ, O GI La , Y Shao-Horn , D Morgan , and Makha. "Instability of Pt/C Electrocatalysts in Proton Exchange Membrane Fuel Cells." *Electrochemical Society* 152 (2005): A2256–71.

Free, Michael L, et al. *Electrometallurgy 2012.* Wiley, 2012.

FuelCellEtc. *FuelCellToday.* 03 12, 2013. (accessed 05 07, 2014).

Garsany Y, OA Baturina, and Swider-Lyons KE. "Impact of Sulfur Dioxide on the Oxygen Reduction Reaction at Pt/Vulcan Carbon Electrocatalysts." *Electrochem Soc* 154 (2007): 670–675.

Geertsma, J. "Estimating the Coefficient of Inertial Resistance in Fluid Flow." *Soc. Pet. Eng. J* 10 (1974): 445–450.

Gevantman, L H. "Solubility of selected gases in water." *Nitric Oxide* , 2000: 80-83.

Giesche, Herbert. "Mercury Porosimetry: a General (Practical) Overview." *Part.part.syst.charact* 23 (2006): 1-11.

Glaser, P. "Power from the Sun: Its Future." *Science* 162 (1968): 857-861.

Gostick, Jeff T, Michael W Fowler, Mark D Pritzker, and Marios A Ioannidis. "Porosimetry and Characterization of the Capillary Properties of Gas Diffusion Media." In *PEM Fuel Cell Diagnostic Tools*, by Hui Li, 515-532. Taylor& Francis, 2012.

Gostick, JT , MW Fowler, MD Pritzker, MA Ioannidis, and LM Behra. "In-plane and through-plane gas permeability of carbon fiber electrode backing layers." *Power Sources* 162 (2006): 228-238.

Gülzow, Erich . "Alkaline Fuel Cells: a Critical View." *Power Sources* 61 (1996): 99–104.

Hadjipaschalis, I, Poullikkas, and Efthimiou Efthimiou. "Overview of Current and Future Energy Storage Technologies for Electric Power Applications." *Renewable and Sustainable Energy Reviews* 13 (2009): 1513–1522.

Heinzel, A , F Mahlendorf, and C Jansen. "Bipolar Plates." *Elsevier*, 2009.

Hermanna, A, Chaudhuria, and T Spagnolb. "Bipolar Plates for PEM Fuel Cells: A Review." (Int J. Hydrogen Energy) 2003: 1297–1302.

Hojjati, Hossein, Kalin Penev, Victor R Pupkevich, and Dimitre G Karamanev. "Modeling, Simulation, and Optimization of Hybrid Fe (II)/Fe (III) Redox Flow Fuel Cell System." *AICHE* 59, no. 06 (2013): 1844–1854.

Hongthong, K, K Pruksathorn, P Piumsomboon, and P Sripakagorn. "Effect of the Geometry and Pattern of the Flow Channel on the Performance of Polymer Electrolyte Membrane Fuel Cell." *Korean J. Chem Eng* 24 (2007): 612-617.

Ismail, M S, T Damjanovicb, D B Inghama, M Pourkashaniana, and A Westwoodc. "Effect of Polytetrafluoroethylene-Treatment and Microporous Layer-coating on the Electrical Conductivity of Gas Diffusion Layers used in Proton Exchange Membrane Fuel Cells." *Power Sources* 195 (2010): 2700–2708.

John, T, and T Weir. *Renewable Energy Resources.* 2. New York: Taylor & Francis, 2006.

Kangasniemi , KH, Condit DA, and Jarvi TD. "Characterization of Vulcan Electrochemically Oxidized under Simulated PEM Fuel Cell Conditions." *Electrochem Soc* 151 (2004): 125–132.

Karamanev, Dimitre Gueorguiev , Victor R Pupkevich, and Hossein Hojjati. Bio-Fuel Cell System. US Patent US8455144 B2. Jun 04, 2013.

Karamanev, Dimitre Gueorguiev, Victor R Pupkevich, and Hossein Hojjati. Bio-Fuel cell System. Canada Patent US 8455144 B2. Jun 04, 2013.

Karimi, Shahram. "A Novel Process for Fabrication Membrane Electrode Assemblies with Low Platinum Loading for Use in Proton Exchange Membrane Fuel Cells." PhD Thesis, Toronto, 2011.

karimi, Shahram, and Frank R Foulkes. "Pulse Electrodeposition of Platinum Catalyst using different Pulse Current Waveforms." *Electrochemistry Communications* 19 (2012): 18-20.

Kim, Hansung , and Branko N Popov. "Development of Novel Method for Preparation of PEMFC Electrodes." *Electrochem. and Solid-State Letters* 7 (2004): A71- A74.

Kim, Hansung, Nalini P Subramanian, and Branko N Popov. " Preparation of PEM Fuel Cell Electrodes using Pulse Electrodeposition ." *Power Sources* 138 (2004): 14–24.

Kong, C S, D Y Kim, H K Lee, Y G Shul, and T H Lee. "Influence of Pore-Size Distribution of Diffusion Layer on Mass-Transport Problems of Proton Exchange Membrane Fuel Cells." *Power Sources*, 2002: 185-191.

Larminie, James, and Andrew Dicks. *Fuel Cell Systems Explained.* 2nd. Wiley, 2003.

Lee, B, and D Gushee. "Renewable Power: Not yet Ready for Prime Time." *Chemical Engineering Progress* 125 (2009): 22-25.

Li, X, and I Sabir. "Review of Bipolar Plates in PEM Fuel Cells: Flow-Field Designs." *Int J. Hydrogen Energy* 30 (2005): 359–371.

Lim1, Chan, and C Y Wang. "Effects of Hydrophobic Polymerc in GDL on Power Performance of a PEM Fuel Cell." *Electrochimica Acta* 49 (2004): 4149–4156.

Lindley, D. "Smart Grid – the Energy Storage Problem. Nature." *Nature* 463 (2010): 18-20.

Litster, S, and G McLean. "PEM Fuel Cell Electrodes." *Power Sources* 130 (2004): 61–76.

McLean, G F, G F Niet, S Prince-Richard, and N Djilali. "An Assessment of Alkaline Fuel Cell Technology." *International Journal of Hydrogen Energy* 27 (2002): 507-526.

Murphy, O J, G D Hitchens, and D J Mank. "High Power Density Proton-Exchange Membrane Fuel Cells." *Power Sources* 47 (1994): 353–368.

O'Hayre, Ryan, Sang-Joon Lee, Suk-Won Cha, and Fritz B Prinz. "A Sharp Peak in the Performance of Sputtered Platinum Fuel Cells at Ultra-Low Platinum Loading." *Power Sources* 109 (2002): 483–493.

O'Hayre, Ryan , Suk-Won Cha, Whitney Colella, and Fritz B Prinz. *Fuel Cell Fundamentals.* New Jersey: Wiley, 2006.

Okada, O, and K Yokoyama. "Development of Polymer Electrolyte Fuel Cell Cogeneration Systems for Residential Applications." *Fuel Cells* 1 (2001).

Park, Sehkyu , Jong-Won Lee, and Branko N Popov. "Effect of Carbon Loading in Microporous Layer on PEM Fuel Cell Performance." *Power Sources* 167 (2006): 357-363.

Park, Sehkyu, Jong-Won Lee, and Branko N Popov. " Effect of PTFE Content in Microporous Layer on Water Management in PEM Fuel Cells." *Power Sources* 177 (2008): 457–463.

Passalacqua, E, F Lufrano, G Squadrito, A Patti, and L Giorgi. "Nafion Content in the Catalyst Layer of Polymer Electrolyte." *Electrochimica Acta* 46 (2001): 799–805.

Passalacqua, E, G Squadrito, F Lufrano, A Patti, and L Giorgi. "Effects of the Diffusion Layer Characteristics on the Performance of Polymer Electrolyte Fuel Cell Electrodes." *Applied Electrochemistry* 31 (2001): 449-454.

Phillips, Ryan K, Brooks R Friess, Anthony D Hicks, Julie Bellerive, and Mina Hoorfar. "Ex-situ Measurement of Properties of Gas Diffusion Layers of PEM Fuel Cells." *Energy Procedia* 22 (2012): 486–495.

Priyanka , H Maheshwari, R B Mathur, and T L Dhami. "The Influence of the Pore Size and Its Distribution in a Carbon Paper Electrode on the Performance of a PEM Fuel Cell." *Electrochimica Acta* 54 (2008): 655–659.

Pupkevich, Victor, Vasili Gilibin, and Dimitre Karamanev. "The effect of activation on the electrochemical behaviour of graphite felt towards the Fe3+/Fe2+ redox electrode reaction. Journal of Power Sources, 2007." *J Power Sources* 9 (2007): 1924–1930.

Pupkevich, Victor, Vassili Glibin, and Dimitre Karamanev. "Phosphorylated polyvinyl alcohol membranes for redox Fe3+/H2 flow cells." *Journal of Power Sources* 228 (2013): 300–307.

R, Borup, and et al. "Scientific Aspects of Polymer Electrolyte Fuel Cell Durability and Degradation." *Chemical Reviews*, 2007: 3904–51.

Rao, Chepuri , and D C Trivedi. "Chemical and Electrochemical Depositions of Platinum Group Metals and their Applications." *Coordination Chemistry Reviews* 249 (2005): 613–631.

Rao, Chepuri R K, and D C Trivedi. "Chemical and Electrochemical Depositions of Platinum Group Metals and their Applications." *Coordination Chemistry Reviews* 249 (2005): 613–631.

Ren, Xiaoming , and Shimshon Gottesfeld. "Electro-osmotic Drag of Water in Poly(perfluorosulfonic acid)." *Electrochemical Society* 181 (2001): A87-A93.

Renewables 2011: Global Status Report. Paris: REN21, 2011, 18,21.

Renewables 2013 Global Status Report . Paris: REN21, 2013, 17-19.

Roen, LM, CH Paik , and TD Jarvi . "Electrocatalytic Corrosion of Carbon Support in PEMFC Cathodes." *Electrochem Solid-State Lett* 7 (2004): 19–22.

MIT- Lect 18 3.091SC Introduction to Solid State Chemistry- Fall 2012. Performed by D Sadoway. 2010.

Schweitzer, Jim . *Biological and Environmental Management- Purdue University.* n.d. http://www.purdue.edu/rem/rs/sem.htm (accessed 05 14, 2014).

Scientific Computing World. January/February 2003. http://www.scientific-computing.com/features/feature.php?feature_id=126 (accessed July 21, 2014).

Sessile drop technique. 05 18, 2014.

Shao, Minhua . *Electrocatalysis in Fuel Cells: A Non- and Low- Platinum Approach.* Springer, 2013.

Shijun, Liao, Baitao Li , and Yingwei Li. "Physical Characterization of Electrocatalysts." In *PEM Fuel Cell Electrocatalysts and Catalyst Layers*, by Jiujun Zhang, 488-510. Springer, 2008.

Song , C, Y Tang, Y Zhang , and JL Zhang . "PEM Fuel Cell Reaction Kinetics in the Temperature Range of 23–120 °C." *Electrochim Acta* 5, no. 2 (2007): 2552–2561.

Song , JM, Cha SY, and Lee WM. ". (2001). Optimal Composition of Polymer Electrolyte Fuel Cell Electrodes Determined by the AC Impedance Method. J. Vol (94), P ." *Power Sources* 94 (n.d.): 78–84.

Sridhar, P , Ramkumar Perumal, N Rajalakshmi, M Raja, and K.S Dhathathreyan. "Humidification studies on polymer electrolyte membrane fuel cell." *Journal of Power Sources* 101, no. 1 (2001): 72–78.

Steele, B.C.H, and A Heinzel. "Materials for Fuel-Cell Technologies." *Nature*, no. 414 (2001): 345-352.

Stevens A, and Dahn JR. "Thermal Degradation of the Support in Carbon-Supported Platinum Electrocatalysts for PEM Fuel Cells. Carbon." 43 (2005): 179–88.

Stock, J T, and M V Omra. *Electrochemistry, Past and Present.* American Chemical Society, 1989.

Summer, J J, S E Creager, J J Ma, and D D Desma. "Proton Conductivity in Nafion® 117 and in a Novel Bis [(perfluoroalkyl)sulfonyl]imide Ionomer Membrane." *Electrochemical Society* 145 (1998).

Vielstich, W, A Lamm, and H A Gasteiger. *Handbook of Fuel Cells.* Vol. 2. New York: Wiley, 2003.

Wang, Haijiang , Hui Li, and Xiao-Zi Yuan. *PEM Fuel Cell Failure Mode Analysis.* CRC Press, 2011.

Wang, Y, K.S Chen, J Mishler, and X.C Adroher. "A Review of Polymer Electrolyte Membrane Fuel Cells: Technology, Applications, and Needs on Fundamental Research." *Applied Energy* 88 (2011): 981–1007.

Wanga, Xiaoli , et al. "A Bi-Functional Micro-porous Layer with Composite Carbon Black for PEM Fuel Cells." *Power Sources* 162 (2006): 474–479.

Watkins, D S, K W Dirks, and D G Epp. Fuel Cell Fluid Flow Field Plate. US Patent 5,108,849. 1992.

Webb, Paul A. *Micromemeritics (Data Collection, Reduction and Presentation).* April 1993.

Weber, Adam Z, and John Newman. "Effects of Microporous Layers in Polymer Electrolyte." *Journal of The Electrochemical Society* 152 (2005): A677-A688 .

Wilson, M S. Membrane Catalyst Layer for Fuel Cells. US Patent 5,234,777. 1993.

Xua, C, T S Zhaoa, and Y L Heb. "Effect of Cathode Gas Diffusion Layer on Water Transport and Cell Performance in Direct Methanol Fuel Cells." *Power Sources* 171 (2007): 268–274.

Yasuda , K, A Taniguchi , T Akita , T Toroi , and Z Siroma . "Characteristics of a Platinum Black Catalyst Layer with Regard to Platinum Dissolution Phenomena in a Membrane Electrode Assembly." *Electrochemical Society* 153 (2006): 1599–603.

Zhou, L. "Progress and Problems in Hydrogen Storage Methods." *Renewable and Sustainable Energy Reviews* 9, no. 4 (2005): 395–408.

Appendices

Appendix 1-1: Sample excel sheet used for calculation of gas permeability

Parameters

Sample Code :	CC4-WU-12	Date :	31-Jan-14	Apparatus :	B	
Sample Type :	CC4-500µm	Sample Thickness (mm)		PTFE Loading Cloth(%wt.)	75.0%	
Barometric Pressure(Pa) :	100600	L1:	0.724	PTFE Loading in MPL(%wt.)	40.0%	
Room Temperature(C) :	22	L2:	0.752	MPL Loading (mg/cm²) :	1.42	
Correction Factor(m) :	0.3282	L3:	0.770	Catalyst Loading(mgPt/cm²)	0.495	
Correction Factor(b) :	0.0179	Average(m) :	7.487E-04	Sample Weight(g)	0.4004	
Sample Test Area(m2) :	0.000506707	Expected Value :		Pressure Conversion:	0.006227223	

Global Constants (DO NOT CHANGE) / **DO NOT CHANGE**

Gas Constant Dry Air :	287.058	Temp(K):	295.15
InH2O to Pascal :	249.088908	Density Air :	1.187368542
Molar Mass of Dry Air :	0.0289652	2LRT/MWair :	126.858457
Dry Air Viscosity :	1.82E-05	Density/Area:	2343.304003
Total Sample Area(cm²) :	9		

READINGS / CALCULATED FINAL VALUES / INTERMEDIATE CALCULATIONS

Pin (H2O)	AP Transducer (mV)	Air Flow (ccm)	K (m2)	Error %	Mass Flow Kg/s	Pin (Pa)	ΔP (Pa)	Pout (Pa)	AP Volt Adjusted	AP Volt Final	Left Side Equation
0.0	0	0.00	N/A	N/A	0.0000E+00	100600	0	100600	-0.0179	0	0
0.5	9	1.28	1.0760E-11	#DIV/0!	4.9990E-05	100724.5445	0.053317506	100724.4911	8.562004	8.562004	84.66727708
1.0	15	2.27	1.1462E-11	#DIV/0!	8.8655E-05	100849.0889	0.088657505	100849.0003	14.237086	14.237086	140.9606411
1.5	21	3.19	1.1489E-11	#DIV/0!	1.2459E-04	100973.6334	0.124140569	100973.5092	19.935142	19.935142	197.620512
2.0	27	4.19	1.1734E-11	#DIV/0!	1.6364E-04	101098.1778	0.159460131	101098.0184	25.606942	25.606942	254.1591053
2.5	33	5.16	1.1812E-11	#DIV/0!	2.0152E-04	101222.7223	0.194841006	101222.5274	31.288588	31.288588	310.9342259
3.0	39	6.14	1.1881E-11	#DIV/0!	2.3980E-04	101347.2667	0.230201443	101347.0365	36.966952	36.966952	367.8156133
3.5	45	7.05	1.1805E-11	#DIV/0!	2.7534E-04	101471.8112	0.265704944	101471.5455	42.66829	42.66829	425.0647112
4.0	52	8.12	1.1749E-11	#DIV/0!	3.1713E-04	101596.3556	0.307108665	101596.0485	49.317116	49.317116	491.9037287
4.5	57	8.99	1.1858E-11	#DIV/0!	3.5111E-04	101720.9001	0.336466694	101720.5636	54.031582	54.031582	539.5878094
5.0	63	9.99	1.1911E-11	#DIV/0!	3.9016E-04	101845.4445	0.371786256	101845.0728	59.703382	59.703382	596.9592943
5.5	69	10.87	1.1814E-11	#DIV/0!	4.2453E-04	101969.989	0.407351071	101969.5816	65.414566	65.414566	654.8637323
6.0	75	11.85	1.1836E-11	#DIV/0!	4.6280E-04	102094.5334	0.442711508	102094.0907	71.09293	71.09293	712.578854
6.5	80	12.78	1.1960E-11	#DIV/0!	4.9912E-04	102219.0779	0.471946911	102218.606	75.787704	75.787704	760.5620934

CC4-WU-14(A) / **CC4-WU-12(B2)** / CC4-WU-14(A2) / CC4-WU-12(A) / CC4-WU-14(B) / Charts and Graphs

Appendix 1-2: Gas permeability data (Figure 4-5)

Paper			Cloth		
PTFE (wt.%)	K (m²)	Standard Deviation	PTFE (wt.%)	K (m²)	Standard Deviation
0	8.52E-12	4.27E-13	0	3.10E-11	5.20E-13
13	7.38E-12	2.55E-13	20	3.54E-11	1.31E-13
20	5.73E-12	1.69E-13	43	4.43E-11	7.60E-13
26	4.89E-12	2.12E-13	61	4.02E-11	6.74E-13
42	2.32E-12	5.57E-14	79	4.11E-11	2.05E-12
63	8.85E-13	1.55E-14	89	4.94E-11	2.44E-13
70	7.11E-13	1.30E-14	124	3.80E-11	8.81E-13
83	7.84E-13	3.22E-14	139	4.42E-11	2.82E-14
96	4.49E-13	7.94E-15	155	4.56E-11	2.21E-12
106	4.92E-13	8.49E-15	176	2.24E-11	1.01E-12
122	6.41E-13	9.74E-15	193	8.23E-12	2.00E-13
133	5.09E-14	1.37E-15	211	4.14E-12	3.05E-13
146	9.17E-15	1.43E-16			

Appendix 2-1: Long-term durability data (Figure 4-13)

The BioGenerator fuel cell voltage using the developed electrode				The BioGenerator fuel cell voltage using commercial electrode					
Time (hr)	Voltage (V)	Time (hr)	Voltage (V)	Time (hr)	Voltage (V)	Time (hr)	Voltage (V)	Time (hr)	Voltage (V)
20	0.579	1380	0.564	0	0.61	498.5	0.59	1253	0.511
63	0.58	1404	0.562	5	0.61	522.5	0.5845	1273	0.509
111	0.567	1452	0.56	22	0.6	546.5	0.578	1321	0.5
121	0.57	1500	0.559	27.5	0.603	570.5	0.562	1337	0.501
145	0.57	1524	0.553	43.5	0.603	594.5	0.551	1347	0.5
193	0.5685	1572	0.55	51.5	0.602	618.5	0.55	1352	0.498
217	0.567	1644	0.536	66.5	0.601	642.5	0.547	1372	0.499
227	0.567	1668	0.547	72	0.6	666.5	0.542	1392	0.497
275	0.563	1692	0.5475	74	0.6	706.5	0.522	1397	0.498
299	0.566	1740	0.545	92	0.599	721.5	0.51	1445	0.5
323	0.566	1812	0.544	99	0.602	729	0.521	1462	0.494
371	0.569	1836	0.543	119.5	0.6	745	0.511	1474	0.489
395	0.565	1860	0.541	146.5	0.597	750.5	0.5125	1489	0.489
419	0.562	1884	0.542	163	0.593	776.5	0.505	1513	0.487
443	0.561	1908	0.543	171.5	0.588	800.5	0.564	1535	0.485
467	0.56	1932	0.542	175.5	0.596	825.5	0.5475	1556	0.494
491	0.561	1956	0.542	176	0.597	849.5	0.5405	1564	0.494
515	0.559	1980	0.543	188	0.596	865	0.5515	1636	0.48
563	0.556	2004	0.542	195	0.597	872	0.5475	1644	0.478
588	0.554	2028	0.542	210.5	0.596	889	0.554	1661	0.477
612	0.553	2052	0.542	218	0.5955	906	0.5545	1669	0.479
636	0.552	2100	0.545	237	0.5945	915.5	0.546	1693	0.477
684	0.554	2148	0.539	256	0.594	931.5	0.5465	1717	0.474
708	0.553	2172	0.547	260	0.594	938.5	0.545	1737	0.468
756	0.555	2196	0.546	263	0.5955	960.5	0.545	1785	0.472
804	0.56	2220	0.544	284.5	0.593	988	0.543	1805	0.462
828	0.559	2244	0.543	286	0.5935	1000	0.5405	1825	0.443
852	0.56	2292	0.542	313.5	0.59	1008	0.5595	1897	0.41
876	0.56	2340	0.541	330	0.587	1024	0.542	1935	0.406
900	0.562	2364	0.531	334	0.588	1037	0.564	1943	0.406
948	0.545	2412	0.54	337.5	0.596	1049	0.559	1970	0.414
972	0.55	2436	0.535	352	0.587	1056	0.555	1994	0.35
996	0.558	2484	0.461	360	0.5865	1074	0.554	2028	0.225
1020	0.558	2508	0.322	376	0.585	1098	0.549	2055	0.103
1044	0.5557	2532	0.451	383	0.585	1105	0.548	2079	0.07
1092	0.56	2556	0.4655	398	0.5845	1126	0.547		
1116	0.56	2580	0.189	405	0.592	1176	0.518		
1164	0.558	2604	0.418	421	0.584	1196	0.5165		
1236	0.556	2628	0.564	430	0.584	1204	0.5155		
1260	0.556	2652	0.566	452	0.579	1221	0.509		
1284	0.556			457.5	0.592	1229	0.534		
1356	0.551			474.5	0.587	1246	0.511		

Appendix 2-2: i-V curve data (Figure 4-14- a)

The BioGenerator fuel cell i-V using commercial electrode								
t= 0			**t= 100 hrs**			**t= 330 hrs**		
I(A)	i(A cm $^{-2}$)	V(v)	I(A)	i(A cm $^{-2}$)	V(v)	I(A)	i(A cm $^{-2}$)	V(v)
0	0	1.005	0	0	0.8625	0	0	0.975
0.0318	0.00795	0.7975	0.0262	0.00655	0.82	0.08	0.02	0.7425
0.1125	0.028125	0.6975	0.1162	0.02905	0.73	0.18	0.045	0.68
0.3325	0.083125	0.6125	0.2412	0.0603	0.6675	0.4803	0.120075	0.5775
0.6025	0.150625	0.5575	0.4862	0.12155	0.595	0.9356	0.2339	0.465
1.2325	0.308125	0.445	0.9118	0.22795	0.4925	1.4206	0.35515	0.3525
1.9031	0.475775	0.3275	1.2768	0.3192	0.41	2.062	0.5155	0.1875
2.5331	0.633275	0.2125	1.8118	0.45295	0.2825	2.45	0.6125	0.0675
3.1318	0.78295	0.09	2.2968	0.5742	0.1575			
			2.516	0.629	0.09			
t= 640 hrs			**t= 1020 hrs**			**t= 1620 hrs**		
I(A)	i(A cm $^{-2}$)	V(v)	I(A)	i(A cm $^{-2}$)	V(v)	I(A)	i(A cm $^{-2}$)	V(v)
0	0	0.98	0	0	0.9775	0	0	0.95
0.08	0.02	0.7175	0.0837	0.020925	0.71	0.079	0.01975	0.7175
0.2	0.05	0.6375	0.2237	0.055925	0.6125	0.1287	0.032175	0.6675
0.445	0.11125	0.5425	0.4447	0.111175	0.525	0.37	0.0925	0.53
0.8606	0.21515	0.42	0.9843	0.246075	0.3625	0.6497	0.162425	0.42
1.30006	0.325015	0.29	1.4347	0.358675	0.2175	0.93	0.2325	0.325
1.5903	0.397575	0.1925	1.7043	0.426075	0.11	1.1993	0.299825	0.2275
1.7756	0.4439	0.1225	1.7843	0.446075	0.075	1.355	0.33875	0.1675
1.91	0.4775	0.055	1.8	0.45	0.0475	1.495	0.37375	0.1075
						1.5547	0.388675	0.085
						1.601	0.40025	0.0425

t= 1900 hrs		
I(A)	i(A cm $^{-2}$)	V(v)
0	0	0.9525
0.08	0.02	0.6825
0.18	0.045	0.58
0.355	0.08875	0.455
0.635	0.15875	0.3086
0.82	0.205	0.2
0.9606	0.24015	0.115
1.0056	0.2514	0.085
1.0505	0.262625	0.05
1.04	0.26	0.03

Appendix 2-3: i-V curve data (Figure 4-14- b)

The BioGenerator fuel cell i-V using the developed electrode								
t= 0			**t=125 hrs**			**t= 250 hrs**		
I(A)	i(A cm $^{-2}$)	V(v)	I(A)	i(A cm $^{-2}$)	V(v)	I(A)	i(A cm $^{-2}$)	V(v)
0	0	1	0	0	0.9825	0	0	0.985
0.065	0.01625	0.745	0.08	0.02	0.7425	0.0793	0.019825	0.7575
0.265	0.06625	0.6	0.2353	0.058825	0.6025	0.2147	0.053675	0.6525
0.4853	0.121325	0.5225	0.4453	0.111325	0.52	0.44	0.11	0.5475
0.7756	0.1939	0.45	0.7306	0.18265	0.44	0.685	0.17125	0.4625
1.1606	0.29015	0.36	1.0556	0.2639	0.355	1.0353	0.258825	0.3675
1.9053	0.476325	0.18	1.5006	0.37515	0.25	1.3703	0.342575	0.2925
2.1256	0.5314	0.145	1.9306	0.48265	0.16	1.7003	0.425075	0.2175
2.369	0.59225	0.0675	2.337	0.58425	0.0675	1.9003	0.475075	0.1775
						2.1056	0.5264	0.1325
						2.2506	0.56265	0.1
						2.339	0.58475	0.0625
t= 520 hrs			**t= 1700 hrs**					
I(A)	i(A cm $^{-2}$)	V(v)	I(A)	i(A cm $^{-2}$)	V(v)			
0	0	1.0125	0	0	1.0075			
0.0837	0.020925	0.735	0.0743	0.018575	0.75			
0.2337	0.058425	0.6275	0.1793	0.044825	0.655			
0.4437	0.110925	0.535	0.3993	0.099825	0.535			
0.8193	0.204825	0.41	0.66	0.165	0.435			
1.304	0.326	0.28	1.0156	0.2539	0.325			
1.6943	0.423575	0.1775	1.36	0.34	0.2325			
1.9793	0.494825	0.1	1.59	0.3975	0.175			
2.06	0.515	0.055	1.8056	0.4514	0.12			
			1.965	0.49125	0.0775			
			1.984	0.496	0.0522			

Name:	Vahid Vajihinejad
Post-secondary Education and Degrees:	Sharif University of Technology Tehran, Iran 2007-2012 B.Sc.
	The University of Western Ontario London, Ontario, Canada 2012-2014 M.E.Sc.
Honors and Awards:	Ranked 900th among more than 250,000 participants in the Iranian Nationwide Universities' entrance exam 2007
Related Work Experience	Teaching Assistant The University of Western Ontario 2012-2014

Publications:

Vajihinejad, V., Brouwers, P., Karamanev, D., Karimi, S. Effect of PTFE in Gas Diffusion Backing Layer of Hydrogen Oxidation Anode Electrode of a Microbial-based Fe^{2+}/Fe^{3+} Redox Flow Fuel Cell International Journal of Hydrogen Energy (to be submitted).

Vajihinejad, V., Cuello, R., Karamanev, D., Karimi, S. Performance Stability Studies of Hydrogen Oxidation Anode Electrodes used in a Microbial-based Fe^{2+}/Fe^{3+} Redox Flow Fuel CellInternational Journal of Hydrogen Energy (to be submitted).

Afsham, N., Vajihinejad, V., Sherafatmand, M., Yaghmaei, S., Roshandel, R. "Ground water Nitrate Removal by means of a Sediment Microbial Fuel Cell (SMFC) Using Biocathode", oral presentation, 3rd International Microbial Fuel Cell Conference, the Netherlands, 2011.

Vajihinejad, V., Sherafatmand, M. Study of Methods Employed in Biological Air Treatment via Biofiltration. The 4th Conference and Exhibition on Environmental Engineering, Iran, 2010.